AD

Research and Development Technical Report
ECOM-0044-F

MICROWAVE ACTIVE NETWORK SYNTHESIS

FINAL REPORT

By

E. G. Cristal A. Podell S. B. Cohn

FEBRUARY 1972

DISTRIBUTION STATEMENT

Approved for Public Release; Distribution Unlimited.

ECOM

UNITED STATES ARMY ELECTRONICS COMMAND · FORT MONMOUTH, N.J. 07703

CONTRACT DAAB07-70-C-0044

STANFORD RESEARCH INSTITUTE
Menlo Park, California 94025

108

PRIOR REPORT - LIMITED

NOTICES

Disclaimers

The findings in this report are not to be construed as an official Department of the Army position, unless so designated by other authorized documents.

The citation of trade names and names of manufacturers in this report is not to be construed as official Government indorsement or approval of commercial products or services referenced herein.

Disposition

Destroy this report when it is no longer needed. Do not return it to the originator.

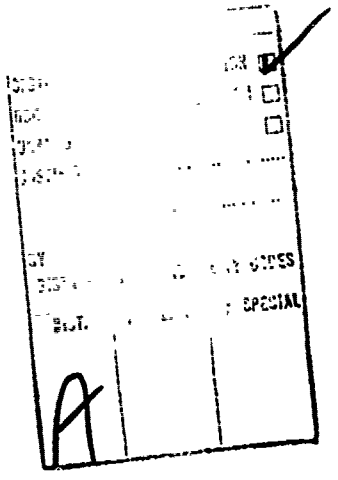

TECHNICAL REPORT ECOM-0044-F

Reports Control Symbol
OSD-1366

FEBRUARY 1972

MICROWAVE ACTIVE NETWORK SYNTHESIS

FINAL REPORT

SRI Project 8245

CONTRACT DAAB07-70-C-0044

Prepared by

E. G. CRISTAL A. PODELL S. B. COHN

STANFORD RESEARCH INSTITUTE

MENLO PARK, CALIFORNIA 94025

For

U.S. ARMY ELECTRONICS COMMAND, FORT MONMOUTH, N.J. 07703

ABSTRACT

This report describes the application of meander lines to impedance transformers, and discusses two types of negative-impedance circuits and two slot-line topics.

It is demonstrated that meander lines constitute a class of impedance transformers of which stepped-impedance transformers are a special case. A design table is presented for nearly-equal-ripple meander-line transformers of from 2 to 6 turns, incorporating a wide range of bandwidths and impedance transformations. Experimental confirmation of the design table is given.

Two types of negative-impedance-converter (NIC) circuits were designed and constructed: (1) a high-power NUNIC, and (2) a FET-NIC filter. A high-power NUNIC circuit intended for operation at 200 to 500 MHz was built and produced negative resistance from below 80 MHz to above 680 MHz. A lossless one-pole filter incorporating the NUNIC was built for operation at 230 MHz and exhibited a 3-dB filter bandwidth of 2.7 MHz. The 1-dB compression point occurred at 1 watt of input power (+30 dBm) and the third-order intermodulation intercept measured +34.5 dB. A FET-NIC filter has been constructed in microwave integrated circuit (MIC) form. It was possible to vary the bandwidth of this filter electrically over a 7:1 range. The size of the complete MIC FET-NIC filter is comparable with a small power-transistor package, approximately 1/2 inch square by 1/16 inch high.

The slot-line topics treated are, firstly, symmetrical four-layer-sandwich slot line, which is discussed for ferrite-phase-shifter applications. Formulas are given for wavelength, characteristic impedance,

and magnetic-field-strength distribution. Curves of the latter are helpful for phase-shifter optimization. Secondly, coupling between two parallel slot lines is analyzed, and a few typical curves of coupling and directivity versus frequency are shown.

PURPOSE OF CONTRACT

The purpose of this contract is to develop techniques for the design of passive and active filters and components in the VHF-to-microwave-frequency range, and to determine the electromagnetic properties of slot line for integration with microstrip technology.

CONTENTS

ILLUSTRATIONS

TABLES

ACKNOWLEDGMENTS

The authors are indebted to Dr. Ulrich Gysel for numerous illuminating discussions concerning the numerical methods used to obtain the meander-line design table, and for allowing the authors the use of his modified computer program of the Fletcher-Powell technique for minimization of a function of several variables. The use of this program undoubtedly saved considerable computer time in compiling the design table. The authors would also like to ackrowledge the excellent work done by Mr. Eldon Fernandes of SRI, who accurately constructed and measured the experimental meander-line transformers.

I INTRODUCTION

A. Meander-Line and Hybrid Meander-Line Transformers

In Section II the application of meander lines to impedance transformers is proposed and developed. Meander-line transformers have less bandwidth than stepped-impedance transformers for a given passband VSWR, but can have greatly superior shape factors in stripline and MIC realizations. Hybrid meander-line transformers allow circuit designers greatly increased flexibility in choosing transformer shape factors, while allowing (basically) the same electrical performance as with either stepped-impedance or meander-line transformers. A comprehensive meander-line-transformer-design table is presented in Section II.

B. Negative-Impedance Converters

Work on the NIC circuit during the past reporting period was conducted in the following areas: (1) increasing the power-handling capabilities of the NIC, (2) increasing its flexibility of application, and (3) decreasing its size. The progress that was made in all three of these areas is described in Section III. In particular, a 1-watt UHF NIC filter was constructed and an integrated-circuit FET-NIC filter was built with electronically variable bandwidth. These circuits were shown to be insensitive to both device-parameter variations and environmental changes.

C. Slot Line

The investigation of slot line is brought to a close in Section IV of this report. One final subject is the symmetrical four-layer-sandwich slot line, which is being applied to ferrite phase shifting in another USAECOM program. Formulas of wavelength, characteristic impedance, and magnetic-field distribution are given. Field computations and plots are useful in selecting parameters for good phase-shifter performance. A second subject is analysis of directional coupling of a pair of slots. Directivity and coupling versus frequency are shown graphically for several cases.

II MEANDER-LINE AND HYBRID MEANDER-LINE TRANSFORMERS

A. General

Transformers are very often required in microwave components and systems. Coupled-transmission-line geometries, such as interdigital and/or combline, are often used for purposes of obtaining impedance transformations.[1]* However, in many applications these structures are quite unsatisfactory for the following reasons:

(1) The required coupling between lines may not be practically realized.

(2) One or more of the coupled lines may require grounding, which is difficult in stripline and microwave-integrated-circuit (MIC) realizations.

(3) The equivalent circuit for these and other coupled-line geometries contains, in addition to ideal transformers, shunt or series reactances that limit the bandwidth over which the transformer may be used.

The stepped-impedance transformer,[2,3,4] consisting of a cascade of unit-elements[5] (UE), is also commonly used. The stepped-impedance transformer can transform widely differing impedances (resistances, to be strictly correct) over narrow to very wide bandwidths, and it can be constructed readily in air-line, stripline, and MIC. However, each section of a stepped-impedance transformer is a quarter-wavelength long at band center.† Consequently, the length of a multisection transformer can be quite large. For example, a three-section stripline transformer

---

* References are listed at the end of the report.
† Excepting the short-step transformer.[6]

constructed on Rexolite 1422 ($\epsilon_r = 2.54$) centered at 1000 MHz would be 5.56 inches long. If, as is sometimes the case, transformers are required at both the input and output of a device, the overall length of the stepped-impedance transformers and device could be excessive. An idealized solution to this problem would be to fold the stepped-impedance transformer accordion fashion, as illustrated in Figures II-1(a) and (b). In order to preserve the electrical characteristics of the circuit, shielding between the folded lines would be needed. Conceptually, this technique is satisfactory, but in practice the required shielding would be impractical. On the other hand, if the shields were removed, there would be sufficient coupling between lines to seriously degrade the transformer performance.

Figures II-2(a) and (b) depict conventional meander-line geometries in stripline and MIC. We note that these structures may be considered as folded, coupled-line, stepped-impedance lines. Thus, from this

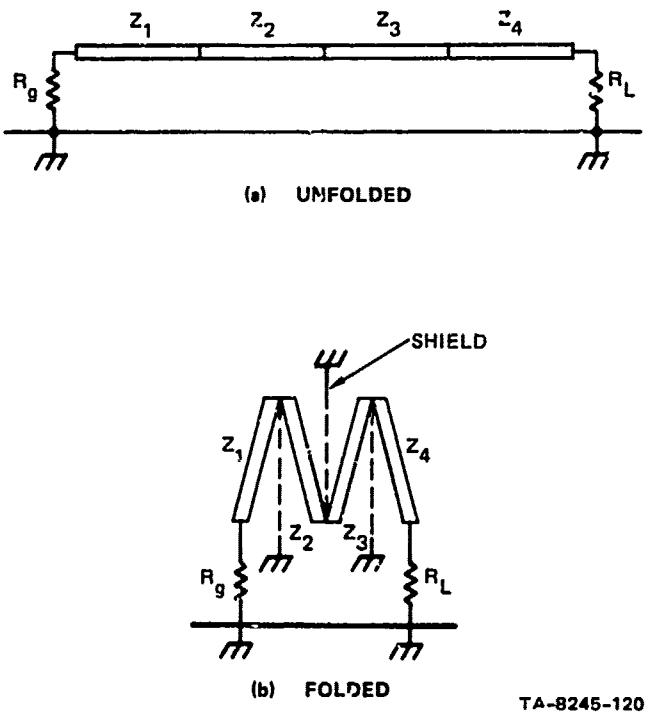

FIGURE II-1 STEPPED-IMPEDANCE TRANSFORMER

(a) STRIPLINE

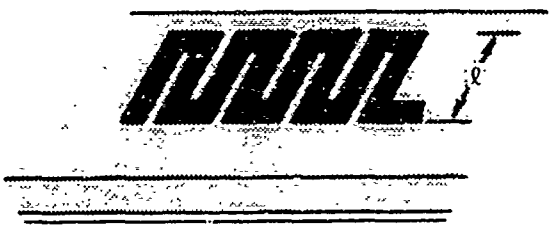

(b) MICROWAVE-INTEGRATED CIRCUIT (MIC)

TA-8245-115

FIGURE II-2 CONVENTIONAL MEANDER-LINE GEOMETRIES

perspective the meander line might be considered as comprising a class of generalized coupled-line transformers within which the stepped-impedance transformer is merely a special case for which coupling between turns is negligible. From this point of view, an extension of meander-line transformers to hybrid meander-line transformers is quite natural. A hybrid meander-line transformer is one in which coupling between some adjacent turns is negligible, whereas for other adjacent turns it is significant. Several examples of hybrid meander-line transformers are given in Figures II-3(a), (b), and (c). Theoretically, the number of hybrid configurations is $2^{(N-1)}$, where N is the order of the transformer. Hybrid geometries allow the circuit designer much greater flexibility in the physical layout of the transformer than he would otherwise have with only meander-line and stepped-impedance transformers.

(a) EXAMPLE 1

(b) EXAMPLE 2

(c) EXAMPLE 3

TA-8245-116

FIGURE II-3 HYBRID MEANDER-LINE GEOMETRIES

The meander line is not a new transmission-line geometry. Butcher[7] studied it from the point of view of its possible application in traveling-wave tubes. Bolljahn and Matthaei[8] computed its image impedance in the general all-coupled-line case, and Hewitt[9] utilized the structure in a microwave compression filter. The most recent and novel treatment of the meander line has been given by Sato.[10] An equivalent circuit for meander lines (presented by Sato) having coupling only between adjacent turns is given in Figure II-4. The coupling between turns is accounted for solely by "S-plane inductors"[5,11] connecting unit elements. A stepped-impedance geometry is obtained by setting all inductive admittance values to zero. A hybrid geometry is obtained by setting some but not all inductive admittance values to zero. The equivalent circuit of

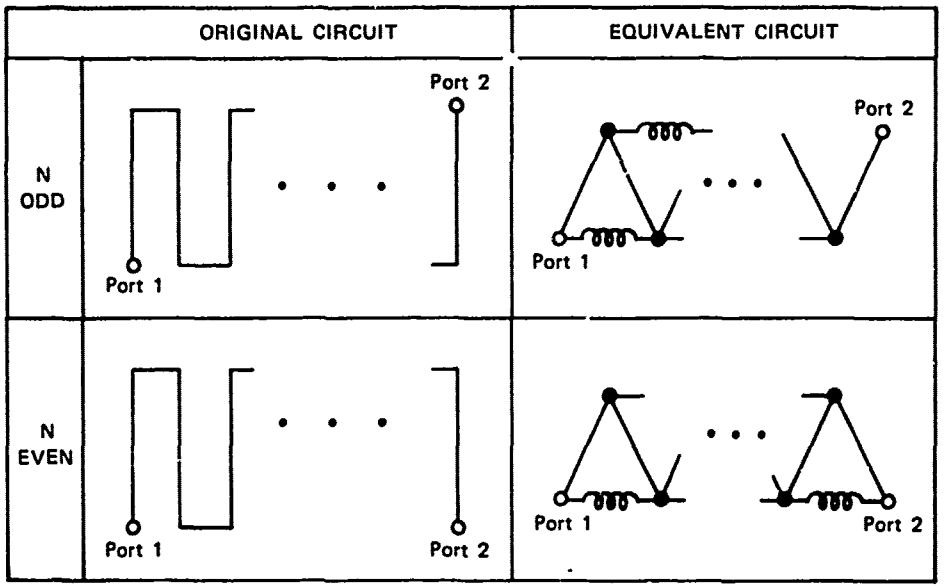

FIGURE II-4 TWO-PORT EQUIVALENT CIRCUITS FOR MEANDER LINES HAVING NEGLIGIBLE COUPLING BETWEEN NONADJACENT TURNS

Figure II-4 forms the basis for the compilation of meander-line transformer designs given later in this section.

B. Meander-Line-Transformer Design Tables

The meander-line transformer tables presented later in this section were compiled using numerical techniques by minimizing a weighted reflection-coefficient function raised to a high integer power (e.g., minimizing a least-p^{th} objective). The weighting function was constructed to assure that the coupling between meander-line turns would be within prescribed limits. The numerical techniques are well known,[12] and consequently specific details will not be given here.

1. Definition of Parameters Used in Design Tables

Figure II-5 depicts a cross-sectional representation of an arbitrary meander-line transformer in any TEM or quasi-TEM medium and depicts the unnormalized distributed capacitance parameters C_{g_i} and $C_{i,i+1}$. These are defined as follows:

$$\begin{aligned} C_{g_i} &= \text{Capacitance to ground per unit length for the } i^{th} \text{ conductor} \\ C_{i,i+1} &= \text{Mutual capacitance per unit length between the } i^{th} \text{ and } i^{th}+1 \text{ conductors.} \end{aligned} \tag{II-1}$$

Coupling between non-adjacent lines is assumed negligible.

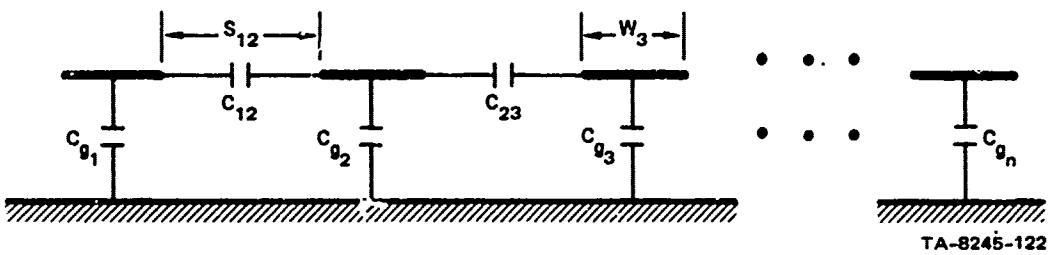

FIGURE II-5 SCHEMATIC CROSS-SECTIONAL REPRESENTATION FOR MEANDER-LINE TRANSFORMERS

The dimensionless, distributed-capacitance parameters that are needed for use with Getsinger's data[13] in order to obtain dimensional parameters from electrical parameters are as follows:

$$\begin{aligned} c_{g_i} &= C_{g_i} / \epsilon \\ c_{i,i+1} &= C_{i,i+1} / \epsilon \\ \epsilon &= \epsilon_r \epsilon_o \\ \epsilon_r &= \text{Relative dielectric constant of the medium} \\ \epsilon_o &= \text{Permittivity of free space in the units of } C_{g_i} \text{ and } C_{i,i+1}. \end{aligned} \tag{II-2}$$

The coupling, $k_{i,i+1}$, between meander-line turns i and i+1 is defined as

$$k_{i,i+1} = -20 \log_{10} \frac{C_{i,i+1}}{\sqrt{\left(C_{g_i} + C_{i,i+1}\right)\left(C_{g_{i+1}} + C_{i,i+1}\right)}} \text{ dB} \quad . \tag{II-3}$$

The meander-line-transformer bandwidth, BW, is defined as

$$BW = \theta_2/\theta_1 \tag{II-4}$$

where θ_1 and θ_2 are the lower and upper passband edges, respectively, in electrical degrees or frequency. The ratio of load to source resistance, always taken as greater than 1, is denoted by the symbol RL/RG, and the peak VSWR in the passband is denoted by VSWR.

The compilation of meander-line-transformer designs is presented in Table II-1, for N = 2 to 6 turns, RL/RG = 1.0 to 20.0, and BW = 1.5 to 10. The normalized self and mutual capacitances are listed under the column headings CGi/E and CMij/E, respectively. These values may be converted to the dimensionless forms C/ε required by Getsinger's data, by the equation

$$\left.\begin{matrix} C_{g_i}/\varepsilon \\ \text{or} \\ C_{i,i+1}/\varepsilon \end{matrix}\right\} = \frac{376.7}{RG\sqrt{\varepsilon_r}} \left\{\text{Table II-1 value}\right\} \tag{II-5}$$

where RG is the source resistance in ohms. Table II-1 was terminated after the peak passband VSWR exceeded 1.5.

Table II-1

MEANDER-LINE-TRANSFORMER DESIGNS

PROGRAM BY
E.G. CRISTAL
OCTOBER 1971

2 SECTION MEANDER-LINE TRANSFORMER TABLE
CAPACITANCES NORMALIZED TO 376.7/SQRT(EPSR)
COUPLING = 10 TO 16 DB
BANDWIDTH = 1.50/1.

RL/RG	CG1/E	CG2/E	CM12/E	VSWR
1.0	.8051	.8051	.2179	1.001
1.1	.8114	.7764	.1754	1.007
1.2	.7994	.7339	.1602	1.013
1.3	.7894	.6981	.1457	1.020
1.4	.7758	.6624	.1388	1.028
1.5	.7375	.6148	.1585	1.031
1.6	.7329	.5890	.1458	1.035
1.7	.7224	.5646	.1400	1.039
1.8	.7127	.5422	.1357	1.044
1.9	.7085	.5255	.1241	1.047
2.0	.7015	.5178	.1182	1.051
2.2	.6772	.4695	.1187	1.059
2.4	.6725	.4478	.1032	1.064
2.6	.6513	.4181	.1045	1.072
2.8	.6395	.3967	.9766E-01	1.078
3.0	.6347	.3812	.8978E-01	1.082
3.5	.6042	.3382	.8598E-01	1.096
4.0	.5882	.3196	.7574E-01	1.108
4.5	.5637	.2811	.7326E-01	1.120
5.0	.5548	.2636	.6557E-01	1.128
6.0	.5225	.2288	.6159E-01	1.150
7.0	.5024	.2050	.5437E-01	1.167
8.0	.4881	.1875	.4954E-01	1.181
9.0	.4727	.1721	.4599E-01	1.199
10.0	.4599	.1599	.4321E-01	1.212
20.0	.3941	.1005	.2659E-01	1.343

Table II-1 (Continued)

PROGRAM BY
E.G. CRISTAL
OCTOBER 1973

2 SECTION MEANDER-LINE TRANSFORMER TABLE
CAPACITANCES NORMALIZED TO 376.7*SQRT(EPSR)
COUPLING = 10 TO 16 DB
BANDWIDTH = 2.00/1.

RL/RG	CG1/E	CG2/E	CM12/E	VSWR
1.0	.7564	.7552	.2727	1.014
1.1	.7428	.7155	.2585	1.022
1.2	.7324	.6816	.2359	1.041
1.3	.7242	.6516	.2156	1.067
1.4	.7185	.6283	.1990	1.078
1.5	.7154	.6106	.1292	1.085
1.6	.7148	.6129	.1235	1.098
1.7	.7139	.5984	.1194	1.113
1.8	.7218	.5862	.1137	1.122
1.9	.7139	.5749	.1100	1.137
2.0	.7021	.5272	.1053	1.146
2.2	.6847	.4932	.9889E-01	1.171
2.4	.6687	.4661	.9275E-01	1.188
2.6	.6519	.4407	.8803E-01	1.204
2.8	.6397	.4189	.8435E-01	1.224
3.0	.6286	.4002	.8099E-01	1.244
3.5	.6108	.3596	.7294E-01	1.286
4.0	.5771	.3275	.6726E-01	1.325
4.5	.5613	.3049	.6157E-01	1.354
5.0	.5451	.2837	.5803E-01	1.393
6.0	.5127	.2489	.5187E-01	1.456
7.0	.4980	.2246	.4701E-01	1.513

Table II-1 (Continued)

PROGRAM BY
E.G. CRISTAL
OCTOBER 1971

2 SECTION MEANDER-LINE TRANSFORMER TABLE
CAPACITANCES NORMALIZED TO 376.7/SQRT(EPSR)
COUPLING = 10 TO 16 DB
BANDWIDTH = 3.00/1.

RL/RG	CG1/E	CG2/E	CM12/E	VSWR
1.0	.7383	.7379	.3072	1.000
1.1	.7164	.6924	.2916	1.091
1.2	.7914	.7452	.1598	1.176
1.3	.7405	.7086	.1504	1.241
1.4	.7529	.6791	.1419	1.345
1.5	.7495	.6641	.1338	1.427
1.6	.7234	.6369	.1234	1.508

PROGRAM BY
E.G. CRISTAL
OCTOBER 1971

2 SECTION MEANDER-LINE TRANSFORMER TABLE
CAPACITANCES NORMALIZED TO 376.7/SQRT(EPSR)
COUPLING = 10 TO 16 DB
BANDWIDTH = 4.00/1.

RL/RG	CG1/E	CG2/E	CM12/E	VSWR
1.0	.7387	.7385	.3175	1.000
1.1	.7104	.6883	.2988	1.070
1.2	.7686	.7214	.1874	1.178
1.3	.7814	.7157	.1398	1.180
1.4	.7663	.6843	.1297	1.235
1.5	.7494	.6604	.1226	1.283
1.6	.7325	.6359	.1164	1.332
1.7	.7173	.6132	.1114	1.380
1.8	.7034	.5929	.1072	1.427
1.9	.6905	.3739	.1031	1.473
2.0	.6789	.5570	.9960E-01	1.517

PROGRAM BY
E.G. CRISTAL
OCTOBER 1971

2 SECTION MEANDER-LINE TRANSFORMER TABLE
CAPACITANCES NORMALIZED TO 376.7/SQRT(EPSR)
COUPLING = 10 TO 16 DB
BANDWIDTH = 5.00/1.

RL/RG	CG1/E	CG2/E	CM12/E	VSWR
1.0	.7556	.7562	.2842	1.001
1.1	.7424	.7198	.2555	1.077
1.2	.7324	.6921	.2287	1.150
1.3	.7845	.7138	.1389	1.210
1.4	.7612	.6890	.1318	1.277
1.5	.7454	.6615	.1234	1.341
1.6	.7233	.6409	.1205	1.397
1.7	.7135	.6141	.1124	1.449
1.8	.7111	.5983	.1051	1.500

Table II-1 (Continued)

PROGRAM BY
E.G. CRISTAL
OCTOBER 1971

2 SECTION MEANDER-LINE TRANSFORMER TABLE
CAPACITANCES NORMALIZED TO 376.7/SQRT(EPSR)
COUPLING = 10 TO 16 DB
BANDWIDTH = 6.00/1.

RL/RG	CG1/E	CG2/E	CM12/E	VSWR
1.0	.7465	.7446	.2964	1.000
1.1	.7324	.7105	.2490	1.083
1.2	.7815	.7348	.1702	1.161
1.3	.7757	.7124	.1450	1.236
1.4	.7601	.6816	.1354	1.312
1.5	.7431	.6598	.1252	1.381
1.6	.7256	.6371	.1198	1.451
1.7	.7113	.6195	.1143	1.518

PROGRAM BY
E.G. CRISTAL
OCTOBER 1971

2 SECTION MEANDER-LINE TRANSFORMER TABLE
CAPACITANCES NORMALIZED TO 376.7/SQRT(EPSR)
COUPLING = 10 TO 16 DB
BANDWIDTH = 6.00/1.

RL/RG	CG1/E	CG2/E	CM12/E	VSWR
1.0	.7321	.7315	.3193	1.000
1.1	.7183	.6935	.2903	1.054
1.2	.7083	.6644	.2635	1.102
1.3	.7849	.7118	.1419	1.133
1.4	.7683	.6830	.1306	1.164
1.5	.7525	.6545	.1240	1.198
1.6	.7389	.6292	.1170	1.231
1.7	.7255	.6068	.1120	1.262
1.8	.7131	.5851	.1069	1.294
1.9	.7026	.5660	.1037	1.325
2.0	.6884	.5470	.9945E-01	1.352
2.2	.6685	.5177	.9376E-01	1.404
2.4	.6521	.4910	.8748E-01	1.458
2.6	.6358	.4668	.8287E-01	1.513

Table II-1 (Continued)

PROGRAM BY
E.G. CRISTAL
OCTOBER 1971

2 SECTION MEANDER-LINE TRANSFORMER TABLE
CAPACITANCES NORMALIZED TO 376.7/SQRT(EPSR)
COUPLING = 10 TO 16 DB
BANDWIDTH = 10.00/1.

RL/RG	CG1/E	CG2/E	CM12/E	VSWR
1.0	.7624	.7629	.2740	1.001
1.1	.7594	.7244	.2432	1.004
1.2	.8004	.7468	.1544	1.184
1.3	.7784	.7141	.1439	1.275
1.4	.7587	.6993	.1369	1.344
1.5	.7372	.6569	.1329	1.451
1.6	.7195	.6251	.1273	1.540

PROGRAM BY
E.G. CRISTAL
OCTOBER 1971

3 SECTION MEANDER-LINE TRANSFORMER TABLE
CAPACITANCES NORMALIZED TO 376.7/SQRT(EPSR)
COUPLING = 10 TO 16 DB
BANDWIDTH = 1.50/1.

RL/RG	CG1/E	CG2/E	CG3/E	CM12/E	CM23/E	VSWR
1.0	.7836	.6132	.7836	.2604	.2604	1.002
1.1	.7749	.6025	.7483	.2560	.2278	1.005
1.2	.7646	.5937	.7185	.2604	.1896	1.028
1.3	.7542	.5849	.6882	.2521	.1595	1.012
1.4	.7665	.5328	.5892	.2487	.2114	1.017
1.5	.7638	.5283	.5662	.2493	.2028	1.023
1.6	.7425	.5142	.5532	.2019	.1595	1.015
1.7	.7246	.4959	.5241	.2035	.1458	1.013
1.8	.72[illegible]	.4934	.5099	.2093	.1395	1.015
1.9	.7221	.4866	.4883	.1874	.1180	1.012
2.0	.7165	.4793	.4752	.1990	.1157	1.014
2.2	.7160	.4697	.4414	.1664	.8976E-01	1.015
2.4	.7170	.4663	.4222	.1720	.8246E-01	1.019
2.6	.7412	.4646	.3905	.1272	.8078E-01	1.018
2.8	.7410	.4574	.3714	.1288	.7565E-01	1.026
3.0	.7292	.4409	.3505	.1181	.6216E-01	1.017
3.5	.7289	.4062	.3028	.1116	.6821E-01	1.034
4.0	.7039	.3694	.2584	.9137E-01	.7333E-01	1.035
4.5	.6982	.3517	.2384	.8841E-01	.6256E-01	1.033
5.0	.6658	.3314	.2237	.9605E-01	.5327E-01	1.042
6.0	.6575	.2992	.1852	.8165E-01	.4971E-01	1.036
7.0	.6502	.2871	.1669	.7425E-01	.4751E-01	1.053
8.0	.6313	.2614	.1470	.7340E-01	.3864E-01	1.049
9.0	.6096	.2451	.1342	.7347E-01	.3519E-01	1.044
10.0	.6023	.2304	.1214	.7058E-01	.3528E-01	1.049
20.0	.5288	.1614	.6837E-01	.5348E-01	.1827E-01	1.088

Table II-1 (Continued)

PROGRAM BY
E.G. CRISTAL
OCTOBER 1971

3 SECTION MEANDER-LINE TRANSFORMER TABLE
CAPACITANCES NORMALIZED TO 376.7/SQRT(EPSR)
COUPLING = 10 TO 16 DB
BANDWIDTH = 2.00/1.

RL/RG	CG1/E	CG2/E	CG3/E	CM12/E	CM23/E	VSWR
1.0	.7713	.5951	.7713	.2737	.2737	1.001
1.1	.7488	.5688	.7233	.2756	.2455	1.011
1.2	.7285	.5476	.6861	.2788	.2163	1.017
1.3	.7129	.5294	.6487	.2707	.1884	1.031
1.4	.7031	.5173	.6219	.2700	.1735	1.031
1.5	.6897	.5024	.5947	.2690	.1566	1.037
1.6	.6791	.4901	.569	.2642	.1433	1.043
1.7	.6712	.4784	.5465	.2598	.1296	1.052
1.7	.6735	.4551	.5293	.2559	.1556	1.053
1.8	.6674	.4542	.5061	.2450	.1492	1.058
1.9	.6581	.4415	.4859	.2403	.1439	1.063
2.0	.6705	.4432	.4649	.2099	.1307	1.064
2.2	.6602	.4271	.4358	.2098	.1222	1.071
2.4	.6652	.4137	.4007	.1775	.1176	1.079
2.6	.7128	.4112	.3564	.1034	.1269	1.077
2.8	.7048	.4014	.3394	.9985E-01	.1135	1.086
3.0	.6957	.3959	.3206	.1059	.1021	1.092
3.5	.6851	.3809	.3019	.9751E-01	.7284E-01	1.099
4.0	.6754	.3744	.2774	.9178E-01	.5041E-01	1.106
4.5	.6576	.3461	.2482	.8239E-01	.3772E-01	1.118
5.0	.6537	.3377	.2316	.7490E-01	.4764E-01	1.123
6.0	.6313	.3054	.1974	.7277E-01	.4490E-01	1.142
7.0	.6021	.2753	.1723	.6913E-01	.4157E-01	1.158
8.0	.5959	.2661	.1581	.6057E-01	.3552E-01	1.169
9.0	.5834	.2534	.1450	.6334E-01	.3080E-01	1.181
10.0	.5678	.2244	.1324	.6145E-01	.2942E-01	1.201
20.0	.5325	.1414	.7604E-01	.3326E-01	.1784E-01	1.320

Table II-1 (Continued)

PROGRAM BY
E.G. CRISTAL
OCTOBER 1971

3 SECTION MEANDER-LINE TRANSFORMER TABLE
CAPACITANCES NORMALIZED TO 376.7/SQRT(EPSR)
COUPLING = 10 TO 16 DB
BANDWIDTH = 3.00/1.

AL/WG	CG1/E	CG2/E	CG3/E	CM12/E	CM23/E	VSWR
1.0	.8038	.6407	.7350	.1334	.3056	1.028
1.1	.8485	.6205	.6973	.1403	.2857	1.025
1.2	.8203	.5877	.6516	.1406	.2617	1.051
1.3	.8089	.5732	.6215	.1358	.2361	1.078
1.4	.7895	.5556	.5962	.1387	.2153	1.096
1.5	.7759	.5415	.5701	.1352	.1999	1.114
1.6	.7661	.5326	.5484	.1250	.1783	1.129
1.7	.7573	.5265	.5324	.1235	.1605	1.145
1.8	.7504	.5208	.5171	.1176	.1434	1.157
1.9	.7406	.5144	.5035	.1150	.1277	1.167
2.0	.7275	.5185	.5036	.1221	.1004	1.173
2.2	.7230	.5161	.4659	.1105	.8817E-01	1.220
2.4	.7109	.4828	.4387	.1020	.8543E-01	1.226
2.6	.6991	.4701	.4175	.9746E-01	.7481E-01	1.240
2.8	.6917	.4566	.3957	.9516E-01	.7181E-01	1.268
3.0	.6766	.4362	.3736	.9228E-01	.7028E-01	1.286
3.5	.6519	.4075	.3342	.8588E-01	.6191E-01	1.326
4.0	.6302	.3757	.2941	.7795E-01	.5389E-01	1.391
4.5	.6142	.3608	.2765	.7626E-01	.5126E-01	1.414
5.0	.5979	.3413	.2542	.7155E-01	.4736E-01	1.457
6.0	.5708	.3125	.2217	.6851E-01	.4117E-01	1.550

Table II-1 (Continued)

PROGRAM BY
E.G. CRISTAL
OCTOBER 1971

3 SECTION MEANDER-LINE TRANSFORMER TABLE
CAPACITANCES NORMALIZED TO 376.7/SQRT(EPSR)
COUPLING = 10 TO 16 DB
BANDWIDTH = 4.00/1.

RL/RG	CG1/E	CG2/E	CG3/E	CM12/E	CM23/E	VSWR
1.0	.8182	.6111	.7584	.1583	.2353	1.130
1.1	.8177	.6287	.734.	.1747	.2307	1.048
1.2	.8181	.6156	.6948	.1633	.1975	1.103
1.3	.786	.597H	.6666	.1577	.1845	1.124
1.4	.7754	.5883	.641	.1453	.1591	1.158
1.5	.7691	.5831	.6186	.1388	.1384	1.197
1.6	.7537	.5773	.6057	.1321	.1195	1.208
1.7	.7456	.57n5	.5861	.1231	.1049	1.232
1.8	.7401	.5607	.5625	.1161	.9979E-01	1.262
1.9	.7286	.5416	.5395	.1132	.9887E-01	1.287
2.0	.7215	.535(	.5252	.1078	.9145E-01	1.305
2.2	.7063	.511H	.4897	.1019	.8605E-01	1.358
2.4	.6886	.4915	.4608	.9808E-01	.8002E-01	1.403
2.6	.6738	.4754	.4369	.9518E-01	.7495E-01	1.445
2.8	.6645	.4632	.4179	.9167E-01	.7064E-01	1.482
3.0	.6503	.4455	.3959	.8835E-01	.6767E-01	1.529

PROGRAM BY
E.G. CRISTAL
OCTOBER 1971

3 SECTION MEANDER-LINE TRANSFORMER TABLE
CAPACITANCES NORMALIZED TO 376.7/SQRT(EPSR)
COUPLING = 10 TO 16 DB
BANDWIDTH = 5.00/1.

RL/RG	CG1/E	CG2/E	CG3/E	CM12/E	CM23/E	VSWR
1.0	.8635	.6376	.737H	.1516	.3167	1.002
1.1	.8126	.613(	.7198	.1799	.2538	1.060
1.2	.7967	.5976	.6848	.1681	.2281	1.115
1.3	.7813	.586H	.6567	.1524	.2017	1.164
1.4	.7588	.5771	.6426	.1569	.1671	1.211
1.5	.7626	.596H	.6403	.1326	.1228	1.246
1.6	.7527	.5895	.6189	.1233	.111H	1.282
1.7	.7390	.5692	.5906	.1202	.1093	1.326
1.8	.7300	.5601	.5719	.1137	.1016	1.361
1.9	.7184	.5454	.5584	.1100	.9895E-01	1.399
2.0	.7075	.5341	.5344	.1072	.9346E-01	1.433
2.2	.6908	.512H	.4999	.1002	.8686E-01	1.507

Table II-1 (Continued)

PROGRAM BY
E.G. CRISTAL
OCTOBER 1971

3 SECTION MEANDER-LINE TRANSFORMER TABLE
CAPACITANCES NORMALIZED TO 376.7/SQRT(EPSR)
COUPLING = 10 TO 16 DB
BANDWIDTH = 6.00/1.

RL/RG	CG1/E	CG2/E	CG3/E	CM12/E	CM23/E	VSWR
1.0	.8405	.6499	.7756	.1723	.2609	1.015
1.1	.8222	.6314	.7319	.1661	.2381	1.068
1.2	.8046	.6134	.6937	.1541	.2120	1.134
1.3	.7927	.6041	.6669	.1415	.1870	1.194
1.4	.7753	.6108	.6676	.1409	.1375	1.246
1.5	.7617	.6057	.6493	.1286	.1207	1.292
1.6	.7501	.5900	.6196	.1242	.1138	1.351
1.7	.7357	.5758	.5991	.1185	.1073	1.396
1.8	.7194	.5561	.5757	.1157	.1039	1.446
1.9	.7100	.5459	.5576	.1099	.9856E-01	1.492
2.0	.6978	.5328	.5399	.1079	.9487E-01	1.539

PROGRAM BY
E.G. CRISTAL
OCTOBER 1971

3 SECTION MEANDER-LINE TRANSFORMER TABLE
CAPACITANCES NORMALIZED TO 376.7/SQRT(EPSR)
COUPLING = 10 TO 16 DB
BANDWIDTH = 8.00/1.

RL/RG	CG1/E	CG2/E	CG3/E	CM12/E	CM23/E	VSWR
1.0	.7992	.6414	.7926	.2315	.2412	1.025
1.1	.7840	.6171	.7484	.2117	.1996	1.086
1.2	.7681	.6075	.7217	.2049	.1781	1.160
1.3	.7902	.6222	.6903	.1457	.1587	1.231
1.4	.7718	.6197	.6673	.1393	.1375	1.301
1.5	.7580	.6019	.6482	.1316	.1239	1.367
1.6	.7432	.5854	.6228	.1237	.1143	1.434
1.7	.7311	.5746	.6054	.1188	.1082	1.498
1.8	.7133	.5589	.5834	.1164	.1028	1.562

PROGRAM BY
E.G. CRISTAL
OCTOBER 1971

3 SECTION MEANDER-LINE TRANSFORMER TABLE
CAPACITANCES NORMALIZED TO 376.7/SQRT(EPSR)
COUPLING = 10 TO 16 DB
BANDWIDTH = 10.00/1.

RL/RG	CG1/E	CG2/E	CG3/E	CM12/E	CM23/E	VSWR
1.0	.8361	.6709	.8014	.1822	.2268	1.004
1.1	.8174	.6514	.7592	.1733	.2009	1.086
1.2	.8017	.6383	.7266	.1615	.1702	1.171
1.3	.7887	.6314	.7005	.1478	.1449	1.253
1.4	.7769	.6243	.6788	.1360	.1248	1.331
1.5	.7563	.6010	.6484	.1329	.1221	1.409
1.6	.7364	.5905	.6208	.1265	.1142	1.485
1.7	.7260	.5694	.6010	.1202	.1119	1.560

Table II-1 (Continued)

PROGRAM BY
E.G. CRISTAL
OCTOBER 1971

4 SECTION MEANDER-LINE TRANSFORMER TABLE
CAPACITANCES NORMALIZED TO 376.7/SQRT(EPSR)
COUPLING = 10 TO 16 DB
BANDWIDTH = 1.50/1.

RL/RG	CG1/E	CG2/E	CG3/E	CG4/E	CM12/E	CM23/E	CM34/E	VSWR
1.0	.8161	.7046	.7046	.8161	.2167	.1598	.2167	1.002
1.1	.8139	.6858	.6919	.7889	.1970	.1583	.1469	1.001
1.2	.8088	.6741	.6640	.7275	.1970	.1315	.1360	1.001
1.3	.8327	.6462	.6059	.6851	.1593	.1765	.1197	1.001
1.4	.8236	.6420	.5752	.6237	.1599	.1449	.1297	1.003
1.5	.8241	.6278	.5497	.5847	.1488	.1439	.1177	1.002
1.6	.8154	.6117	.5299	.5588	.1517	.1395	.1088	1.002
1.7	.8116	.6042	.5083	.5240	.1492	.1280	.1091	1.002
1.8	.8029	.5915	.4878	.4938	.1521	.1205	.1081	1.002
1.9	.7945	.5769	.4727	.4728	.1539	.1171	.9923E-01	1.002
2.0	.7954	.5695	.4617	.4566	.1533	.1228	.9287E-01	1.003
2.2	.7916	.5593	.4291	.4099	.1454	.1055	.9533E-01	1.003
2.4	.7796	.5443	.4104	.3854	.1555	.1017	.8283E-01	1.004
2.6	.7682	.5225	.3918	.3484	.1521	.9323E-01	.8765E-01	1.005
2.8	.7673	.4981	.3622	.3338	.1433	.1083	.7231E-01	1.005
3.0	.7626	.4961	.3496	.3109	.1401	.9122E-01	.7068E-01	1.004
3.5	.7521	.4741	.3158	.2684	.1373	.8080E-01	.6488E-01	1.005
4.0	.7509	.4637	.2986	.2405	.1345	.7618E-01	.5735E-01	1.006
4.5	.7318	.4360	.2715	.2153	.1353	.6989E-01	.5070E-01	1.006
5.0	.7302	.4236	.2525	.1950	.1300	.6823E-01	.4883E-01	1.007
6.0	.7209	.4048	.2300	.1677	.1295	.6351E-01	.4111E-01	1.008
7.0	.7146	.3840	.2062	.1453	.1178	.5690E-01	.3534E-01	1.009
8.0	.6982	.3631	.1881	.1282	.1214	.5350E-01	.3292E-01	1.010
9.0	.6948	.3491	.1741	.1158	.1132	.5173E-01	.2905E-01	1.010
10.0	.6768	.3318	.1630	.1057	.1186	.4984E-01	.2688E-01	1.011
20.0	.6929	.3020	.1148	.5905E-01	.9002E-01	.3798E-01	.1606E-01	1.029

Table II-1 (Continued)

PROGRAM BY
E.G. CRISTAL
OCTOBER 1971

4 SECTION MEANDER-LINE TRANSFORMER TABLE
CAPACITANCES NORMALIZED TO 376.7/SQRT(EPSR)
COUPLING = 10 TO 16 DB
BANDWIDTH = 2.00/1.

WL/WG	CG1/E	CG2/E	CG3/E	CG4/E	CM12/E	CM23/E	CM34/E	VSWR
1.0	.8365	.7172	.7233	.8436	.1818	.1559	.1731	1.000
1.1	.8379	.6955	.6725	.7732	.1658	.1575	.1626	1.003
1.2	.8232	.6677	.6357	.7165	.1713	.1527	.1510	1.005
1.3	.8208	.6539	.6059	.6685	.1622	.1448	.1399	1.008
1.4	.8157	.6480	.5826	.6290	.1587	.1372	.1276	1.009
1.5	.8129	.6315	.5635	.5942	.1530	.1273	.1179	1.011
1.6	.8056	.6166	.5495	.5593	.1530	.1224	.1143	1.014
1.7	.7977	.6024	.5146	.5248	.1531	.1167	.1152	1.016
1.8	.7980	.5900	.4951	.5013	.1454	.1188	.1069	1.017
1.9	.7917	.5816	.4839	.4801	.1463	.1113	.9929E-01	1.019
2.0	.7894	.5734	.4682	.4582	.1424	.1072	.9580E-01	1.020
2.2	.7817	.5499	.4363	.4204	.1380	.1070	.8947E-01	1.023
2.4	.7735	.5338	.4123	.3883	.1350	.1009	.8404E-01	1.026
2.6	.7671	.5208	.3938	.3626	.1325	.9512E-01	.7754E-01	1.028
2.8	.7656	.5105	.3756	.3395	.1259	.9115E-01	.7321E-01	1.030
3.0	.7586	.4940	.3580	.3190	.1273	.8977E-01	.6975E-01	1.033
3.5	.7441	.4681	.3236	.2778	.1212	.8265E-01	.6209E-01	1.038
4.0	.7331	.4482	.2985	.2470	.1178	.7540E-01	.5542E-01	1.042
4.5	.7278	.4333	.2778	.2231	.1113	.7015E-01	.4994E-01	1.045
5.0	.7165	.4183	.2592	.2031	.1102	.6684E-01	.4623E-01	1.050
6.0	.7044	.3920	.2317	.1731	.1035	.5934E-01	.3950E-01	1.055
7.0	.6992	.3705	.2106	.1514	.1010	.5464E-01	.3442E-01	1.062
8.0	.6798	.3532	.1934	.1347	.9687E-01	.5097E-01	.3099E-01	1.067
9.0	.6717	.3384	.1787	.1212	.9219E-01	.4813E-01	.2832E-01	1.072
10.0	.6698	.3295	.1685	.1110	.8795E-01	.4514E-01	.2567E-01	1.074
20.0	.6197	.2545	.1085	.6054E-01	.7259E-01	.3099E-01	.1468E-01	1.111

Table II-1 (Continued)

PROGRAM BY
E.G. CRISTAL
OCTOBER 1971

4 SECTION MEANDER-LINE TRANSFORMER TABLE
CAPACITANCES NORMALIZED TO 376.7/SQRT(EPSR)
COUPLING = 10 10 16 DB
BANDWIDTH = 3.00/1.

RL/RG	CG1/E	CG2/E	CG3/E	CG4/E	CM12/E	CM23/E	CM34/E	VSWR
1.0	.8551	.7455	.7433	.8526	.1591	.1388	.1621	1.000
1.1	.8269	.6817	.6693	.7761	.1755	.1659	.1638	1.014
1.2	.8122	.6666	.6516	.7287	.1772	.1440	.1430	1.027
1.3	.8151	.6589	.6209	.6789	.1584	.1344	.1360	1.039
1.4	.8114	.6421	.5926	.6391	.1503	.1329	.1264	1.050
1.5	.8062	.6294	.5696	.6026	.1443	.1257	.1194	1.060
1.6	.7979	.6147	.5483	.5704	.1423	.1202	.1139	1.068
1.7	.7941	.6043	.5297	.5424	.1363	.1151	.1079	1.075
1.8	.7864	.5908	.5128	.5178	.1351	.1116	.1021	1.082
1.9	.7832	.5821	.4973	.4948	.1303	.1070	.9729E-01	1.089
2.0	.7757	.5699	.4826	.4744	.1298	.1041	.9295E-01	1.095
2.2	.7662	.5516	.4562	.4382	.1247	.9820E-01	.8567E-01	1.107
2.4	.7566	.5351	.4334	.4076	.1213	.9283E-01	.7974E-01	1.118
2.6	.7484	.5203	.4134	.3814	.1176	.8843E-01	.7439E-01	1.129
2.8	.7406	.5068	.3955	.3587	.1144	.8477E-01	.6980E-01	1.139
3.0	.7337	.4946	.3796	.3386	.1109	.8138E-01	.6580E-01	1.148
3.5	.7171	.4678	.3469	.2987	.1057	.7480E-01	.5730E-01	1.168
4.0	.7022	.4465	.3208	.2672	.1022	.6816E-01	.5172E-01	1.189
4.5	.6900	.4274	.2985	.2421	.9734E-01	.6390E-01	.4710E-01	1.208
5.0	.6794	.4112	.2800	.2219	.9314E-01	.6037E-01	.4323E-01	1.223
6.0	.6600	.3841	.2514	.1913	.8787E-01	.5481E-01	.3697E-01	1.255
7.0	.6452	.3633	.2293	.1686	.8227E-01	.5040E-01	.3254E-01	1.283
8.0	.6300	.3451	.2114	.1510	.7877E-01	.4667E-01	.2944E-01	1.310
9.0	.6183	.3305	.1973	.1373	.7525E-01	.4372E-01	.2678E-01	1.334
10.0	.6077	.3179	.1857	.1262	.7278E-01	.4122E-01	.2463E-01	1.358
20.0	.5429	.2507	.1263	.7344E-01	.5083E-01	.2738E-01	.1443E-01	1.550

Table II-1 (Continued)

PROGRAM BY
E.G. CRISTAL
OCTOBER 1971

4 SECTION MEANDER-LINE TRANSFORMER TABLE
CAPACITANCES NORMALIZED TO 376.7/SQRT(EPSR)
COUPLING = 10 TO 16 DB
BANDWIDTH = 4.00/1.

WL/RG	CG1/E	CG2/E	CG3/E	CG4/E	CM12/E	CM23/E	CM34/E	VSWR
1.0	.8179	.7126	.7265	.8339	.2054	.1393	.1851	1.000
1.1	.8052	.6800	.6870	.7802	.1985	.1435	.1623	1.028
1.2	.8185	.6730	.6514	.7313	.1614	.1445	.1467	1.052
1.3	.8143	.6618	.6217	.6816	.1481	.1328	.1425	1.074
1.4	.8048	.6433	.6014	.6486	.1438	.1283	.1261	1.095
1.5	.7993	.6324	.5771	.6099	.1358	.1191	.1234	1.115
1.6	.7886	.6139	.5590	.5835	.1351	.1174	.1115	1.134
1.7	.7831	.6034	.5426	.5569	.1300	.1111	.1043	1.152
1.8	.7746	.5899	.5253	.5320	.1282	.1075	.9950E-01	1.170
1.9	.7676	.5788	.5094	.5097	.1248	.1039	.9524E-01	1.185
2.0	.7607	.5681	.4949	.4896	.1219	.1005	.9115E-01	1.199
2.2	.7482	.5489	.4698	.4554	.1167	.9508E-01	.8312E-01	1.224
2.4	.7363	.5313	.4471	.4253	.1125	.9014E-01	.7739E-01	1.249
2.6	.7254	.5159	.4274	.3998	.1089	.8598E-01	.7249E-01	1.272
2.8	.7155	.5021	.4096	.3769	.1056	.8204E-01	.6856E-01	1.294
3.0	.7065	.4893	.3941	.3573	.1027	.7867E-01	.6471E-01	1.315
3.5	.6872	.4641	.3633	.3180	.9690E-01	.7065E-01	.5649E-01	1.363
4.0	.6691	.4407	.3369	.2871	.9270E-01	.6626E-01	.5078E-01	1.410
4.5	.6522	.4197	.3133	.2612	.8825E-01	.6200E-01	.4679E-01	1.455
5.0	.6384	.4028	.2951	.2409	.8442E-01	.5859E-01	.4294E-01	1.495
6.0	.6176	.3794	.2692	.2108	.7994E-01	.5229E-01	.3727E-01	1.572

Table II-1 (Continued)

PROGRAM BY
E.G. CRISTAL
OCTOBER 1971

4 SECTION MEANDER-LINE TRANSFORMER TABLE
CAPACITANCES NORMALIZED TO 376.7/SQRT(EPSR)
COUPLING = 10 TO 16 DB
BANDWIDTH = 5.00/1.

RL/RG	CG1/E	CG2/E	CG3/E	CG4/E	CM12/E	CM23/E	CM34/E	VSWR
1.0	.8285	.7028	.7194	.8481	.1924	.1675	.1679	1.000
1.1	.8332	.6879	.6805	.7907	.1641	.1662	.1491	1.046
1.2	.8232	.6805	.6576	.7361	.1536	.1406	.1425	1.083
1.3	.8084	.6612	.6296	.6896	.1498	.1298	.1376	1.115
1.4	.8026	.6466	.6086	.6562	.1381	.1250	.1240	1.144
1.5	.7893	.6283	.5853	.6213	.1356	.1191	.1193	1.173
1.6	.7802	.6130	.5673	.5942	.1306	.1150	.1100	1.200
1.7	.7709	.6001	.5505	.5679	.1269	.1095	.1041	1.226
1.8	.7623	.5872	.5333	.5442	.1228	.1060	.9907E-01	1.251
1.9	.7535	.5759	.5177	.5219	.1204	.1016	.9513E-01	1.277
2.0	.7458	.5646	.5029	.5021	.1178	.9889E-01	.9099E-01	1.303
2.2	.7307	.5446	.4776	.4679	.1126	.9323E-01	.8403E-01	1.347
2.4	.7175	.5269	.4559	.4393	.1081	.8867E-01	.7783E-01	1.388
2.6	.7046	.5109	.4366	.4143	.1043	.8448E-01	.7254E-01	1.427
2.8	.6925	.4963	.4191	.3923	.1010	.8080E-01	.6799E-01	1.464
3.0	.6813	.4830	.4032	.3726	.9791E-01	.7754E-01	.6409E-01	1.500

PROGRAM BY
E.G. CRISTAL
OCTOBER 1971

4 SECTION MEANDER-LINE TRANSFORMER TABLE
CAPACITANCES NORMALIZED TO 376.7/SQRT(EPSR)
COUPLING = 10 TO 16 DB
BANDWIDTH = 6.00/1.

RL/RG	CG1/E	CG2/E	CG3/E	CG4/E	CM12/E	CM23/E	CM34/E	VSWR
1.0	.8587	.7382	.7338	.8536	.1548	.1535	.1611	1.000
1.1	.8239	.6902	.6897	.7911	.1736	.1524	.1502	1.056
1.2	.8214	.6799	.6552	.7340	.1563	.1403	.1467	1.107
1.3	.8079	.6584	.6297	.6950	.1466	.1348	.1340	1.150
1.4	.7951	.6416	.6091	.6597	.1414	.1262	.1244	1.191
1.5	.7845	.6266	.5892	.6281	.1334	.1193	.1170	1.228
1.6	.7734	.6115	.5703	.5992	.1293	.1139	.1113	1.265
1.7	.7631	.5975	.5538	.5746	.1252	.1096	.1046	1.300
1.8	.7528	.5847	.5375	.5515	.1212	.1050	.9980E-01	1.334
1.9	.7427	.5726	.5223	.5306	.1180	.1010	.9556E-01	1.366
2.0	.7334	.5611	.5083	.5121	.1152	.9874E-01	.9146E-01	1.399
2.2	.7168	.5403	.4836	.4791	.1100	.9297E-01	.8406E-01	1.461
2.4	.7011	.5215	.4612	.4502	.1061	.8853E-01	.7871E-01	1.521

Table II-1 (Continued)

PROGRAM BY
E.G. CRISTAL
OCTOBER 1971

4 SECTION MEANDER-LINE TRANSFORMER TABLE
CAPACITANCES NORMALIZED TO 376.7/SQRT(EPSR)
COUPLING = 10 TO 16 DB
BANDWIDTH = 8.00/1.

RL/RG	CG1/E	CG2/E	CG3/E	CG4/E	CM12/E	CM23/E	CM34/E	VSWR
1.0	.8545	.7397	.7481	.8642	.1598	.1462	.1481	1.000
1.1	.8215	.6916	.6875	.7862	.1748	.1484	.1576	1.071
1.2	.8190	.6786	.6563	.7371	.1537	.1408	.1459	1.137
1.3	.8052	.6589	.6319	.6968	.1483	.1329	.1336	1.201
1.4	.7902	.6411	.6106	.6621	.1414	.1239	.1259	1.257
1.5	.7770	.6238	.5903	.6319	.1346	.1187	.1190	1.312
1.6	.7644	.6084	.5728	.6051	.1294	.1138	.1129	1.365
1.7	.7520	.5932	.5566	.5819	.1248	.1097	.1064	1.416
1.8	.7398	.5797	.5408	.5601	.1211	.1059	.1017	1.466
1.9	.7284	.5675	.5265	.5405	.1177	.1022	.9749E-01	1.515

PROGRAM BY
E.G. CRISTAL
OCTOBER 1971

4 SECTION MEANDER-LINE TRANSFORMER TABLE
CAPACITANCES NORMALIZED TO 376.7/SQRT(EPSR)
COUPLING = 10 TO 16 DB
BANDWIDTH = 10.00/1.

RL/RG	CG1/E	CG2/E	CG3/E	CG4/E	CM12/E	CM23/E	CM34/E	VSWR
1.0	.8634	.7548	.7631	.8729	.1490	.1361	.1377	1.000
1.1	.8318	.6932	.6877	.7812	.1654	.1573	.1610	1.062
1.2	.8157	.6752	.6596	.7381	.1560	.1425	.1401	1.155
1.3	.8041	.6592	.6273	.6927	.1465	.1323	.1411	1.229
1.4	.7896	.6402	.6088	.6623	.1412	.1261	.1272	1.300
1.5	.7737	.6216	.5901	.6339	.1358	.1203	.1191	1.369
1.6	.7594	.6052	.5722	.6077	.1303	.1154	.1138	1.431
1.7	.7462	.5901	.5565	.5844	.1260	.1106	.1080	1.495
1.8	.7331	.5755	.5410	.5637	.1222	.1075	.1035	1.556

Table II-1 (Continued)

PROGRAM BY
E.G. CRISTAL
OCTOBER 1971

5 SECTION MEANDER-LINE TRANSFORMER TABLE
CAPACITANCES NORMALIZED TO 376.7/SQRT(EPSR)
COUPLING = 10 TO 16 DB
BANDWIDTH = 2.00/1.

AL/A0	C01/E	C02/E	C03/E	C04/E	C05/E	CM12/E	CM23/E	CM34/E	CM45/E	VSWR
1.0	.8310	.6853	.6719	.6641	.8147	.1867	.1940	.2066	.2091	1.001
2.0	.8080	.5587	.4741	.4097	.4239	.1530	.1952	.1643	.1217	1.008
2.2	.8031	.5553	.4629	.4056	.4087	.1512	.1818	.9680E-01	.8484E-01	1.009
2.4	.7898	.5665	.4625	.3700	.3704	.1604	.1337	.9236E-01	.8527E-01	1.010
2.6	.7895	.5700	.4514	.3494	.3456	.1549	.1144	.8974E-01	.7715E-01	1.010
2.8	.7885	.5651	.4394	.3324	.3241	.1523	.1097	.8509E-01	.7108E-01	1.011
3.0	.7854	.5529	.4212	.3156	.3046	.1484	.1100	.8224E-01	.6623E-01	1.011
3.5	.7802	.5347	.3902	.2804	.2634	.1408	.1022	.7310E-01	.5812E-01	1.012
4.0	.7767	.5211	.3683	.2569	.2341	.1355	.9746E-01	.6558E-01	.4985E-01	1.013
4.5	.7692	.5074	.3493	.2351	.2096	.1346	.9076E-01	.5960E-01	.4546E-01	1.015
5.0	.7620	.4900	.3269	.2120	.1865	.1302	.8624E-01	.5460E-01	.4494E-01	1.017
6.0	.7566	.4732	.3004	.1877	.1596	.1255	.8052E-01	.5053E-01	.3607E-01	1.020
7.0	.7467	.4593	.2809	.1678	.1389	.1256	.7277E-01	.4679E-01	.3160E-01	1.020
8.0	.7352	.4376	.2624	.1530	.1227	.1260	.7362E-01	.4125E-01	.2789E-01	1.023
9.0	.7297	.4272	.2488	.1379	.1098	.1233	.6902E-01	.3805E-01	.2597E-01	1.024
10.0	.7273	.4173	.2328	.1283	.1080	.1171	.6382E-01	.3803E-01	.2294E-01	1.028
20.0	.6943	.3508	.1660	.7736E-01	.5264E-01	.9965E-01	.4912E-01	.2297E-01	.1288E-01	1.040

Table II-1 (Continued)

PROGRAM BY
E.G. CRISTAL
OCTOBER 1971

5 SECTION MEANDER-LINE TRANSFORMER TABLE
CAPACITANCES NORMALIZED TO 376.7/SQRT(EPSR)
COUPLING = 10 TO 16 DB
BANDWIDTH = 3.00/1.

RL/RO	C01/E	C02/E	C03/E	C04/E	C05/E	CM12/E	CM23/E	CM34/E	CM45/E	VSWR
1.0	.7669	.6433	.7038	.6434	.7669	.2758	.1796	.1794	.2758	1.000
1.1	.7687	.6396	.6850	.6273	.7266	.2573	.1648	.1573	.2237	1.008
1.2	.7627	.6315	.6737	.6018	.6752	.2519	.1561	.1333	.2034	1.015
1.3	.7765	.6301	.6461	.5870	.6476	.2301	.1444	.1398	.1520	1.021
1.4	.7717	.6264	.6236	.5682	.6251	.2190	.1360	.1299	.1302	1.027
1.5	.8086	.6467	.5931	.5371	.5859	.1633	.1347	.1261	.1237	1.031
1.6	.8082	.6332	.5822	.5200	.5576	.1565	.1296	.1172	.1116	1.034
1.7	.8066	.6310	.5653	.4973	.5278	.1508	.1252	.1131	.1058	1.038
1.8	.8035	.6225	.5580	.4773	.5011	.1479	.1220	.1085	.1010	1.043
1.9	.8083	.6143	.5398	.4596	.4776	.1456	.1193	.1048	.9593E-01	1.048
2.0	.7967	.6065	.5229	.4433	.4564	.1435	.1161	.1013	.9173E-01	1.050
2.2	.7894	.5871	.4923	.4108	.4182	.1392	.1158	.9884E-01	.8597E-01	1.057
2.4	.7845	.5802	.4800	.3880	.3859	.1360	.1048	.8863E-01	.8043E-01	1.062
2.6	.7782	.5635	.4584	.3660	.3598	.1324	.1060	.8367E-01	.7574E-01	1.067
2.8	.7747	.5584	.4455	.3492	.3377	.1295	.9693E-01	.8016E-01	.6851E-01	1.071
3.0	.7688	.5447	.4288	.3335	.3182	.1279	.9802E-01	.7687E-01	.6405E-01	1.076
3.5	.7567	.5231	.3994	.2994	.2776	.1245	.9062E-01	.6847E-01	.5651E-01	1.087
4.0	.7474	.5044	.3744	.2731	.2461	.1199	.8620E-01	.6213E-01	.5020E-01	1.096
4.5	.7397	.4981	.3541	.2515	.2218	.1160	.8140E-01	.5748E-01	.4504E-01	1.105
5.0	.7341	.4774	.3364	.2342	.2025	.1108	.7708E-01	.5389E-01	.4079E-01	1.111
6.0	.7189	.4518	.3063	.2054	.1720	.1065	.7146E-01	.4787E-01	.3502E-01	1.128
7.0	.7085	.4323	.2840	.1847	.1505	.1030	.6666E-01	.4350E-01	.3038E-01	1.140
8.0	.6962	.4163	.2659	.1682	.1338	.9944E-01	.6277E-01	.3975E-01	.2710E-01	1.153
9.0	.6885	.4038	.2515	.1549	.1204	.9383E-01	.5993E-01	.3654E-01	.2474E-01	1.165
10.0	.6796	.3911	.2386	.1444	.1102	.9354E-01	.5765E-01	.3426E-01	.2236E-01	1.175
8.0	.6211	.3176	.1698	.8968E-01	.6037E-01	.7728E-01	.4135E-01	.2123E-01	.1242E-01	1.256

Table II-1 (Continued)

PROGRAM BY
E.G. CRISTAL
OCTOBER 1971

5 SECTION MEANDER-LINE TRANSFORMER TABLE
CAPACITANCES NORMALIZED TO 376.7/SQRT(EPSR)
COUPLING = 10 TO 16 DB
BANDWIDTH = 4.00/1.

RL/RO	C01/E	C02/E	C03/E	C04/E	C05/E	CM12/E	CM23/E	CM34/E	CM45/E	VSWR
1.0	.8556	.7288	.7312	.7333	.8543	.1588	.1633	.1552	.1603	1.000
1.1	.8368	.6974	.6816	.6648	.7757	.1664	.1643	.1654	.1619	1.017
1.2	.8293	.6863	.6681	.6385	.7226	.1594	.1487	.1409	.1482	1.031
1.3	.8214	.6726	.6419	.6050	.6769	.1554	.1410	.1370	.1352	1.044
1.4	.8160	.6614	.6216	.5772	.6361	.1496	.1360	.1285	.1260	1.056
1.5	.8099	.6496	.6024	.5507	.5987	.1456	.1298	.1217	.1195	1.068
1.6	.8037	.6399	.5865	.5275	.5661	.1430	.1231	.1156	.1135	1.079
1.7	.7983	.6295	.5701	.5067	.5375	.1399	.1194	.1103	.1074	1.090
1.8	.7931	.6202	.5554	.4884	.5125	.1373	.1159	.1056	.1016	1.100
1.9	.7894	.6120	.5436	.4742	.4907	.1345	.1127	.9955E-01	.9486E-01	1.110
2.0	.7833	.6010	.5273	.4561	.4693	.1329	.1118	.9827E-01	.9142E-01	1.119
2.2	.7793	.5858	.5038	.4291	.4338	.1283	.1071	.9213E-01	.8272E-01	1.137
2.4	.7667	.5714	.4841	.4051	.4026	.1254	.1022	.8608E-01	.7664E-01	1.153
2.6	.7595	.5593	.4666	.3846	.3765	.1220	.9783E-01	.8140E-01	.7124E-01	1.165
2.8	.7515	.5467	.4502	.3659	.3534	.1196	.9468E-01	.7711E-01	.6699E-01	1.178
3.0	.7444	.5357	.4356	.3500	.3338	.1177	.9151E-01	.7406E-01	.6276E-01	1.189
3.5	.7297	.5123	.4054	.3170	.2935	.1123	.8520E-01	.6636E-01	.5456E-01	1.214
4.0	.7177	.4930	.3795	.2893	.2618	.1084	.7946E-01	.6084E-01	.4895E-01	1.242
4.5	.7048	.4750	.3593	.2687	.2376	.1040	.7589E-01	.5597E-01	.4395E-01	1.264
5.0	.6947	.4600	.3408	.2504	.2176	.9997E-01	.7214E-01	.5260E-01	.3999E-01	1.284
6.0	.6774	.4358	.3122	.2213	.1861	.9274E-01	.6500E-01	.4623E-01	.3482E-01	1.325
7.0	.6689	.4145	.2899	.2010	.1643	.9010E-01	.6170E-01	.4165E-01	.3027E-01	1.359
8.0	.6475	.3981	.2715	.1838	.1472	.8640E-01	.5764E-01	.3864E-01	.2714E-01	1.395
9.0	.6376	.3852	.2574	.1709	.1338	.8337E-01	.5449E-01	.3576E-01	.2471E-01	1.426
10.0	.6417	.3840	.2580	.1620	.1248	.7807E-01	.5096E-01	.3350E-01	.2280E-01	1.460
20.0	.5801	.3172	.1878	.1083	.7334E-01	.6739E-01	.3268E-01	.2176E-01	.1330E-01	1.723

Table II-1 (Continued)

PROGRAM BY
E.G. CRISTAL
OCTOBER 1971

5 SECTION MEANDER-LINE TRANSFORMER TABLE
CAPACITANCES NORMALIZED TO 376.7/SQRT(EPSR)
COUPLING = 10 TO 10 DB
BANDWIDTH = 5.00/1.

RL/R0	C01/E	C02/E	C03/E	C04/E	C05/E	C12/E	C23/E	C34/E	C45/E	VSWR
1.0	.8332	.7079	.7193	.7149	.6445	.1468	.1662	.1700	.1728	1.001
1.1	.8323	.6984	.6919	.6751	.7807	.1702	.1545	.1566	.1568	1.033
1.2	.8261	.6831	.6636	.6405	.7255	.1607	.1459	.1432	.1453	1.060
1.3	.8195	.6731	.6479	.6121	.6805	.1524	.1382	.1318	.1352	1.081
1.4	.8111	.6595	.6261	.5851	.6422	.1473	.1359	.1255	.1254	1.101
1.5	.8035	.6474	.6175	.5612	.6078	.1425	.1244	.1125	.1171	1.119
1.6	.7962	.6356	.5898	.5394	.5772	.1384	.1218	.1130	.1100	1.136
1.7	.7894	.6247	.5733	.5197	.5432	.1346	.1196	.1083	.1037	1.153
1.8	.7823	.6143	.5586	.5016	.5254	.1319	.1144	.1039	.9854E-01	1.169
1.9	.7765	.6048	.5448	.4849	.5038	.1289	.1106	.9983E-01	.9379E-01	1.184
2.0	.7698	.5952	.5320	.4694	.4825	.1267	.1078	.9710E-01	.8986E-01	1.198
2.2	.7580	.5782	.5085	.4424	.4475	.1229	.1026	.9028E-01	.8161E-01	1.226
2.4	.7482	.5627	.4875	.4186	.4168	.1194	.9893E-01	.8503E-01	.7588E-01	1.255
2.6	.7387	.5493	.4699	.3983	.3908	.1163	.9488E-01	.8037E-01	.7036E-01	1.281
2.8	.7306	.5372	.4539	.3800	.3682	.1132	.9163E-01	.7637E-01	.6603E-01	1.304
3.0	.7214	.5256	.4391	.3636	.3483	.1104	.8796E-01	.7312E-01	.6241E-01	1.326
3.5	.7036	.5022	.4107	.3321	.3085	.1054	.8139E-01	.6483E-01	.5454E-01	1.376
4.0	.6879	.4818	.3843	.3052	.2776	.9960E-01	.7698E-01	.5989E-01	.4881E-01	1.422
4.5	.6721	.4613	.3617	.2817	.2521	.9521E-01	.7262E-01	.5567E-01	.4463E-01	1.468
5.0	.6589	.4455	.3441	.2640	.2324	.9215E-01	.6960E-01	.5196E-01	.4080E-01	1.509

Table II-1 (Continued)

PROGRAM BY
E.G. CRISTAL
OCTOBER 1971

5 SECTION MEANDER-LINE TRANSFORMER TABLE
CAPACITANCES NORMALIZED TO 376.7/SQRT(EPSR)
COUPLING = 10 TO 16 DB
BANDWIDTH = 6.00/1.

RL/RG	C01/E	C02/E	C03/E	C04/E	C05/E	CM12/E	CM23/E	CM34/E	CM45/E	VSWR
1.0	.8171	.6912	.7200	.7054	.8286	.2071	.1737	.1638	.1922	1.000
1.1	.8155	.6872	.6963	.6745	.7783	.1886	.1586	.1545	.1818	1.043
1.2	.8270	.6831	.6669	.6434	.7274	.1575	.1490	.1424	.1456	1.084
1.3	.8176	.6726	.6491	.6167	.6855	.1511	.1368	.1317	.1327	1.116
1.4	.8076	.6578	.6276	.5890	.6461	.1452	.1356	.1244	.1252	1.144
1.5	.7980	.6440	.6081	.5662	.6136	.1406	.1259	.1182	.1166	1.171
1.6	.7894	.6318	.5907	.5458	.5847	.1361	.1272	.1127	.1091	1.196
1.7	.7809	.6200	.5744	.5266	.5582	.1326	.1173	.1080	.1039	1.220
1.8	.7730	.6093	.5599	.5083	.5334	.1289	.1130	.1032	.9865E-01	1.243
1.9	.7652	.5994	.5462	.4924	.5122	.1260	.1092	.9961E-01	.9368E-01	1.265
2.0	.7581	.5898	.5334	.4773	.4923	.1230	.1061	.9603E-01	.8954E-01	1.286
2.2	.7439	.5719	.5111	.4514	.4578	.1195	.1006	.8956E-01	.8242E-01	1.327
2.4	.7318	.5561	.4903	.4284	.4285	.1151	.9586E-01	.8457E-01	.7599E-01	1.366
2.6	.7202	.5416	.4721	.4080	.4030	.1117	.9188E-01	.8014E-01	.7138E-01	1.402
2.8	.7095	.5283	.4556	.3895	.3804	.1085	.8835E-01	.7630E-01	.6705E-01	1.439
3.0	.6996	.5163	.4409	.3731	.3606	.1058	.8539E-01	.7305E-01	.6358E-01	1.474
3.5	.6781	.4901	.4104	.3413	.3213	.1002	.7942E-01	.6572E-01	.5562E-01	1.554

PROGRAM BY
E.G. CRISTAL
OCTOBER 1971

5 SECTION MEANDER-LINE TRANSFORMER TABLE
CAPACITANCES NORMALIZED TO 376.7/SQRT(EPSR)
COUPLING = 10 TO 16 DB
BANDWIDTH = 8.00/1.

RL/RG	C01/E	C02/E	C03/E	C04/E	C05/E	CM12/E	CM23/E	CM34/E	CM45/E	VSWR
1.0	.8555	.7236	.7300	.7484	.8672	.1590	.1735	.1496	.1445	1.000
1.1	.8297	.6951	.6937	.6715	.7732	.1709	.1570	.1517	.1684	1.063
1.2	.8236	.6847	.6721	.6478	.7314	.1557	.1430	.1406	.1458	1.114
1.3	.8135	.6683	.6469	.6172	.6874	.1496	.1372	.1337	.1358	1.168
1.4	.8016	.6534	.6268	.5932	.6528	.1446	.1310	.1257	.1245	1.215
1.5	.7900	.6394	.6085	.5717	.6208	.1390	.1250	.1186	.1169	1.257
1.6	.7787	.6263	.5917	.5520	.5932	.1344	.1198	.1130	.1102	1.298
1.7	.7679	.6138	.5759	.5338	.5683	.1303	.1155	.1081	.1064	1.336
1.8	.7577	.6018	.5611	.5169	.5454	.1267	.1117	.1038	.9972E-01	1.374
1.9	.7474	.5905	.5476	.5012	.5245	.1239	.1079	.9973E-01	.9540E-01	1.411
2.0	.7382	.5798	.5345	.4870	.5060	.1210	.1050	.9694E-01	.9118E-01	1.447
2.2	.7222	.5622	.5126	.4628	.4739	.1158	.9886E-01	.9027E-01	.8362E-01	1.515

Table II-1 (Continued)

PROGRAM BY
E.G. CRISTAL
OCTOBER 1971

5 SECTION MEANDER-LINE TRANSFORMER TABLE
CAPACITANCES NORMALIZED TO 376.7/SQRT(EPSR)
COUPLING = 10 TO 16 DB
BANDWIDTH = 10.00/1.

RL/RO	C01/E	C02/E	C03/E	C04/E	C05/E	CM12/E	CM23/E	CM34/E	CM45/E	VSWR
1.0	.8476	.7345	.7522	.7532	.8477	.1682	.1452	.1434	.1439	1.000
1.1	.8334	.6989	.6950	.6826	.7851	.1665	.1564	.1505	.1530	1.074
1.2	.8255	.6868	.6694	.6493	.7366	.1538	.1433	.1454	.1398	1.140
1.3	.8092	.6651	.6480	.6225	.6927	.1505	.1370	.1327	.1328	1.202
1.4	.7983	.6501	.6255	.5944	.6546	.1441	.1320	.1262	.1265	1.264
1.5	.7848	.6357	.6078	.5730	.6236	.1395	.1257	.1195	.1180	1.321
1.6	.7719	.6219	.5908	.5540	.5972	.1346	.1202	.1137	.1119	1.373
1.7	.7596	.6087	.5752	.5363	.5730	.1303	.1157	.1089	.1064	1.425
1.8	.7476	.5961	.5605	.5200	.5513	.1267	.1115	.1046	.1015	1.476
1.9	.7364	.5841	.5464	.5049	.5317	.1234	.1084	.1011	.9703E-01	1.526

Table II-1 (Continued)

PROGRAM BY
E.G. CRISTAL
OCTOBER 1971

6 SECTION MEANDER-LINE TRANSFORMER TABLE
CAPACITANCES NORMALIZED TO 376.7/SQRT(EPSR)
COUPLING = 10 TO 16 DB
BANDWIDTH = 3.00/1.

RL/HG	CG1/E	CG2/E	CG3/E	CG4/E	CG5/E	CG6/E	CM12/E	CM23/E	CM34/E	CM45/E	CM56/E	VSWR
1.0	.8216	.6677	.6727	.6892	.6888	.6264	.2003	.2094	.1902	.1821	.1915	1.004
1.2	.8440	.6891	.6652	.6525	.6227	.7110	.1581	.1729	.1485	.1420	.1491	1.007
1.4	.8228	.6655	.6309	.5893	.5429	.5094	.1691	.1527	.1396	.1294	.1375	1.013
1.6	.8164	.6557	.6099	.5504	.4991	.5469	.1667	.1381	.1257	.1141	.1106	1.017
1.8	.8163	.6441	.5834	.5127	.4514	.4878	.1579	.1349	.1168	.1070	.1029	1.022
2.0	.8107	.6358	.5646	.4831	.4203	.4455	.1563	.1243	.1111	.9595E-01	.8874E-01	1.025
2.5	.8021	.6048	.5109	.4204	.3471	.3572	.1467	.1218	.9976E-01	.8183E-01	.7881E-01	1.034
3.0	.7956	.5912	.4849	.3810	.3052	.3052	.1424	.1093	.8683E-01	.7049E-01	.6173E-01	1.040
4.0	.7804	.5580	.4300	.3165	.2422	.2334	.1363	.9731E-01	.7849E-01	.5853E-01	.4808E-01	1.052
6.0	.7544	.5097	.3666	.2486	.1767	.1609	.1305	.8697E-01	.6302E-01	.4390E-01	.3343E-01	1.067
8.0	.7512	.4904	.3311	.2112	.1415	.1232	.1146	.7602E-01	.5155E-01	.3435E-01	.2564E-01	1.079
10.0	.7421	.4674	.3030	.1861	.1199	.1007	.1085	.7309E-01	.4597E-01	.2892E-01	.2080E-01	1.092
20.0	.7058	.4080	.2336	.1237	.7103E-01	.5390E-01	.9505E-01	.5377E-01	.3157E-01	.1821E-01	.1121E-01	1.134

Table II-1 (Continued)

PROGRAM BY
E.G. CRISTAL
OCTOBER 1971

6 SECTION REACTIVE-LIVE TRANSFORMER TABLE
CAPACITANCES NORMALIZED TO 376.7/SQRT(EPSR)
COUPLING = 10 TO 16 DB
BANDWIDTH = 4.00/1.

RL/RG	CG1/E	CG2/E	CG3/E	CG4/E	CG5/E	CG6/E	CM12/E	CM23/E	CM34/E	CM45/E	CM56/E	VSWR
1.0	.8480	.7314	.7326	.7235	.7241	.6492	.1679	.1497	.1065	.1025	.1004	1.0062
1.2	.8374	.6959	.6667	.63	.6460	.6118	.1587	.1519	.1000	.1535	.1525	1.0041
1.4	.8210	.6675	.6345	.5979	.5592	.5725	.1608	.1453	.1369	.1251	.1291	1.0037
1.6	.8196	.6598	.6085	.5615	.5043	.5526	.1474	.1298	.1254	.1165	.1137	1.0050
1.8	.8090	.6392	.5792	.5160	.4626	.4968	.1459	.1263	.1174	.1031	.1020	1.0061
2.0	.8019	.6250	.5561	.4867	.4479	.4513	.1424	.1209	.1101	.9625E-01	.9380E-01	1.0072
2.5	.7916	.6005	.5147	.4429	.3886	.3733	.1328	.1090	.9454E-01	.7931E-01	.7192E-01	1.0093
3.0	.7778	.5759	.4792	.3891	.3401	.3160	.1285	.1010	.8537E-01	.6977E-01	.6187E-01	1.1112
4.0	.7563	.5356	.4256	.3299	.2891	.2449	.1215	.9390E-01	.7302E-01	.5857E-01	.4751E-01	1.1144
6.0	.7281	.4895	.3632	.2611	.1921	.1711	.1086	.7903E-01	.5703E-01	.4171E-01	.3296E-01	1.1171
8.0	.7056	.4569	.3245	.2216	.1563	.1330	.1039	.7044E-01	.4942E-01	.3395E-01	.2555E-01	1.1236
10.0	.7020	.4422	.3018	.1983	.1342	.1101	.9324E-01	.6531E-01	.4299E-01	.2890E-01	.2100E-01	1.1269
20.0	.6481	.3777	.2360	.1372	.8370E-01	.5166E-01	.4494E-01	.4860E-01	.2971E-01	.1009E-01	.1183E-01	1.1407

Table II-1 (Continued)

PROGRAM BY
E.G. CRISTAL
OCTOBER 1971

6 SECTION MEANDER-LINE IMPEDANCE TABLE
CAPACITANCES NORMALIZED TO 376.7/SQRT(EPSR)
COUPLING = 10 TO 16 DB
BANDWIDTH = 5.00/1.

RL/RG	CG1/E	CG2/E	CG3/E	CG4/E	CG5/E	CG6/E	CM12/E	CM23/E	CM34/E	CM45/E	CM56/E	VSWR
1.0	.8244	.7145	.7179	.7050	.6743	.7985	.1937	.1548	.1761	.1705	.2297	1.004
1.2	.8279	.6925	.6774	.6543	.6388	.7255	.1647	.1456	.1514	.1384	.1390	1.042
1.4	.8209	.6725	.6399	.6097	.5694	.6316	.1536	.1402	.1328	.1234	.1238	1.076
1.6	.8108	.6526	.6102	.5815	.5454	.5628	.1462	.1296	.1215	.1116	.1098	1.100
1.8	.8010	.6350	.5831	.5561	.4775	.5089	.1457	.1226	.1129	.1023	.9800E-01	1.121
2.0	.7915	.6190	.5590	.4974	.4448	.4851	.1364	.1173	.1068	.9318E-01	.8884E-01	1.139
2.5	.7734	.5861	.5123	.4414	.3819	.3847	.1279	.1068	.9277E-01	.7818E-01	.7104E-01	1.181
3.0	.7568	.5592	.4748	.3968	.3346	.3283	.1210	.9886E-01	.8381E-01	.6938E-01	.6098E-01	1.218
4.0	.7312	.5209	.4242	.3387	.2736	.2569	.1159	.8727E-01	.7030E-01	.5574E-01	.4725E-01	1.277
6.0	.6915	.4688	.3634	.2725	.2071	.1829	.1108	.7483E-01	.5474E-01	.4143E-01	.3324E-01	1.372
8.0	.6661	.4380	.3242	.2373	.1710	.1444	.9352E-01	.6721E-01	.4792E-01	.3396E-01	.2604E-01	1.460
10.0	.6443	.4097	.2966	.2064	.1489	.1204	.8858E-01	.6147E-01	.4247E-01	.2947E-01	.2169E-01	1.535

Table II-1 (Continued)

PROGRAM BY
E.G. CRISTAL
OCTOBER 1971

6 SECTION MEANDER-LINE TRANSFORMER TABLE
CAPACITANCES NORMALIZED TO 376.7/SQRT(EPSR)
COUPLING = 10 TO 16 DB
BANDWIDTH = 6.00/1.

RL/RG	CG1/E	CG2/E	CG3/E	CG4/E	CG5/E	CG6/E	CM12/E	CM23/E	CM34/E	CM45/E	CM56/E	VSWR
1.0	.8474	.7198	.7407	.7527	.7494	.8883	.1696	.1663	.1385	.1494	.1433	1.000
1.2	.8274	.6857	.6759	.6586	.6375	.7248	.1634	.1525	.1443	.1418	.1429	1.060
1.4	.8184	.6699	.6417	.6055	.5735	.6361	.1495	.1361	.1314	.1246	.1239	1.112
1.6	.8035	.6471	.6096	.5656	.5259	.5699	.1436	.1279	.1203	.1109	.1087	1.150
1.8	.7912	.6282	.5836	.5324	.4883	.5186	.1377	.1208	.1104	.1005	.9599E-01	1.182
2.0	.7813	.6124	.5601	.5042	.4559	.4757	.1317	.1147	.1034	.9248E-01	.8689E-01	1.211
2.5	.7585	.5778	.5140	.4501	.3934	.3945	.1222	.1031	.8943E-01	.7681E-01	.7226E-01	1.277
3.0	.7372	.5479	.4757	.4060	.3486	.3399	.1147	.9520E-01	.8161E-01	.6920E-01	.6127E-01	1.336
4.0	.7073	.5103	.4292	.3507	.2879	.2694	.1067	.8338E-01	.6714E-01	.5563E-01	.4821E-01	1.435
6.0	.6706	.4651	.3696	.2843	.2231	.1965	.9315E-01	.6942E-01	.5472E-01	.4283E-01	.3453E-01	1.607

PROGRAM BY
E.G. CRISTAL
OCTOBER 1971

6 SECTION MEANDER-LINE TRANSFORMER TABLE
CAPACITANCES NORMALIZED TO 376.7/SQRT(EPSR)
COUPLING = 10 TO 16 DB
BANDWIDTH = 8.00/1.

RL/RG	CG1/E	CG2/E	CG3/E	CG4/E	CG5/E	CG6/E	CM12/E	CM23/E	CM34/E	CM45/E	CM56/E	VSWR
1.0	.8214	.6929	.7073	.7135	.7165	.8412	.2124	.1727	.1804	.1637	.1764	1.001
1.2	.8278	.6874	.6753	.6586	.6381	.7238	.1669	.1483	.1472	.1412	.1464	1.099
1.4	.8099	.6632	.6402	.6112	.5832	.6446	.1471	.1334	.1290	.1232	.1241	1.172
1.6	.7938	.6404	.6088	.5749	.5368	.5805	.1395	.1251	.1181	.1107	.1079	1.245
1.8	.7773	.6195	.5820	.5385	.5004	.531	.1322	.1168	.1088	.1009	.9651E-01	1.301
2.0	.7618	.5998	.5586	.5096	.4685	.4897	.1276	.1107	.1017	.9379E-01	.8808E-01	1.356
2.5	.7304	.5647	.5107	.4561	.4094	.4127	.1143	.9861E-01	.8869E-01	.7869E-01	.7304E-01	1.477
3.0	.7015	.5271	.4707	.4124	.3650	.3597	.1064	.9118E-01	.8068E-01	.7012E-01	.6305E-01	1.594

Table II-1 (Concluded)

PROGRAM BY
E.G. CRISTAL
OCTOBER 1971

5 SECTION MEANDER-LINE TRANSFORMER TABLE
CAPACITANCES NORMALIZED TO 376.7/SQRT(EPSR)
COUPLING = 10 TO 14 DB
BANDWIDTH = 10.00/1.

WL/WG	CG1/E	CG2/E	CG3/E	CG4/E	CG5/E	CG6/E	CM12/E	CM23/E	CM34/E	CM45/E	CM56/E	VSWR
1.0	.8579	.7291	.7261	.7344	.7171	.8424	.1559	.1759	.1493	.1642	.1745	1.001
1.2	.8243	.6834	.6755	.6573	.6377	.7252	.1456	.1504	.1454	.1438	.1441	1.129
1.4	.8066	.6598	.6390	.6131	.5979	.6882	.1443	.1337	.1298	.1229	.1231	1.227
1.6	.7861	.6360	.6086	.5736	.5626	.5968	.1367	.1220	.1169	.1112	.1089	1.319
1.8	.7656	.6106	.5789	.5397	.5057	.5382	.1312	.1162	.1089	.1027	.9833E-01	1.405
2.0	.7483	.5912	.5555	.5128	.4774	.4996	.1243	.1092	.1017	.9479E-01	.8942E-01	1.482
2.5	.7076	.5466	.5049	.4572	.4174	.4246	.1141	.9748E-01	.8924E-01	.8126E-01	.7534E-01	1.664

2. Discussion of Design Tables

For the data presented in Table II-1 the coupling between meander-line turns was arbitrarily (after some analytical experimentation) required to be within the range 10 to 16 dB. This range of coupling generally yields a realizable and compact structure for co-planar coupled strips. Tighter than 10 dB coupling tends to become difficult to realize, while greater than 16 dB coupling is entering a region that is beginning to separate the adjacent strips farther than is desirable. Since the effects of the finite-length interconnections between strips were neglected in compiling the Table II-1, the interconnection lengths should be made as small as possible, if the measured performance of the transformer is to correspond well with the theoretical performance. In the realization of the transformers, compensation of the interconnections will generally be required.

The effects of varying the coupling between meander-line turns are shown in the graph of Figure II-6. This graph is for the particular case of N = 4 turns, RL/RG = 2, and BW = 3:1, but is typical of the results in the general case. The graph plots maximum VSWR in the pass-band as a function of coupling between turns. The horizontal arrow depicts the range of coupling allowed. The right-hand sides of the arrows are connected by a smooth curve. This is somewhat arbitrary, but is justified by the fact that coupling values determined by the computer tend toward weaker coupling in most cases. In any event, the qualitative result is the same regardless of the way the curve is connected. The data show that for a given bandwidth the peak VSWR is minimized when the coupling is weakest. Thus, for the class of meander-line transformers, stepped-impedance transformers yield the lowest VSWRs. This is not an especially surprising result, since the coupling between turns introduces constraints on the physical realizability of the meander line. Also, the

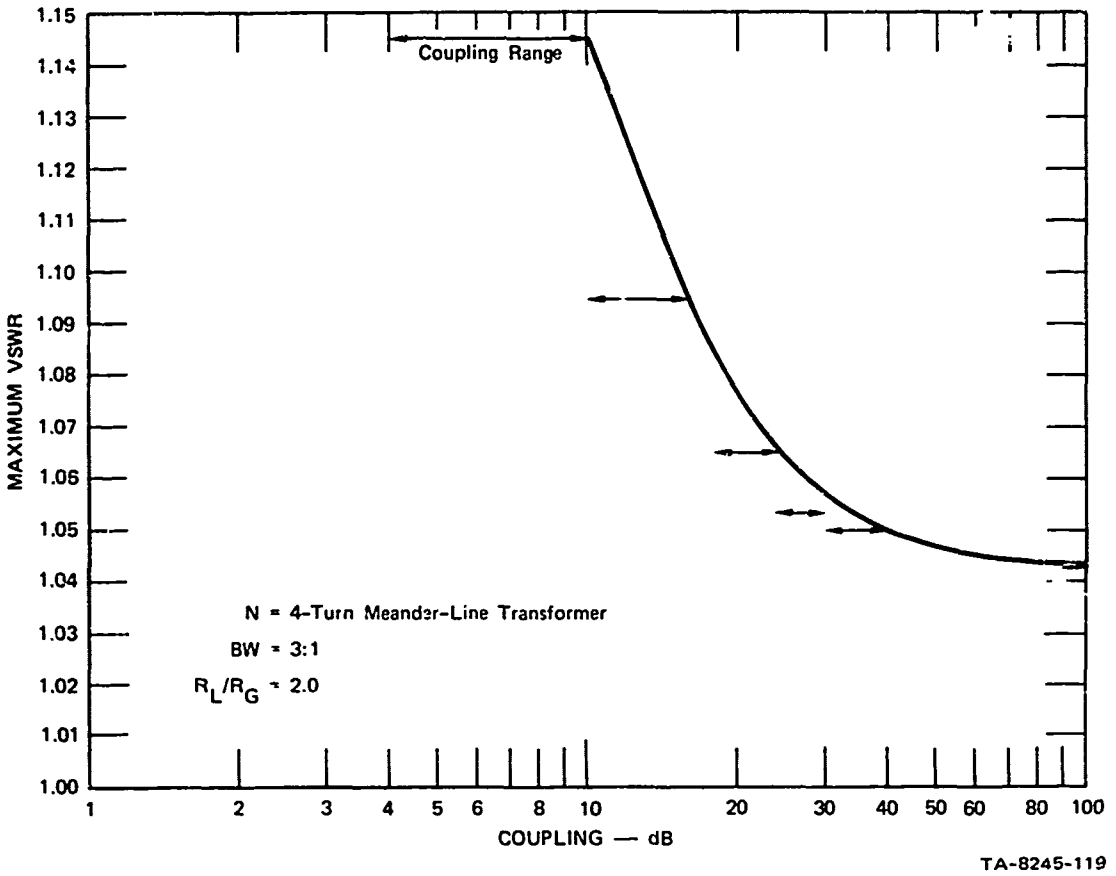

FIGURE II-6 VARIATION OF PEAK VSWR FOR VARIOUS COUPLING VALUES BETWEEN MEANDER-LINE TURNS

same conclusion might be inferred from the data of Wenzel,[14,15] which showed that C-section transiormers* have smaller bandwidths than stepped-impedance transformers for a given VSWR and number of sections.

Since Table II-1 was developed using numerical techniques, it is worthwhile to examine the responses of the transformers in some detail. Figure II-7 shows typical computed responses for 3- , 4- , and 5-turn-meander-line transformers, all having 3:1 bandwidths, 3:1

---

* A C-section transformer may also be considered a two-turn-meander-line transformer.

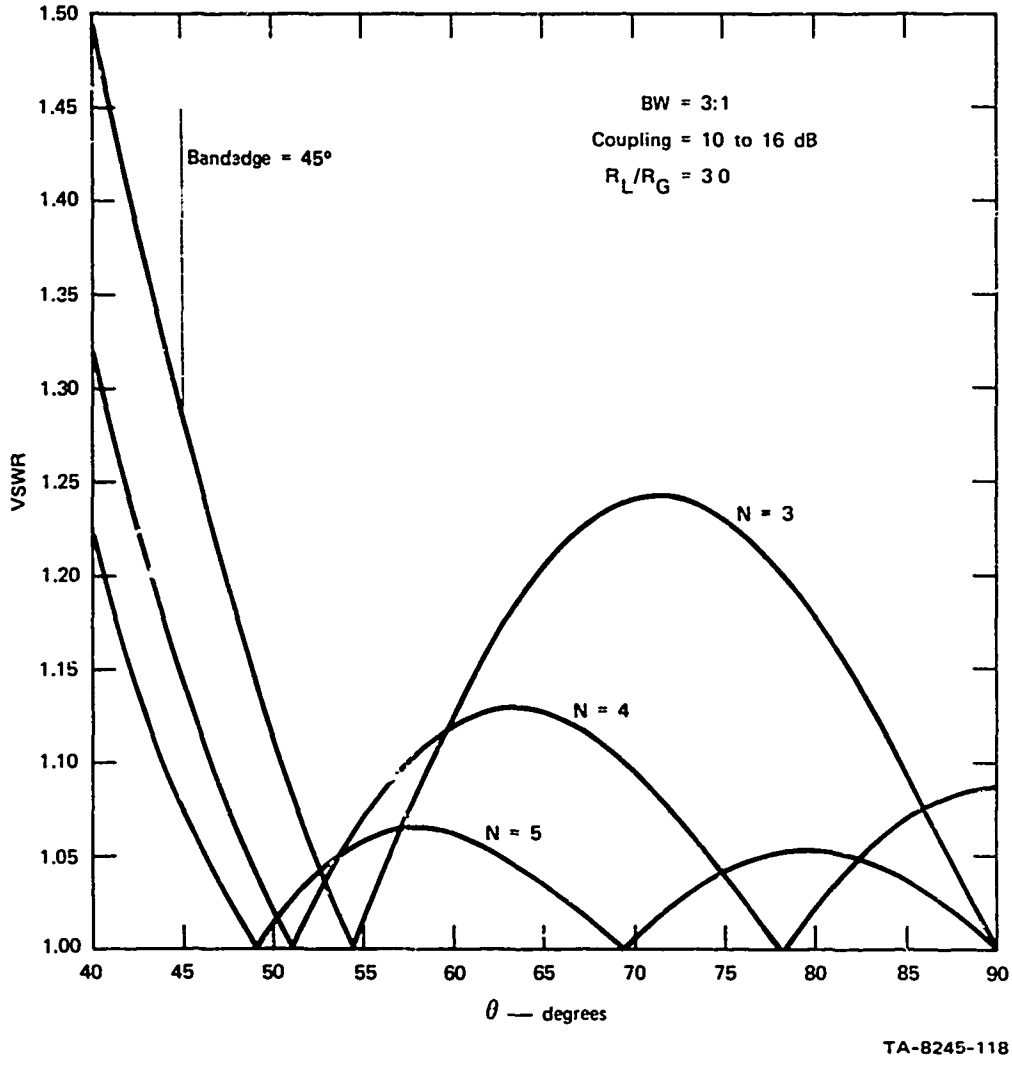

FIGURE II-7 VSWR vs. ELECTRICAL DEGREES FOR N = 3-, 4-, AND 5-TURN MEANDER-LINE TRANSFORMERS

impedance transformation ratios, and 10 to 16 dB coupling between turns. The improvement in VSWR with increasing N is evident. The VSWRs are not quite equal-ripple, but, on the other hand, are so close to equal-ripple that the difference is virtually academic. Certainly, in any realization of these designs, the effect of losses, interconnections, and parasitics would completely obscure any differences between these and precisely equal-ripple designs. Note also that the peak VSWR occurs at the band edge.* Since it is the peak VSWR that is given in Table II-1, and since the band edge performance is almost always degraded in actual hardware realizations, a user may generally assume that the maximum VSWR is slightly lower than that given in Table II-1 over the band of application.

Figure II-8 presents representative data of maximum VSWR versus bandwidth (BW), with the number of meander-line turns as a parameter. Also plotted are the corresponding data for stepped-impedance transformers. The impedance transformation ratio is 2:1 and the coupling between meander-line turns is 10 to 16 dB. The data show that superiority of the stepped-impedance transformer with regard to electrical performance. However, equivalent or improved performance is always possible with meander-line transformers by adding additional turns. Again, we reiterate that the principal advantage of meander-line and hybrid meander-line transformers is the reduction in overall length and the increased flexibility in obtaining suitable shape factors for the stripline or MIC transformers being considered.

---

* This is not always the case, but is usually so.

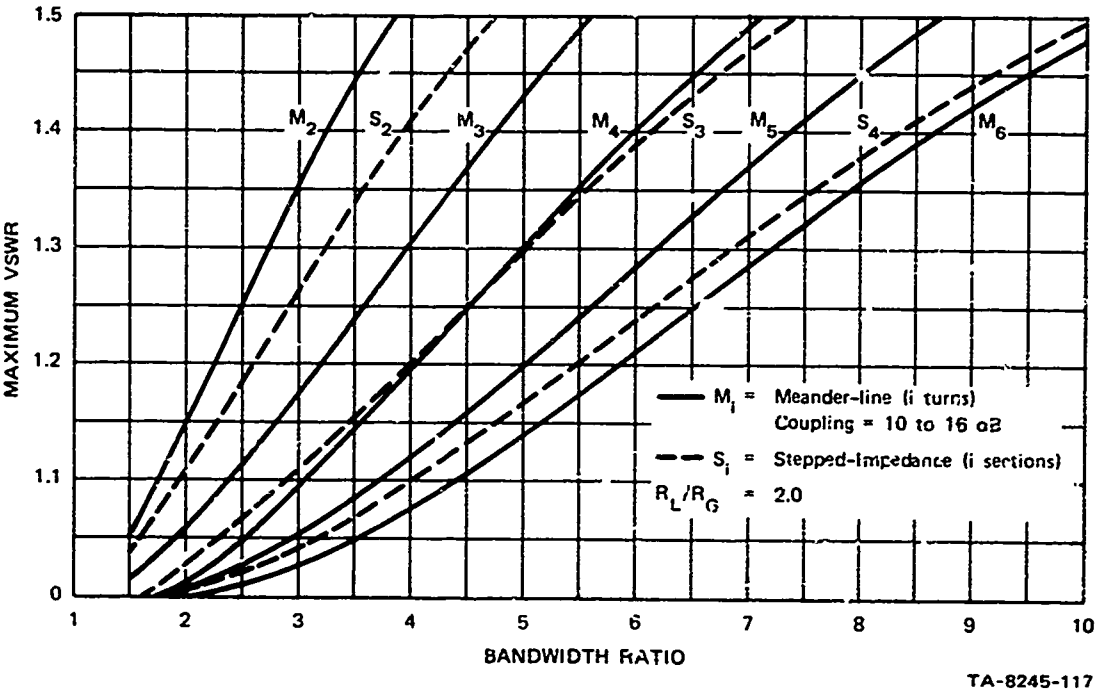

FIGURE II-8 VSWR vs. BANDWIDTH FOR MEANDER-LINE AND STEPPED-IMPEDANCE TRANSFORMERS

3. Example Design

The use of the meander-line-transformer design tables (Table II-1) will be illustrated in the following example. It is required to match 25 to 50 ohms over a 3:1 bandwidth. The maximum VSWR allowed is 1.1. Checking Table II-1 for RL/RG = 50/25 = 2, and for N = 2. 3, and 4, shows that the maximum VSWRs are 1.352, 1.288, and 1.095, respectively. Thus, N = 4 turns is sufficient. The parameters from the N = 4, BW = 3:1 tables are as follows:

$$\begin{aligned} CG1/E &= 0.7757 \\ CG2/E &= 0.5699 \\ CG3/E &= 0.4826 \\ CG4/E &= 0.4744 \\ CM12/E &= 0.1298 \\ CM23/E &= 0.1041 \\ CM34/E &= 0.09295 \quad . \end{aligned} \tag{II-6}$$

We will assume that the transformer is to be constructed in stripline on 1-oz copper-clad Rexolite 1422, which has a relative dielectric constant of 2.54. Since the tables are calculated on the basis that the "load" is always greater than the source, the generator resistance in this case is identified as 25 ohms. Consequently, substituting Eq. (II-6) into Eq. (II-5) (page 9) yields

$$C_{g_1}/\epsilon = \frac{376.7}{25\sqrt{2.54}}\{0.7757\} = 9.454(0.7757) = 7.334$$

$$C_{g_2}/\epsilon = 9.454(0.5699) = 5.388$$

$$C_{g_3}/\epsilon = 9.454(0.4826) = 4.563$$

$$C_{g_4}/\epsilon = 9.454(0.4744) = 4.485 \qquad \text{(II-7)}$$

$$C_{12}/\epsilon = 9.454(0.1298) = 1.227$$

$$C_{23}/\epsilon = 9.454(0.1041) = 0.9842$$

$$C_{34}/\epsilon = 9.454(0.09295) = 0.8788 \quad .$$

Substituting Eq. (II-7) into Getsinger's data yields the results given in Table II-2.

C. Experimental Results

1. Three-Turn-Meander-Line Transformer

A three-turn-meander-line transformer was designed to match a 25-ohm load to a 50-ohm source over a 60-percent bandwidth (BW = 1.857). It was constructed in stripline using 1-oz copper-clad Rexolite 1422, and a ground-plane spacing of 0.250 inch. The electrical and dimensional

Table II-2

EXAMPLE FOUR-TURN-MEANDER-LINE
3:1-BANDWIDTH TRANSFORMER DESIGN
(RL/RG = 2)

Conductor	w/b*	s/b†
1 (25 .. end)	1.550	0.1059
2	1.224	0.1508
3	0.9911	0.1767
4	0.8137	

* w/b = Strip-width-to-ground-plane spacing.

† s/b = Interstrip-spacing-to-ground-plane spacing.

parameters are given in Table II-3. The nominal center frequency was 1 GHz. The interconnections between meander-line turns were mitered experimentally for a satisfactory VSWR. Four 1/8-watt, 100-ohm carbon

Table II-3

ELECTRICAL AND DIMENSIONAL PARAMETERS FOR AN EXPERIMENTAL
STRIPLINE THREE-TURN-MEANDER-LINE TRANSFORMER

Line	C_{g_i}/ε	$C_{i,i+1}/\varepsilon$	Linewidth, w (inch)	Inter-Line Spacing, s (inch)
1 (25-.. side)	6.7191	1.6005	0.354	0.015
2	4.2162	1.5074	0.246	0.018
3 (50-.. side)	4.1891		0.196	
Impedance transformation 2:1 Fractional bandwidth 0.60 (BW = 1.857)			Theoretical VSWR = 1.048	

resistors connected in parallel were used for the 25-ohm load. A photograph of the final design is given in Figure II-9. The measured and computed VSWR's are shown in Figure II-10. Note that although the center frequency of the transformer is slightly high, and although there is some degradation in the response near the upper band edge, generally speaking, there is excellent agreement between the two curves. Also, a photograph of the measured reflection coefficient from 400 to 1400 MHz is shown on an expanded Smith chart overlay in Figure II-11.

2. Fourth-Order Hybrid Meander-Line Transformer

In order to confirm the theory and design procedure for hybrid meander-line transformers, an N = 4 hybrid transformer covering a 4:1 bandwidth and matching 25 to 50 ohms was designed. The theoretical VSWR is 1.14. It was also constructed in stripline using 1-oz copper-clad Rexolite 1422, and a ground-plane spacing of 0.250 inch. Its nominal center frequency was 1.250 GHz. The electrical and dimensional parameters are given in Table II-4, and a photograph of the transformer after the interconnections were mitered is given in Figure II-12. The measured data at the high-frequency end of the passband indicate that the interconnections are not completely compensated; nevertheless, the mean return loss is about 23 dB. Hence, the correspondence with the theory is very good.

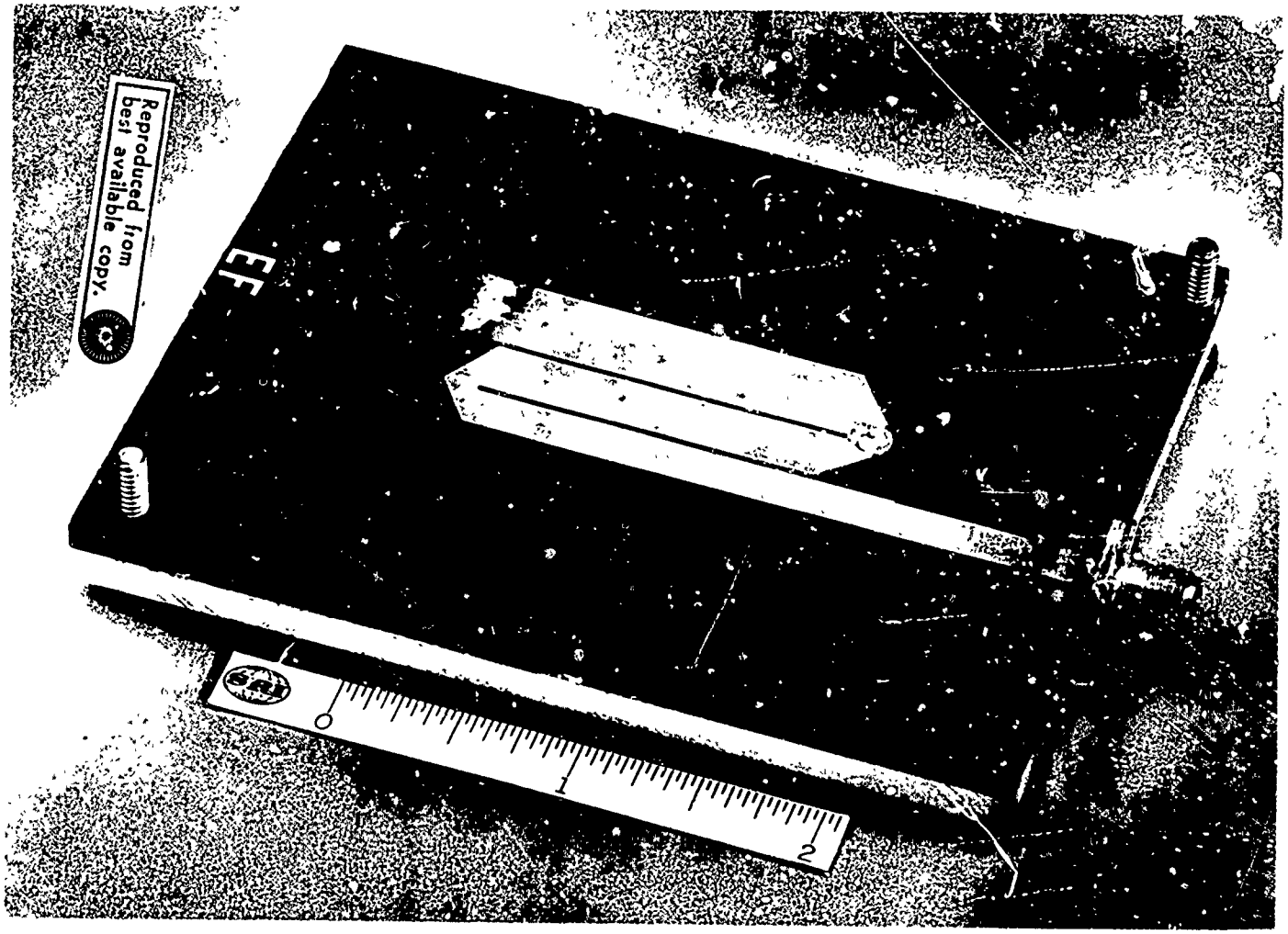

FIGURE II-9 PHOTOGRAPH OF EXPERIMENTAL THREE-TURN-MEANDER-LINE TRANSFORMER

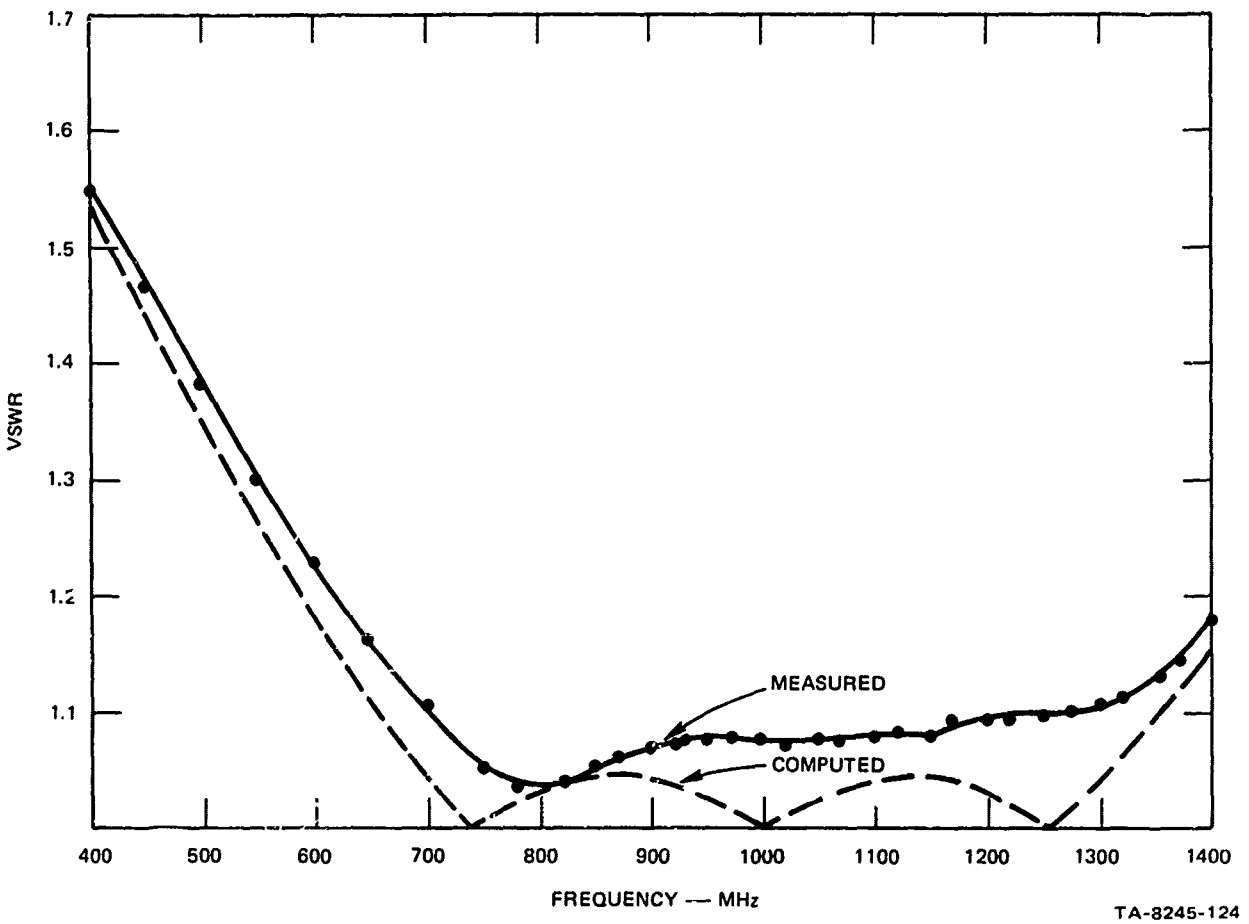

FIGURE II-10 MEASURED AND COMPUTED VSWRs FOR EXPERIMENTAL THREE-TURN-MEANDER-LINE TRANSFORMER

FIGURE II-11 MEASURED REFLECTION COEFFICIENT ON A SMITH-CHART OVERLAY FOR THE EXPERIMENTAL THREE-TURN-MEANDER-LINE TRANSFORMER

Table II-4

ELECTRICAL AND DIMENSIONAL PARAMETERS FOR AN EXPERIMENTAL FOURTH-ORDER STRIPLINE HYBRID MEANDER-LINE TRANSFORMER

Line	C_{g_i}/ϵ	$C_{i,i+1}/\epsilon$	Linewidth, w (inch)	Inter-Line Spacing, s (inch)
1 (25-Ω side)	7.208	1.2300	0.380	0.026
2	6.182	0.0	0.316	--
3	5.2792	0.9006	0.253	0.043
4 (50-Ω side)	4.5239		0.206	

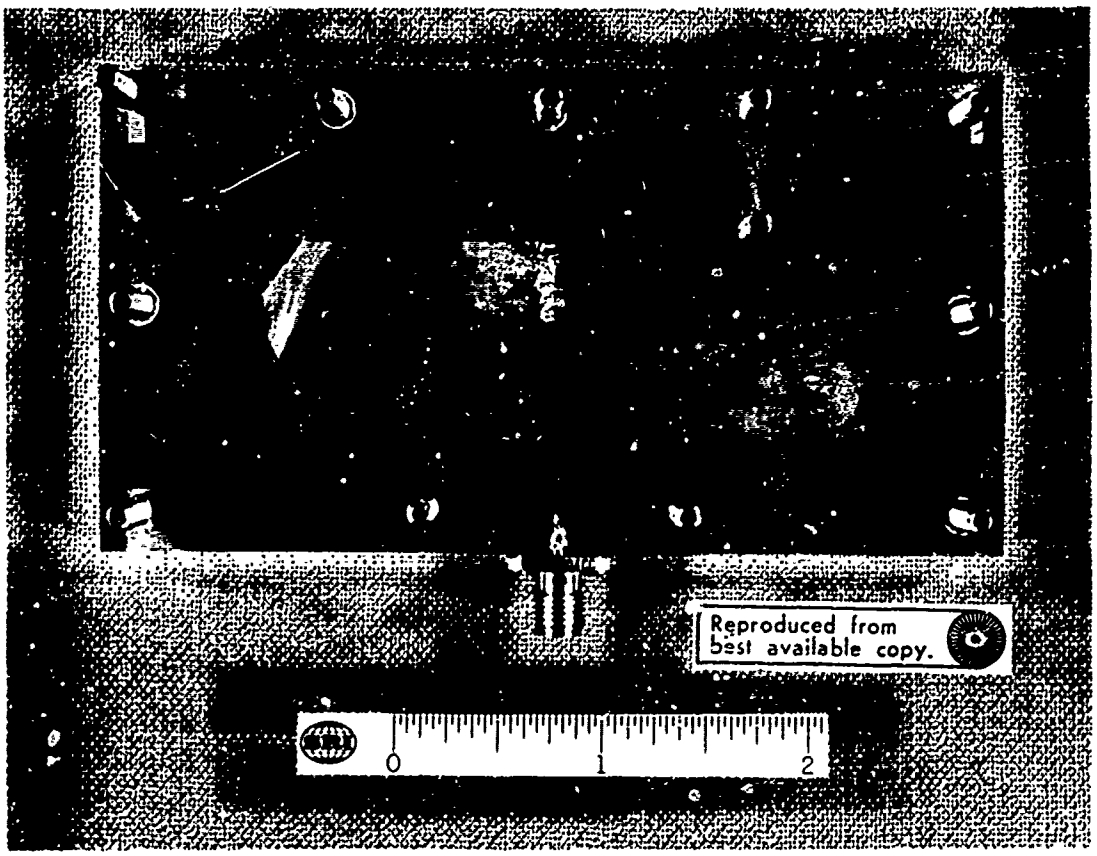

FIGURE II-12 PHOTOGRAPH OF AN EXPERIMENTAL N = 4 HYBRID MEANDER-LINE TRANSFORMER

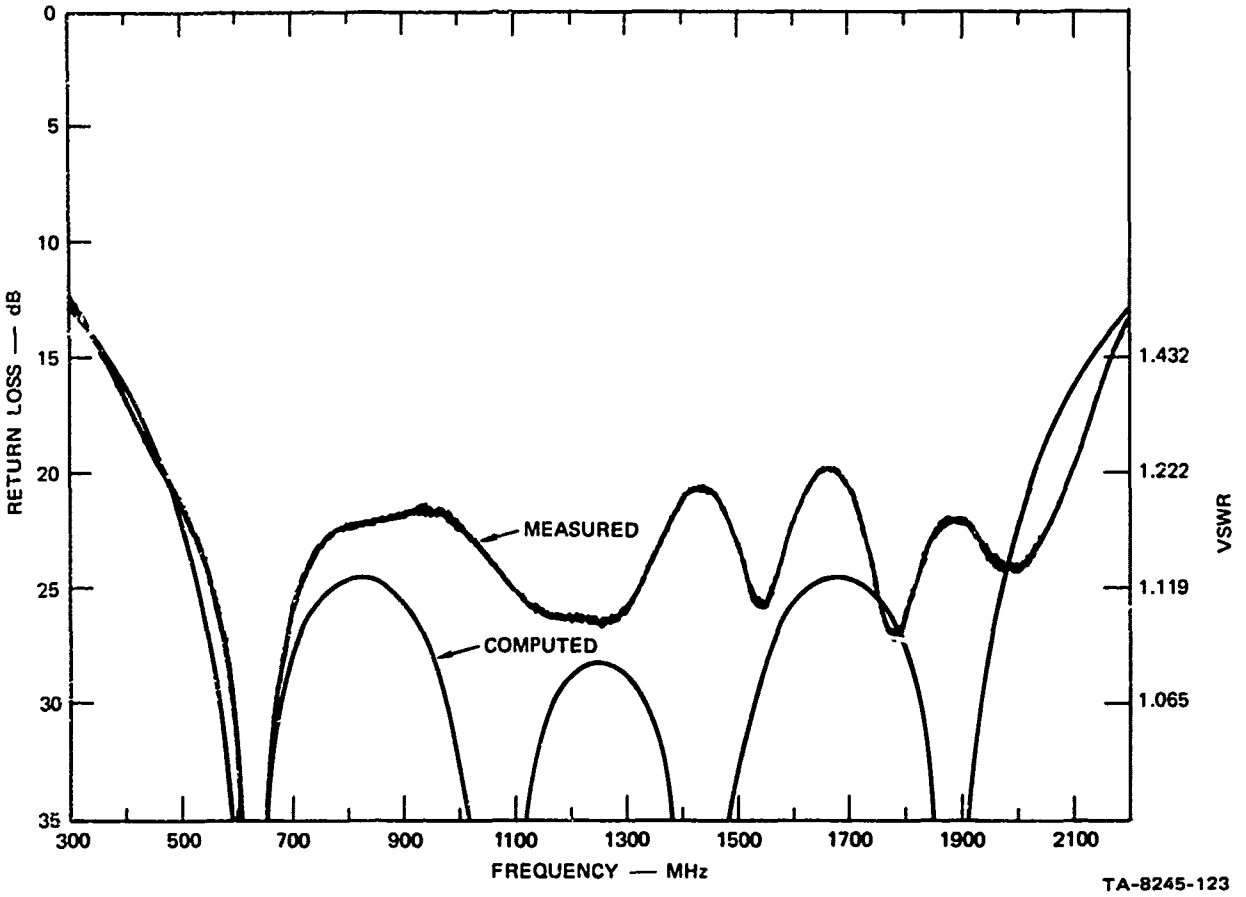

FIGURE II-13 MEASURED AND COMPUTED RETURN LOSS FOR EXPERIMENTAL N = 4 HYBRID MEANDER-LINE TRANSFORMER

III NEGATIVE-IMPEDANCE CONVERTERS

A. General

During the final reporting period, two types of negative-impedance converter (NIC) circuits were designed and constructed: (1) a high-power NUNIC filter and (2) a FET-NIC filter. A high-power NUNIC filter was built to show the applicability of the NUNIC design approach to the realization of large-signal as well as small-signal devices. A FET-NIC filter in integrated form was built to show that active filters can compete with crystal filters in stability, bandwidth, and size.

The design and performance of the high-power NUNIC circuit is discussed in Section III-B, and that of the integrated FET-NIC filter in Section III-C.

B. The NUNIC Circuit

1. Qualitative Analysis

A description of the operation of the NUNIC circuit, along with some measured results, was presented in the Semiannual Report 1 on this contract.[16] A high-power filter operating at 230 MHz was designed and built using this circuit because the NUNIC utilizes the inherent time delays in high-power transistors and their interconnections in order to operate at much higher frequencies than are possible using conventional NIC circuits. However, temperature and transistor parameter sensitivity may be a problem with the NUNIC because the common-emitter transistor, whose gain is beta-dependent, operates with no negative feedback. The addition of negative feedback can be easily implemented

by inserting a resistor (or more complex load) in the emitter-to-ground path. This complicates the analysis of the circuit because h_{11} is no longer small and is a strong function of the emitter load. Collector-to-base feedback in the common-emitter stage is not useful for achieving negative feedback, for two reasons: (1) Such feedback tends to lower the output impedance of the common-emitter transistor, which in turn increases the sensitivity of the circuit to parameter changes in the common-base transistor, and (2) unavoidable parasitic effects tend to make such feedback much less effective at microwave frequencies. Therefore, negative feedback was applied to the NUNIC circuit as an emitter load Z_e, as shown in Figure III-1.

The common-base stage, because its gain is dependent on alpha rather than on beta, is much less sensitive to parameter variations. This is because alpha changes much less than beta with changes in operating voltage, current, and frequency. Consequently, no attempt was made to add negative feedback to the common-base stage.

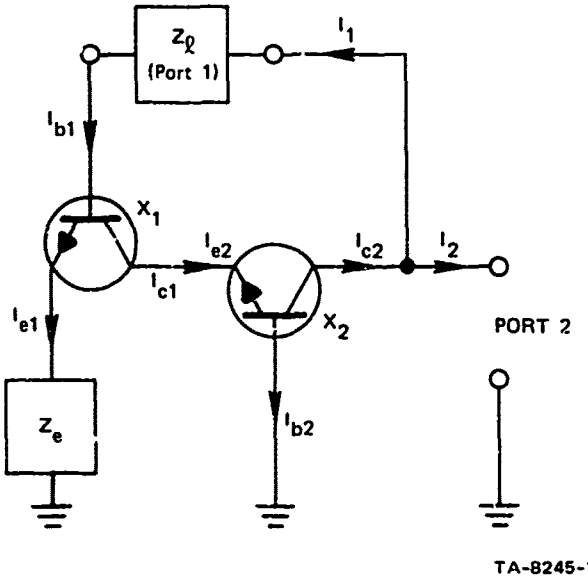

FIGURE III-1(a) NUNIC WITH NEGATIVE FEEDBACK-SCHEMATIC DIAGRAM

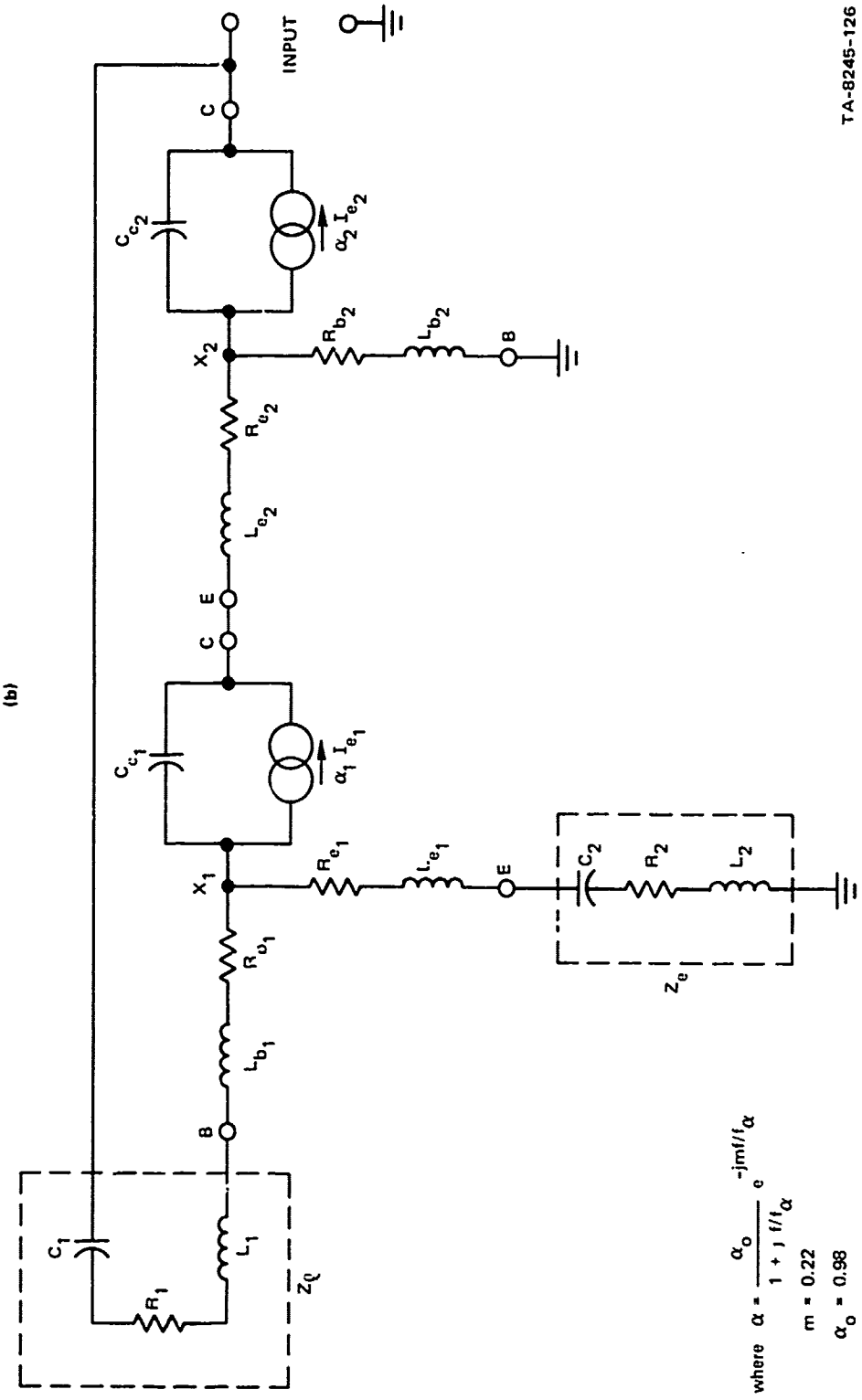

FIGURE III-1 (Concluded)

The element values for the NUNIC circuit with emitter feedback were chosen to give the desired impedance function at Port 2 while maintaining as much negative feedback as possible in the common-emitter stage. This is accomplished most efficiently by using a computer program designed to chose element values that minimize the sensitivity of the input impedance at Port 2 to transistor variations, while still maintaining the proper impedance at that port. However, the development of such a program was beyond the scope of this contract. Instead, the following procedure was adopted. (Each step will be explained in detail as we come to it.) One first chooses an emitter impedance Z_e, and then tries a series of load impedances Z_ℓ, from which one computes the input impedance Z_{in} at Port 2. After a series of trial-and-error calculations to obtain the desired Z_{in}, one thus selects the "optimum" Z_e and Z_ℓ -- they are "optimum" in the sense they give not only the desired Z_{in}, but also low sensitivity to variations in the transistor parameter, f_α. Refer to Section 4 for a more explicit design procedure.

It should be mentioned that there is another practical limitation on the magnitude of Z_e. Since the emitter current of transistor X_1 flows through this impedance, there is a voltage drop across it that may be considerable. The collector current I_{c1} of transistor X_1 is approximately βI_b, where I_b is its base current. The emitter current I_{e1} of transistor X_1 is approximately $(\beta + 1)I_b$. At the frequency where the NUNIC circuit is used, the magnitude and angle of β are likely to range from 2 to 5, and from 140° to 120°, respectively. Consequently, the magnitude of the collector current $|\beta I_b|$ is generally quite close to the magnitude of the emitter current $|(\beta + 1)I_b|$, as is indicated in Figure III-2; in symbols, I_{e1} is approximately equal to I_{c1}. The collector current of X_2, which is I_{c2}, is approximately equal to its emitter current, I_{e2}, for the same reason. Referring to

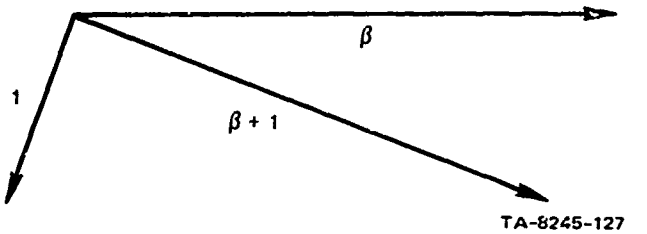

FIGURE III-2 PHASE AND AMPLITUDE OF β AND $\beta + 1$

Figure III-1(a), I_{c2} is therefore approximately equal to $I_{e2} = I_{c1}$, hence approximately equal to I_{e1}. Now, I_1 and I_2 are both supplied by the collector current of transistor X_2, and I_1 and I_2 are approximately in phase in order for NIC action to occur. Therefore, any X_2 collector current flowing into I_1 is not available at Port 2. I_1 may be decreased by increasing the beta of transistor X_1. Thus it is important that transistor X_1 have as high an f_t as possible in order to maximize the power output of the NIC. A second constraint on transistor X_1 is that it must be capable of handling at least as much current as the output transistor, X_2. A third constraint on transistor X_1 is breakdown voltage. An impedance in the emitter-to-ground path of transistor X_1 has flowing through it a current at least as large as the output current I_2. Thus, an emitter impedance comparable in magnitude with the impedance seen by the output transistor, X_2, will result in comparable voltage swings in the emitter of transistor X_1. Although this results in a large amount of negative feedback, it also means that transistor X_1 must have a voltage-breakdown rating similar to that of transistor X_2. This requirement is in conflict with the requirement for a high-gain transistor at X_1, because raising the breakdown voltage of a transistor of given geometry tends to lower its gain. Therefore, voltage-breakdown considerations may limit the magnitude of the emitter impedance of transistor X_1.

To recapitulate, transistor X_1 should be a high-f_t, low-voltage device, and transistor X_2 should be a lower-f_t, high-voltage device. At the highest frequency of operation the beta of transistor X_1 would be chosen to be no less than 2, so that not too much of the output current from transistor X_2 would be lost to feedback. Similarly, transistor X_2 would be chosen to operate below its alpha-cutoff frequency. In a later section, techniques that raise the upper frequency at which negative resistance can be generated will be discussed. However, such techniques will tend to reduce bandwidth.

2. Choosing Transistors

The common-base transistor X_2 operates "Class A" and is therefore limited in efficiency to less than 50 percent. A power output capability of 2.5 watts from this transistor requires that it dissipate at least 2.5 watts at full output. The total dc input of at least 5 watts must be dissipated by the transistor when no input signal is present. A transistor with internal emitter-balancing resistors is essential for operation at this power level. Experience with the Fairchild MSA 8505 transistor has shown it to be rugged which, combined with its alpha-cutoff frequency of 500 MHz, makes it quite suitable. An operating voltage of 20 volts from collector to base was chosen, to be on the conservative side, and an operating current of 250 mA was chosen because it is approximately in the middle of the linear operating range of the smaller common-emitter transistor that was initially used. The MSA 8505 transistor is capable of operation at 500 mA of collector current if a larger common-emitter transistor is used.

The common-emitter transistor X_1 can operate with a lower collector-emitter voltage than X_2, but it should have an f_t of approximately 1 GHz. For this application, another readily available transistor, the MT 5764, was chosen together with a backup device, the MT 5765. The

current capabilities of the MT 5764 appeared barely adequate; therefore the slightly-lower-gain MT 5765 capable of nearly twice the current swing was also acquired. The MT 5764 is capable of continuous operation with 10 volts from collector to emitter and 250 mA of collector current. It was anticipated that the MT 5765 transistor would replace the smaller device, once some experience was gained in mounting, heat sinking, biasing, and stabilizing the transistors.

3. Load Impedance and Power Capabilities

If all the collector current of transistor X_2 was assumed to flow through the external load at Port 2, then one could easily compute the maximum sinusoidal RF power, P_1, available at that port. This power would be

$$P_1 = \frac{I_c \cdot V_{cb}}{2} \qquad \text{(III-1)}$$

which is the maximum undistorted power output from a Class A amplifier operating at I_c collector amperes and V_{cb} collector-to-base volts.* At 230 MHz, nearly $0.2P_1$ was calculated to be fed back to the base of the common-emitter transistor. A higher-gain, more exotic transistor than the MT 5764 would help to lower this loss, but the attempt here is not to wring the last dB of output from the NUNIC at all cost, but rather to achieve a practical design with transistors that represent a practical compromise in cost-versus-performance at the operating frequency. The expected undistorted power output from the NUNIC, P_0, would therefore be given by:

$$P_0 \doteq 0.4 I_c \cdot V_{cb} \quad . \qquad \text{(III-2)}$$

---

* See Ref. 16, p. 36.

When the NUNIC is embedded in a one-pole filter, thereby rendering the filter lossless, the maximum undistorted RF power output from the filter, P_{OUT}, is given by*

$$P_{OUT} \doteq \frac{P_0}{2Q_L/Q_u} \quad . \tag{III-3}$$

The quantity Q_L is defined as the loaded Q of the filter with the NUNIC embedded, and Q_u is defined as the Q of the tuned circuit alone, with nothing else connected.

In a lossless one-pole filter the positive load resistance on the NUNIC would be R_p, the parallel-equivalent loss resistance of the tuned circuit.† This loss resistance is neutralized by the NUNIC's negative input resistance to make the tuned circuit effectively lossless. R_a, the optimum load on the NUNIC for maximum power output would be given by‡

$$R_a \doteq \frac{V_{cb}}{0.8I_c} \quad . \tag{III-4}$$

The 0.8 in the denominator results from the loss of 20 percent of the output current to the feedback loop. For the maximum filter power capability, R_p would be made equal to R_a in order to maximize the power delivered by the NUNIC.

Equations (III-2), (III-3), and (III-4) can now be used to establish the operating conditions and the load for the transistors used in the high-power NUNIC.

---

* See Ref. 15, pp. 41-44.
† See Ref. 16, p. 45.
‡ See Ref. 16, pp. 35-36.

For example, if the NUNIC is operated at 250 mA of collector current and with 20 volts from collector to base on the common-base transistor, then the NUNIC power output, P_0, as calculated from Eq. (III-2) would be

$$P_0 = 0.4 I_c V_{cb} = 0.4 \times 0.25 \times 20 = 2 \text{ watts } (+33 \text{ dBm}) \quad .$$

The power output from the filter would depend on the relative Q multiplication desired. Suppose the NUNIC filter utilizes a tuned circuit whose unloaded Q (Q_u) is 80. If this tuned circuit is used in a filter whose loaded Q (Q_L) is 85 (2.7 MHz bandwidth at 230 MHz), the maximum undistorted filter output power, P_{OUT}, would be [from Eq. (III-3)]:

$$P_{OUT} \doteq \frac{P_0}{2Q_L/Q_u} = \frac{2}{170/80} = 0.94 \text{ watt } (+29.7 \text{ dBm}) \quad .$$

Also, the optimum load resistance R_a, is found to be [from Eq. (III-4)]:

$$R_a \doteq \frac{V_{cb}}{0.8 I_c} = \frac{20}{0.8(0.25)} = 100 \text{ ohms} \quad .$$

A theoretical basis for the calculation of intermodulation (IM) distortion in a NUNIC filter has yet been worked out. An emitter impedance of 10 or 20 ohms will minimize the distortion generated by the common-emitter transistor. However, it is likely that the varactor effect of the collector-base junction of the common-base transistor is a significant source of IM distortion in the NUNIC, just as it is in linear-transistor power amplifiers at these frequencies. Replacement of the MT 5764 by the MT 5765 transistor having twice the current-handling capability will allow twice the filter power output for the same collector-voltage swing, with a corresponding increase in the third-order intercept.

In addition, R_a would be decreased to 50 ohms, thereby further reducing the IM distortion because a smaller fraction of the NUNIC output current would flow through the varactor and a larger fraction through the increased load conductance. Therefore, the replacement of the MT 5764 with a MT 5765 should increase the third-order intercept of the NUNIC filter by 6 dB.

4. NUNIC Load and Emitter Impedances

A NUNIC circuit design that will generate -100 ohms at 230 MHz will now be presented. This will satisfy the specifications of the previous section and will also neutralize tuned-circuit losses. To design such a NUNIC circuit it is necessary to compute the input impedance of the NUNIC whose equivalent circuit was shown in Figure III-1(b).

We adjusted Z_e and Z_ℓ, as described in Section III.1, calculating the input impedance Z_{in} (as a function of both Z_e and Z_ℓ) until Z_{in} not only equalled -100 ohms but also showed little sensitivity to variations in f_α.* The final element values for the circuit shown in Figure III-1(b) are given in Table III-1, and a negative-conductance comparison is given in Table III-2.

A capacitor, C_2, had to be added to the emitter feedback circuit in order to narrow the frequency range over which the NUNIC circuit developed negative resistance. This helped to stabilize the circuit, reducing the tendency to oscillate.

---

*In this calculation the starting point for Z_e was taken as 25 ohms, because this would give almost unity loop gain; Z_ℓ was then varied until $|Z_{in}|$ was a minimum with respect to Z_ℓ. It was found that $|Z_{in}|$ was too large, and to reduce it, Z_e had to be reduced (always looking for a minimum of $|Z_{in}|$ with respect to Z_ℓ). Once the desired value of Z_{in} (namely -100 ohms) had been obtained, the alpha-cutoff frequency (f_α) of both transistors was varied by ±10 percent, and the effect on $|Z_{in}|$ was calculated. Since the sensitivity of $|Z_{in}|$ to the two f_α was considered satisfactory, no further changes in Z_e and Z_ℓ were made. Clearly, there may exist other choices of Z_e and Z_ℓ which will further reduce the sensitivity of the circuit to changes in f_α.

Table III-1

FINAL ELEMENT VALUES

L_1	16 nH	L_{b_1}	1 nH	L_{b_2}	2 nH
C_1	22 pF	L_{e_1}	1 nH	L_{e_2}	10 nH
R_1	100 ohms	R_{b_1}	1 ohm	R_{b_2}	0.3 ohm
		R_{e_1}	1 ohm	R_{e_2}	0.3 ohm
L_2	110 nH	C_{c_1}	5 pF	C_{c_2}	10 pF
C_2	5 pF	α_1	0.98	α_2	0.98
R_2	12 ohms	f_{α_1}	2700	f_{α_2}	1400

Table III-2

CONDUCTANCE CHANGE WITH f_α VARIATION

$-G_{IN}$	f_{α_1}	f_{α_2}
0.01022	2400	1260
0.01032	2700	1400
0.01039	3000	1540

Note that a ±10 percent change in f_α for both transistors resulted in a change of less than ±1 percent in the negative conductance generated by the NUNIC.

5. NUNIC Measurements

Unfortunately, there was insufficient time to replace the MT 5764 transistor with the larger device, so the following measurements were all made with only the MT 5764 and the MSA 8505 transistors in the NUNIC. The collector bias current was thus limited to about 250 mA.

At 230 MHz the third-order intercept and the 1-dB compression point were measured under the following conditions:

V_{cb} (MSA 8505)	20 V
V_{ce} (MT 5764)	10 V
I_c (both)	220 to 250 mA (optimum range)
Q_u	80
Bandwidth	2.7 MHz
Q_L	85
Two-Tone Input Power (each tone)	+8 dBm (for IM test)

The third-order intercept measured +35 dBm, and the output level for 1 dB compression was +29 dBm. The noise figure was also measured, but it was necessary to lower the collector current to 30 mA in order to obtain a 21-dB reading on the available equipment. At 220 mA the noise figure was unreadably high, probably 25 or 26 dB.

6. Noise Figure

Presently, there are no FETs that operate at 250 to 500 mA of drain current, and yet have reasonable gain at 400 MHz. Hence, a bipolar transistor was used in the common-emitter stage of the NUNIC, with the

resulting consequences for noise figure* that were noted in Section III-B-5, above. This high noise figure occurs because the source impedance seen by the base of the common-emitter transistor (about 200 ohms) is more than an order of magnitude larger than the optimum source impedance for minimum MT 5764 noise figure (about 7 ohms at 250 mA). In this respect the MT 5765 operating at 500 mA of collector current should be even worse. The MT 5764 transistor is not a particularly low-noise device, and it is being operated at a relatively high frequency, so it is expected that a noise-matched noise figure of around 10 dB would be obtained from this device at 230 MHz. Therefore, even without adding in the noise contribution of the common-base stage, a noise figure of 18 to 20 dB could be expected for the high-power NUNIC. To this would be added the noise contribution of the loss resistance of the tuned circuit, which should result in a noise figure for the complete active filter of well over 20 dB.

7. Circuit Modifications

For operation over narrow bandwidths, some changes can be made in the NUNIC circuit that will improve its performance if it is used mostly to generate negative resistance (as, for example, in a filter). Consider the one-pole filter of Figure III-3, in which the feedback from the output of transistor X_2 to the base of transistor X_1 has been changed from a direct RF feedback to a tapped-coil (or transformer) feedback, as shown in Figure III-3(a). It is no longer necessary for the current gain of transistor X_1 to be large in order to prevent loss of output current. Because of transformer action, the base current I_1 fed back to transistor X_1 may be larger than the transformer current

---

* See Ref. 16, p. 44.

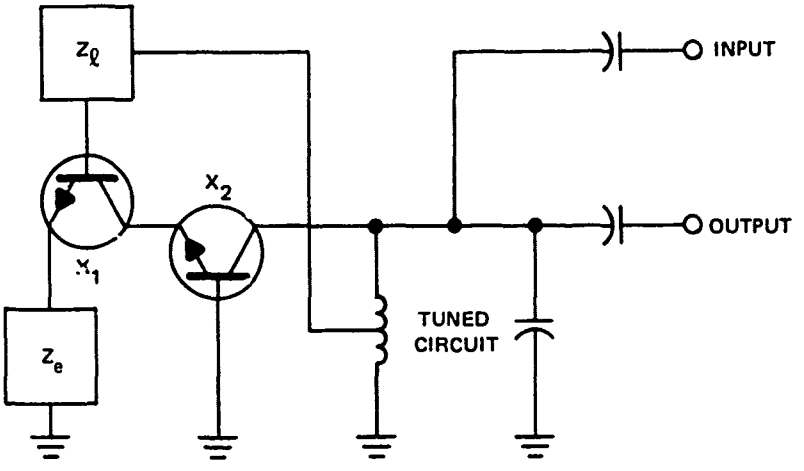

(a) TAPPED-TRANSFORMER FEEDBACK

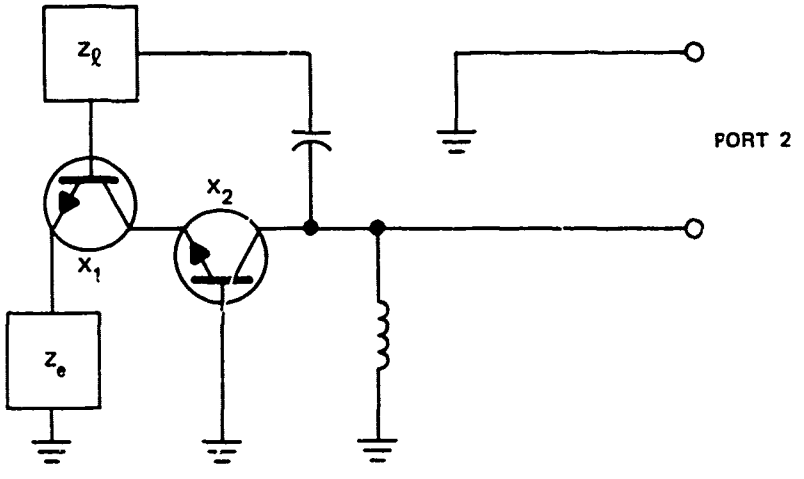

(b) REACTIVE-TRANSFORMER FEEDBACK

TA-8245-128

FIGURE III-3 MODIFIED NUNIC CIRCUITS

flowing from the collector circuit of transistor X_2. Z_ℓ and Z_e will be affected by such tapping down, and it may even be possible to eliminate Z_ℓ for certain combinations of Z_e, transistor gain, and transformer ratio. Since "tapping down" lowers the source impedance seen by the base of transistor X_1, the noise figure of the filter should improve.

The high-frequency performance of the NUNIC may be improved at the expense of bandwidth by the use of a reactive transformer in the feedback loop. A shunt inductor from the collector of transistor X_2 to ground and a series capacitor from the collector of X_2 feeding back to the base of X_1 will add a negative transmission phase shift (thus decreasing the loop phase shift at high frequencies). At the same time, the base input impedance of transistor X_1, as viewed by the collector of transistor X_2, is raised. Figure III-3(b) shows this circuit. It is likely that the capacitor could be absorbed into Z_ℓ, or that Z_ℓ could be eliminated entirely.

None of these circuits has been built and tested, but they are suggested here to show the direction to be taken in future investigation.

C. The Integrated FET-NIC

1. Circuit Design

The FET-NIC* filter circuit discussed in this section was implemented in microwave-integrated-circuit (MIC) form. The schematic diagram for the MIC realization is shown in Figure III-4, and a picture of the MIC substrate in Figure III-5. Note that all RF chokes have been removed from the circuit in order to reduce production cost; the

---

* See Ref. 16, p. 48.

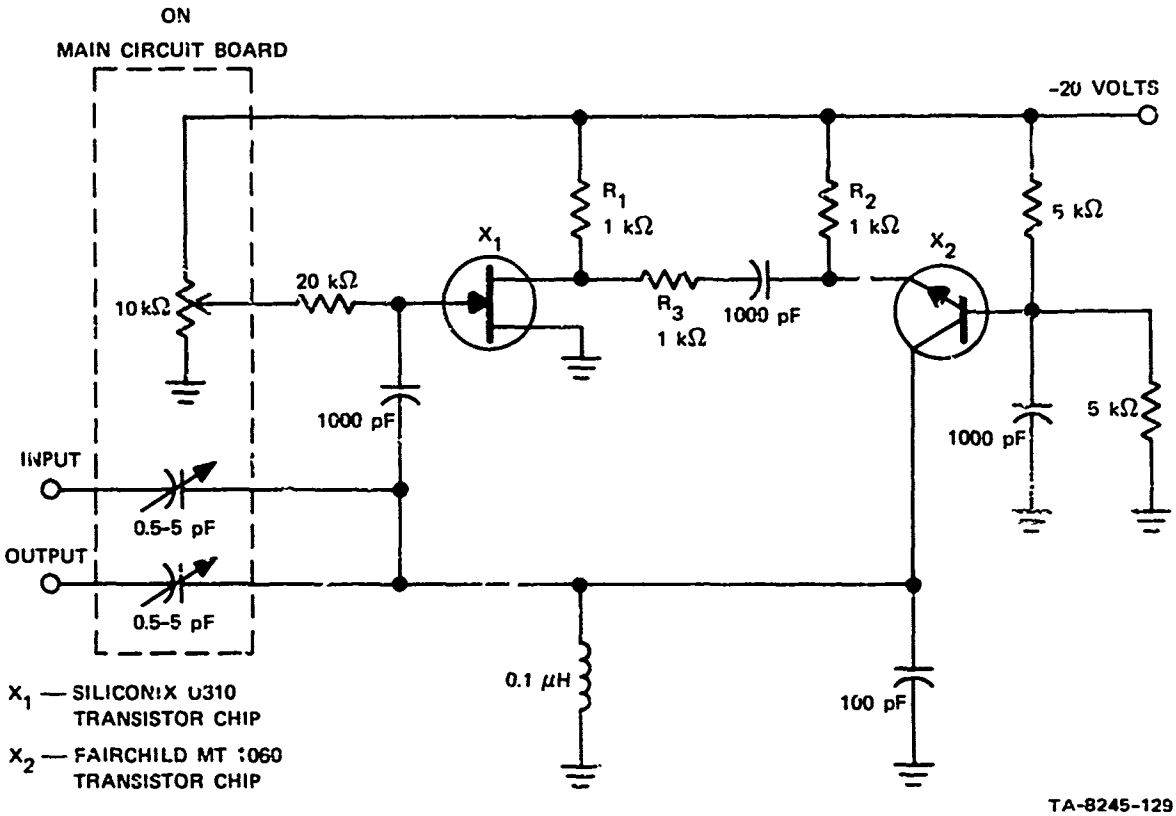

FIGURE III-4 SCHEMATIC DIAGRAM OF FIRST INTEGRATED FET-NIC FILTER

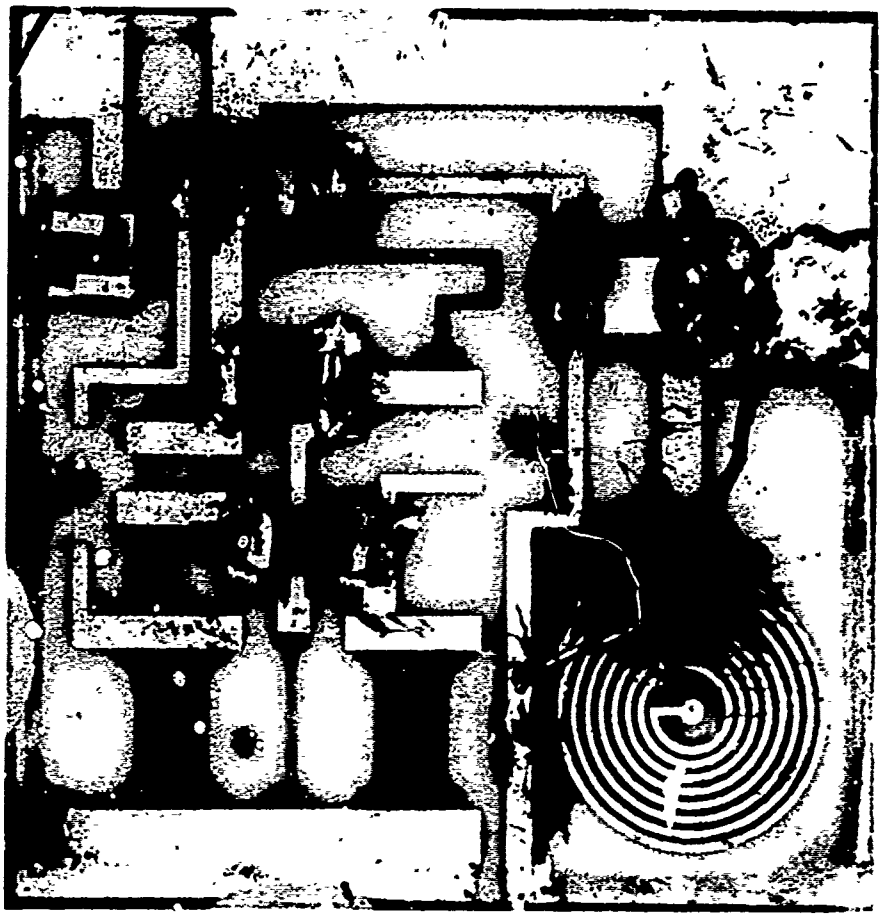

FIGURE III-5 PHOTOGRAPH OF MIC REALIZATION OF FET-NIC FILTER

PIN diodes have been replaced by a fixed resistor R_3, and the variable-coupling trimmer capacitors are located on the main circuit board (Duroid material). The 0.1-μH tuned-circuit inductor was initially implemented as a spiral inductor etched on the substrate. The Q of this inductor was so low (about 8) that it was decided to replace it with a ferrite-core toroidal inductor of much higher Q and smaller area. The only disadvantage of the ferrite toroid is that the particular material on hand limited the experimental filter to an operating frequency of 37 MHz because of the rapidly decreasing inductor Q at high frequencies. However, materials suitable for higher-frequency operation are available. The potentiometer on the main circuit board was an unnecessary frill, but it was useful for setting the bias on the FET.

The elimination of the RF chokes should have a harmful effect on the power-handling ability and the noise figure of the active filter. This can be deduced from the low-frequency equivalent circuit of the FET-NIC filter as shown in Figure III-6. The Kirchoff equations for the loops in this circuit are:

$$I_2[R_e + (1 - \alpha)R_b] = (I_3 - I_2)R_2$$

$$(I_1 - I_3)R_1 = I_3R_3 + (I_3 - I_2)R_2$$

$$V_{gate} = I_1 \frac{1}{g_m} + (I_1 - I_3)R_1$$

$$V_{gate} = \alpha I_2 R_p \quad .$$

Solving for $\frac{I_2}{I_1}$, one obtains

$$\frac{I_2}{I_1} = \frac{R_1R_2}{[R_1 + R_2 + R_3][R_e + (1 - \alpha)R_b + R_2] - R_2^2} \quad .$$

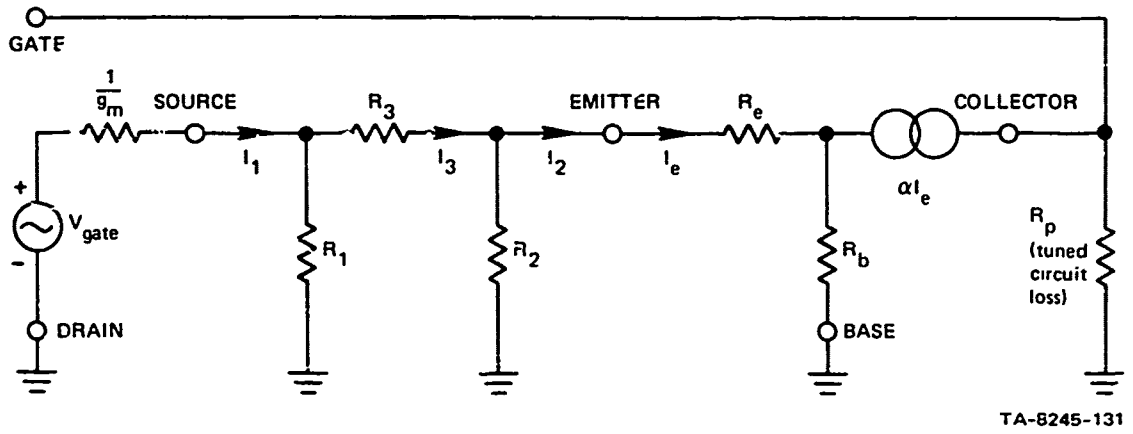

FIGURE III-6 EQUIVALENT CIRCUIT OF FET-NIC

However, since R_1, R_2, and R_3 are about 1 kilohm, while R_e and R_b are about 5 ohms, one may make the approximation that $R_2 + R_e + (1 - \alpha)R_b \doteq R_2$. Therefore,

$$\frac{I_2}{I_1} \doteq \frac{R_1}{R_1 + R_3} \quad . \tag{III-5}$$

Thus, a large fraction of the current I_1 is shunted to ground by the decoupling resistor R_1, unless R_1 can be made much larger than R_3. This is impractical because of power dissipation. In the first integrated FET-NIC, R_1 and R_3 were about equal; therefore, only half of the RF source current from the FET flows into the emitter of the bipolar transistor. In this case the current swing of the FET will limit the power output of the active filter, because the FET and the bipolar transistors are biased to draw about 8 mA each.

In addition, the noise figure of the filter will suffer because only half of the signal current from the FET will reach the emitter of the bipolar transistor. Therefore, some way of eliminating the decoupling loss was essential for the second integrated FET-NIC.

The integrated FET-NIC operated at a slightly higher current than the first non-integrated FET-NIC,* which would have increased the power handling capability of the FET-NIC filter by 1.5 dB. However, the decoupling loss of 6.7 dB resulted in a calculated net decrease in power-handling ability of 5.2 dB. The measured power-handling capability of the integrated FET-NIC was only 4 5 dB less than that of the non-integrated FET-NIC. Thus, the first integrated FET-NIC performed close to expectations.

2. Circuit Redesign

The relatively large microminiature coupling trimmer capacitors were replaced by tiny Siliconix B7140 varactor chips. The NPN bipolar transistor was replaced by a PNP device, which made possible the complete elimination of the coupling loss previously experienced in resistors R_1 and R_2. This PNP device was a Fairchild 2N4957 chip designed for small-signal 450 MHz RF amplifier applications. The circuit was made rather compact, so that a realistic estimate could be made of the degree of miniaturization possible with these techniques. Figure III-7(a) shows a schematic of the redesigned FET-NIC filter and Figure III-7(b) shows the substrate layout.

The measured performance of the redesigned integrated FET-NIC indicated that no electrical sacrifice was necessary for miniaturization. At a comparable percentage bandwidth the newest integrated FET-NIC was essentially identical in performance to the lumped-circuit FET-NIC reported previously (see Section III-D). In addition, the bandwidth of the integrated filter could be electrically varied from 0.2 to 1.4 percent.

---

* See Ref. 16, p 48.

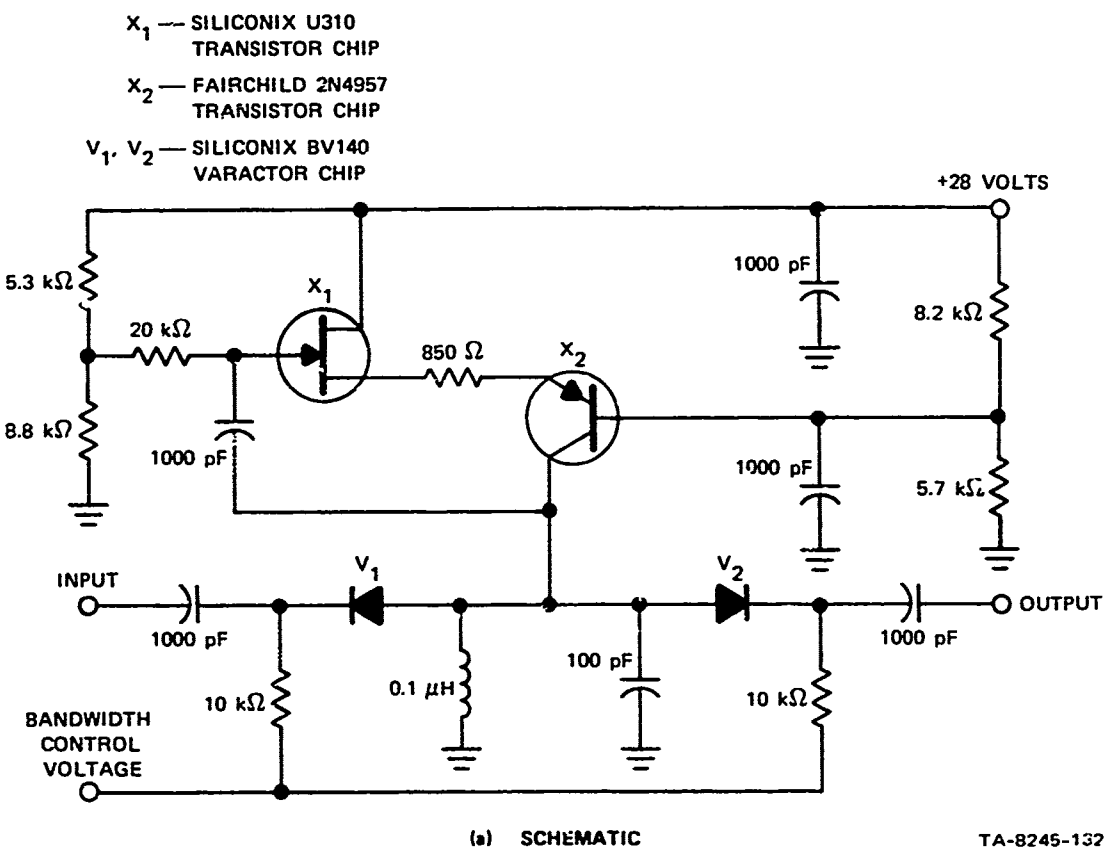

FIGURE III-7 SCHEMATIC DIAGRAM AND SUBSTRATE LAYOUT OF SECOND INTEGRATED FET-NIC FILTER

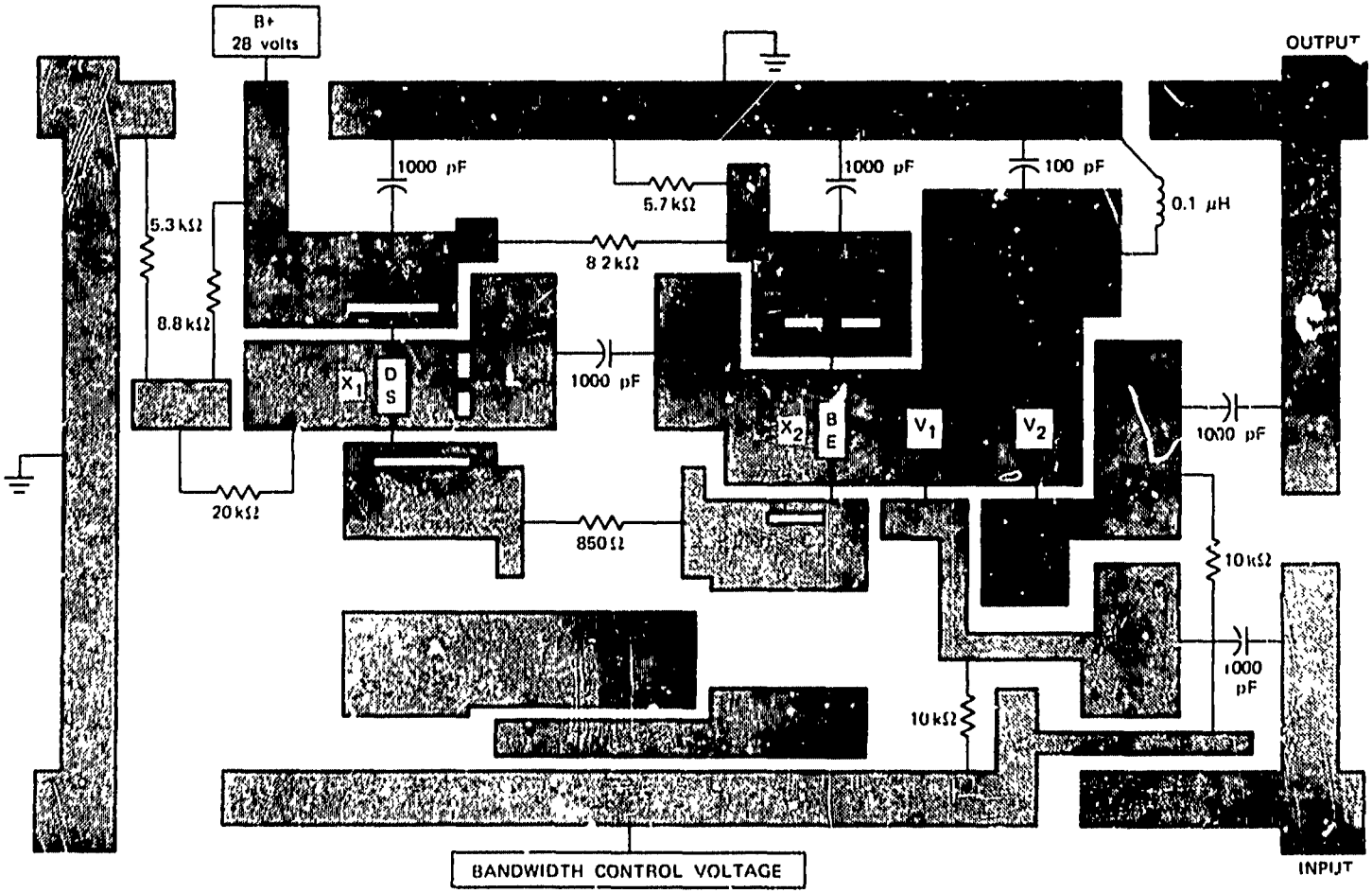

(b) SUBSTRATE LAYOUT

TA-8245-133

FIGURE III-7 (Concluded)

D. Final Results

In Table III-3 the new integrated FET-NIC and the high-power NUNIC are compared with the first FET-NIC circuits and the trial NIC of 1970.

Table III-3

NIC FILTER PERFORMANCE

	Bandwidth and Center Frequency (MHz)	Noise Figure (dB)	Power Output 1-dB Compression (dBm)	Third-Order Intercept (dBm)	Total Variation in Gain, 25°C to 60°C (dB)
Trial NIC (1970)*	0.6 and 50	17	-20	-1'	5.2
1st FET-NIC†	0.6 and 50	7 - 10	+9	+20	0.9
Improved 2nd FET-NIC†	0.6 and 50	7 - 10	+12	+23	‡
1st Integrated FET-NIC	0.6 and 50	9 - 12	+5	+15	0.9
2nd Integrated FET-NIC	0.6 and 50	6 - 7	+12	+23	0.9
High-Power NUNIC Filter	2.7 and 230	>21	+29	+35	0.8

* Source: Ref. 17, p. 51.
† Source: Ref. 16.
‡ Not yet measured.

IV SLOT LINE

A. General

The idea of using slot line to realize transmission and resonator elements in microwave integrated circuits was originally described in an earlier report in this series,[18] and has been treated theoretically in a sequence of reports since then.[16,17,19-21] This study has now been brought to a close, and its last topics are contained in the following section.

Numerous additional papers and reports on slot-line subjects have been published by SRI and USAECOM personnel,[22-27] as well as by others.[28-33] These cover many theoretical, experimental, and application aspects of slot line. Practical use of slot line appears particularly promising for ferrite phase shifters, hybrid junctions, mixers, frequency multipliers, amplifiers, etc. In most of these applications, slot line would be used in conjunction with microstrip line to achieve results not possible with the latter alone.

The basic slot-line configuration is shown in Figure IV-1, and a sandwich-slot-line cross section is shown in Figure IV-2. Their wavelength and impedance parameters have been analyzed with parallel electric or magnetic wall boundaries[17,19,22] and with rectangular shields.[16,17] Formulas for their E- and H-field distributions have been derived.[16,20,21,26] Wideband transitions to coaxial line and microstrip have been analyzed and shown to be practical.[21]

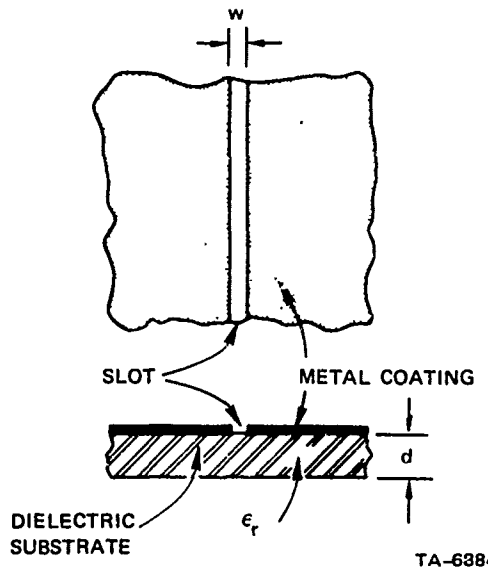

FIGURE IV-1 SLOT LINE ON A DIELECTRIC SUBSTRATE

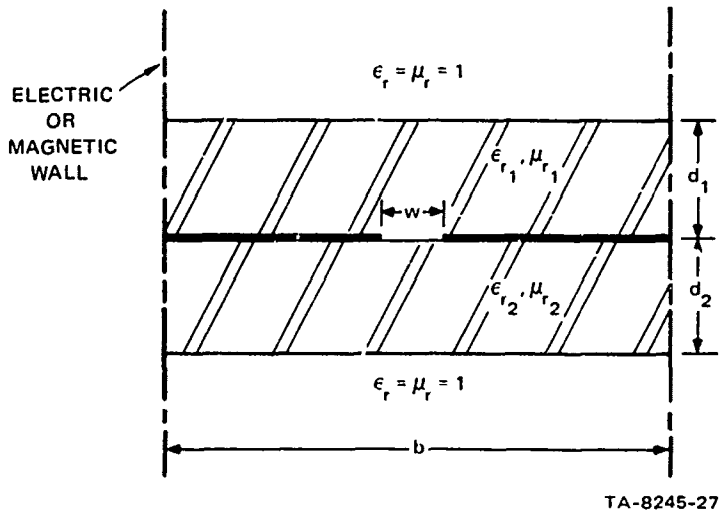

FIGURE IV-2 SANDWICH-SLOT-LINE CROSS SECTION WITH A PAIR OF ELECTRIC OR MAGNETIC WALLS

In this section, two additional aspects of slot lines are treated. These are four-layer symmetrical sandwich slot line, and coupling between a parallel pair of slot lines. Because the former is especially interesting for ferrite phase shifters, the analysis allows the scalar relative permeabilities to differ from unity. In addition to obtaining formulas for Z_{oe}, v/v_g, and λ'/λ, the magnetic-field-strength components in the various layers are evaluated. Graphs of these allow the choice of favorable sets of parameters for best phase-shifter performance. A method of computing coupling between parallel slot lines is given, and several curves of coupling and directivity versus frequency are shown.

B. Multilayer Sandwich Slot Line

Figure IV-3 shows the multilayer slot-line configuration that will be treated in this report. For the computations, b was selected large enough so that wall proximity effects would be negligible. (Generally, $b > 1.5\lambda'$ is sufficient.) In that case, either electric or magnetic walls at $y = \pm b/2$ would yield the same results. Magnetic walls were chosen for the analysis because they lead to simpler formulas and computation. If electric walls are desired, the approaches of earlier reports[18,19,22] may be used to make the necessary changes in the formulas. Electric walls may also be added at $z = \pm(d_1 + d_2 + \ell)$ to surround the multilayer sandwich slot line by a rectangular electric-wall shield. This modification can be carried out as in earlier cases of shields around single-substrate slot line and double-substrate sandwich line.[16,17] In addition, the same principles may be used to treat any number of substrate layers beyond the total of four considered in this report.[17]

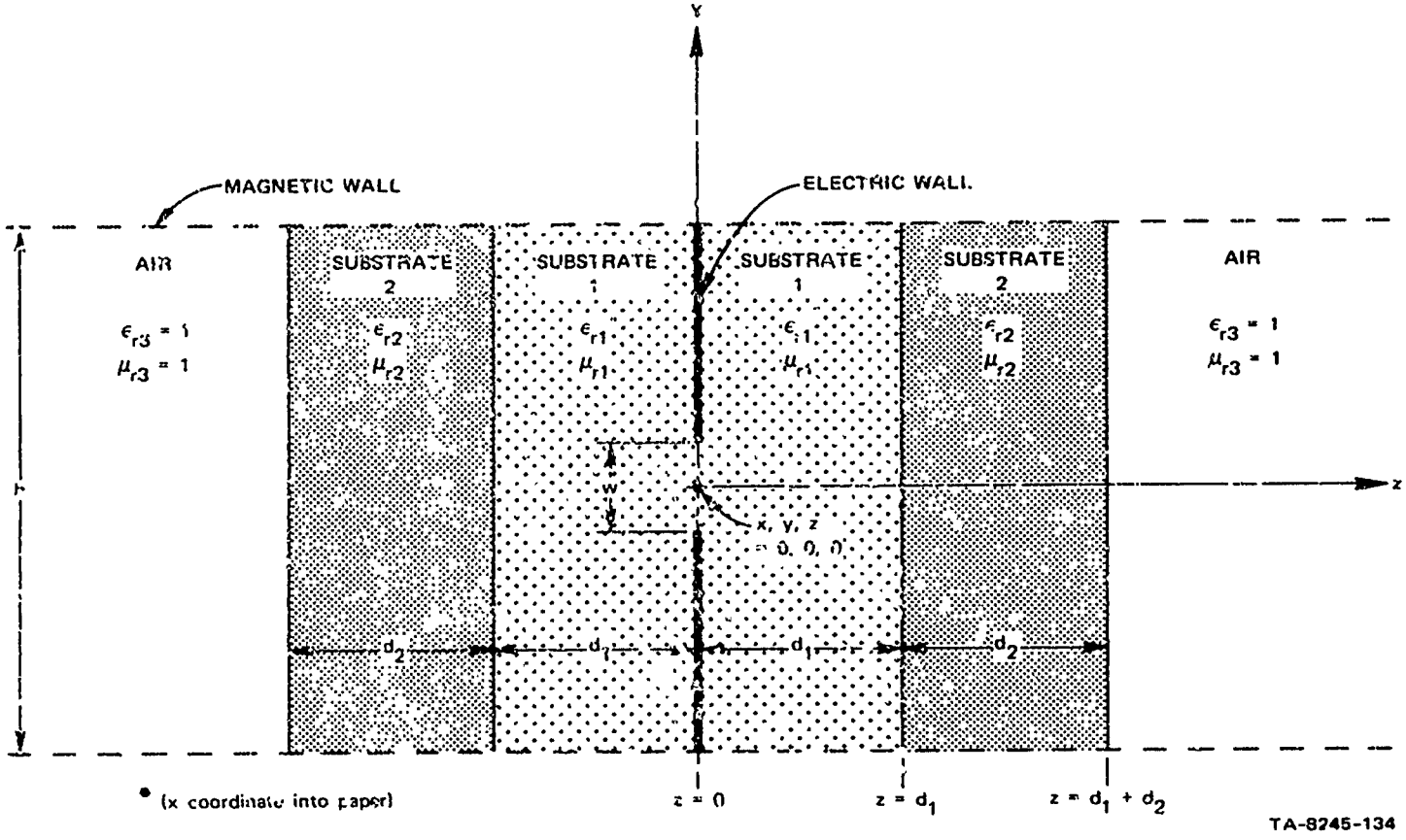

FIGURE IV-3 SYMMETRICAL MULTILAYER-SANDWICH SLOT LINE

Formulas for the configuration in Figure IV-3 were obtained by a straightforward extension of the previous analyses.[16-22] The total normalized susceptance at z = 0 looking toward the right and left must be zero, as follows:

$$0 = \eta B_t = \frac{u_1^2}{p} \ln \frac{8}{\pi\delta} + \frac{1}{p} \sum_{n=1/2,3/2,\ldots} \left[\frac{\epsilon_{r1} \tanh r_n - \frac{p^2 F_{n1}^2}{\mu_{r1}} \coth q_n}{\left[1 + \left(\frac{b}{n\lambda'}\right)^2\right] F_{n1}} - u_1^2 \right] \frac{\sin^2 \pi n\delta}{n(\pi n\delta)^2} \quad . \tag{IV-1}$$

Notation for dimensions, permeabilities, and permittivities are indicated in Figure IV-3, while λ' = slot-line wavelength, η = 376.7 ohms per square, and δ = w/b. (Note that μ_{r1} and μ_{r2} are scalar quantities. Nonisotropic and nonreciprocal effects are neglected.) The value of p satisfying $B_t = 0$ is $p = \lambda/\lambda'$. Other parameters are:

$$r_n = \gamma_{n1} d_1 + \tanh^{-1}\left[\frac{\epsilon_{r2} F_{n1}}{\epsilon_{r1} F_{n2}} \tanh\left(\gamma_{n2} d_2 + \tanh^{-1} \frac{F_{n2}}{\epsilon_{r2} F_n}\right)\right] \tag{IV-2}$$

$$q_n = \gamma_{n1} d_1 + \coth^{-1}\left[\frac{\mu_{r1} F_{n2}}{\mu_{r2} F_{n1}} \coth\left(\gamma_{n2} d_2 + \coth^{-1} \frac{F_n \mu_{r2}}{F_{n2}}\right)\right] \tag{IV-3}$$

$$v = \sqrt{p^2 - 1} \quad , \quad u_1 = \sqrt{\mu_{r1}\epsilon_{r1} - p^2} \quad , \quad u_2 = \sqrt{\mu_{r2}\epsilon_{r2} - p^2} \tag{IV-4}$$

$$F_n = \sqrt{1 + \left(\frac{bv}{n\lambda' p}\right)^2} \quad , \quad F_{n1} = \sqrt{1 - \left(\frac{bu_1}{n\lambda' p}\right)^2} \quad ,$$

$$F_{n2} = \sqrt{1 - \left(\frac{bu_2}{n\lambda' p}\right)^2} \qquad \text{(IV-5)}$$

$$\gamma_n = \frac{2\pi n}{b} F_n \quad , \quad \gamma_{n1} = \frac{2\pi n}{b} F_{n1} \quad , \quad \gamma_{n2} = \frac{2\pi n}{b} F_{n2} \quad . \qquad \text{(IV-6)}$$

In evaluating Eqs. (IV-1) through (IV-6), care must be taken to make the correct changes in the various functions when their arguments are imaginary.[17,19,22]

A similar extension of the earlier analyses[16-22] was carried out by W. Mohuchi of Sedco Systems, Inc., differing in that $\mu_{r1} = 1$ and electric walls were used in place of magnetic walls.[33] The two sets of equations agree when these minor differences are reconciled.

The characteristic impedance defined in terms of power flow and voltage V_0 across the slot is given by[19,22]

$$Z_0 = 376.7\pi \frac{\lambda'}{\lambda} \cdot \frac{v}{v_g} \cdot \frac{\Delta p}{-\Delta \eta B_t} \text{ ohms} \qquad \text{(IV-7)}$$

where $\Delta \eta B_t$ is computed from Eq. (IV-1) with λ' held constant and p incremented slightly about the value $p = \lambda'/\lambda$ at $\eta B_t = 0$. The ratio of phase velocity to group velocity v/v_g is

$$\frac{v}{v_g} = 1 + \frac{f}{\lambda/\lambda'} \cdot \frac{\Delta(\lambda/\lambda')}{\Delta f} \quad . \qquad \text{(IV-8)}$$

In this case $\Delta(\lambda/\lambda')$ and Δf are computed from two separate solutions of $\eta B_t = 0$ for two slightly different values of λ' incremented about the desired λ'. The value f may be assumed to lie midway in the Δf interval.

A time-shared computer program in BASIC language was prepared to compute λ'/λ, v/v_g, and Z_0 versus the various parameters at specified frequencies. This program was used to evaluate values of λ'/λ needed in the field-component computations.

Formulas for field computation have been derived for the multilayer sandwich-slot-line cross section of Figure IV-3. These apply in the $z \geq 0$ region; however, in the $z < 0$ region they also apply when the sign of H_x is reversed. If the sandwich is symmetrical, H_x is necessarily zero at $z = 0$. The field components are expressed as infinite summations of the individual TE- and TM-mode components with respect to z-axis propagation.

Formulas for the complete set of six E and H components were given in Refs. 21 and 22 for single-substrate slot line and a double-substrate sandwich. The work has now been extended to the case of multilayer configurations. The H_x and H_z components are as follows, with the factor $e^{j(\omega t - 2\pi x/\lambda')}$ suppressed:*

---

* This factor implies wave propagation in the +x direction.

- **First substrate, $0 \le z \le d_1$**

$$H^{(1)}_{xTEn} = \frac{j2V_0}{\eta\lambda}\left(\frac{\lambda}{\lambda'}\right)^2 \frac{F_{n1}}{\mu_{r1}{}^n} \frac{\sin \pi n\delta}{\pi n\delta} \cos \frac{2\pi my}{b} \cdot \left[\frac{\coth q_n \cosh \gamma_{n1}z - \sinh \gamma_{n1}z}{1 + (b/n\lambda')^2}\right] \tag{IV-9}$$

$$H^{(1)}_{xTMn} = \frac{-j2V_0}{\eta\lambda} \frac{\epsilon_{r1}}{nF_{n1}} \frac{\sin \pi n\delta}{\pi n\delta} \cos \frac{2\pi my}{b} \cdot \left[\frac{\tanh r_n \cosh \gamma_{n1}z - \sinh \gamma_{n1}z}{1 + (b/n\lambda')^2}\right] \tag{IV-10}$$

$$H^{(1)}_{zTEn} = \frac{2V_0}{\eta b\mu_{r1}} \frac{\lambda}{\lambda'} \frac{\sin \pi n\delta}{\pi n\delta} \cos \frac{2\pi my}{b} \cdot [\cosh \gamma_{n1}z - \coth q_n \sinh \gamma_{n1}z] \tag{IV-11}$$

- **Second substrate, $d_1 \le z \le d_1 + d_2$**

$$H^{(2)}_{xTEn} = \left[H^{(1)}_{xTEn}\right]_{z=d_1} \cdot [\cosh \gamma_{n2}(z - d_1) - \tanh q_{n2} \sinh \gamma_{n2}(z - d_1)] \tag{IV-12}$$

$$H^{②}_{xTMn} = \left[H^{①}_{xTMn}\right]_{z=d_1} \cdot [\cosh \gamma_{n2}(z - d_1) - \coth r_{n2} \sinh \gamma_{n2}(z - d_1)] \quad \text{(IV-13)}$$

$$H^{②}_{zTEn} = \frac{\mu_{r1}}{\mu_{r2}} \left[H^{①}_{zTEn}\right]_{z=d_1} \cdot [\cosh \gamma_{n2}(z - d_1) - \coth q_{n2} \sinh \gamma_{n2}(z - d_1)] \quad \text{(IV-14)}$$

- Air region, $d_1 + d_2 \leq z \leq \infty$

$$H^{③}_{xTEn} = \left[H^{②}_{xTEn}\right]_{z=d_1+d_2} \cdot e^{-\gamma_n(z-d_1-d_2)} \quad \text{(IV-15)}$$

$$H^{③}_{xTMn} = \left[H^{②}_{xTMn}\right]_{z=d_1+d_2} \cdot e^{-\gamma_n(z-d_1-d_2)} \quad \text{(IV-16)}$$

$$H^{③}_{zTEn} = \mu_{r2}\left[H^{②}_{zTEn}\right]_{z=d_1+d_2} \cdot e^{-\gamma_n(z-d_1-d_2)} . \quad \text{(IV-17)}$$

In each region, the modes are summed as follows to yield the H_x and H_z components for the magnetic-wall-boundary configuration of Figure IV-3:

$$H_x = \sum_{n=1/2,3/2,\ldots} [H_{xTEn} + H_{xTMn}] \quad \text{(IV-18)}$$

$$H_z = \sum_{n=1/2,3/2,\ldots} H_{zTEn} . \quad \text{(IV-19)}$$

The variables r_n, q_n, F_{n1}, etc., are defined by Eqs. (IV-2) through (IV-6), while r_{n2} and q_{n2} are:

$$r_{n2} = \gamma_{n2} d_2 + \tanh^{-1}\left(\frac{F_{n2}}{\epsilon_{r2} F_n}\right) \qquad \text{(IV-20)}$$

$$q_{n2} = \gamma_{n2} d_2 + \coth^{-1}\left(\frac{F_n \mu_{r2}}{F_{n2}}\right) . \qquad \text{(IV-21)}$$

A computer program in BASIC language was prepared yielding H_x and H_z in all regions. The H_y, E_x, E_y, and E_z components can be obtained from Eqs. (IV-9) through (IV-19) by straightforward use of Maxwell's equations; however, for ferrite-substrate devices, H_x and H_z in the principal plane $y = 0$ are of primary interest.

Derivation of the mode-summation formulas, Eqs. (IV-9) through (IV-19), was based on the simplifying assumption of constant E_y field across the slot. When w is small compared to b, disregarding the true variation of E_y causes negligible amplitude error for low-order modes, but appreciable error for high-order modes. As a result, the field components are predicted with excellent accuracy at distances from the slot greater than about one slot width, while very near the slot the error is quite large. In an earlier report[16] quasi-static formulas were introduced that yield good accuracy in the vicinity of the slot. For symmetrical sandwich slot line these are as follows, on the z axis between $z = -d_1$ and $z = d_1$:

$$H_x = \frac{j2V_0}{\lambda \eta_{r1}} \left[\epsilon_{r1}\mu_{r1} - \left(\frac{\lambda}{\lambda'}\right)^2\right] \sinh^{-1}\left(\frac{2z}{w}\right) , \quad |z| \le d_1 \qquad \text{(IV-22)}$$

$$H_z = \frac{2V_0}{\pi w \eta_{r1}} \frac{\lambda}{\lambda'} \left[1 - \left(\frac{2z}{w}\right)^2\right]^{-1/2} , \quad |z| \le d_1 . \qquad \text{(IV-23)}$$

Equations (IV-22) and (IV-23) hold for $|z|$ out to about 0.75 w (unless d_1 is smaller), while for greater $|z|$ the mode-summation equations, Eqs. (IV-9) through (IV-19), are valid. In the vicinity of $|z| = 0.75$ w, accuracy may be improved by plotting the two solutions and judiciously blending the curves together.

Graphs of H_x/j and H_z versus z are shown in Figures IV-4 and IV-5. The quasi-static and mode-summation formulas were used in plotting the curves. The discontinuities in H_z are the result of μ_{r2} discontinuities at the interfaces. In both graphs, the second substrate is characterized by $\epsilon_{r2} = 13$ and $\mu_{r2} = 0.8$, which are typical values for ferrite phase shifters. Figure IV-4 has $\epsilon_{r1} = 9.6$ and $\mu_{r1} = 1$, while Figure IV-5 has $\epsilon_{r1} = 30$ and $\mu_{r1} = 1$. The dimensions w, d_1, and d_2 are the same in both cases, and their values are shown in the figures. In each case b was

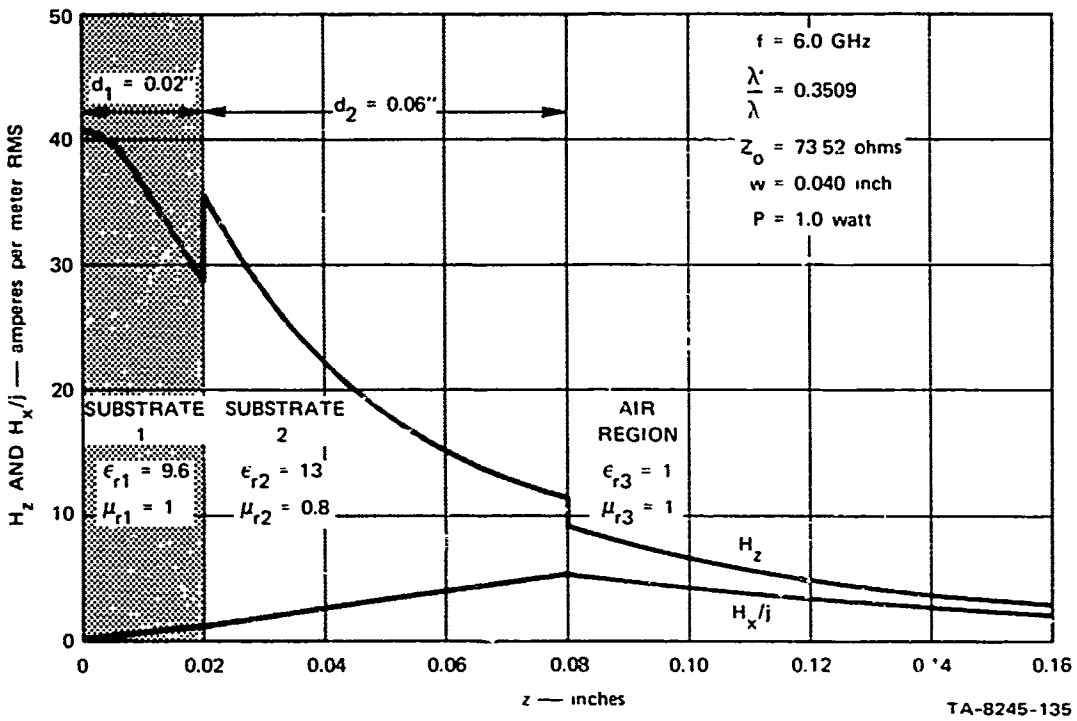

FIGURE IV-4 FIELDS H_z AND H_x/j vs. z iN y = 0 PLANE, $\epsilon_{rl} = 9.6$

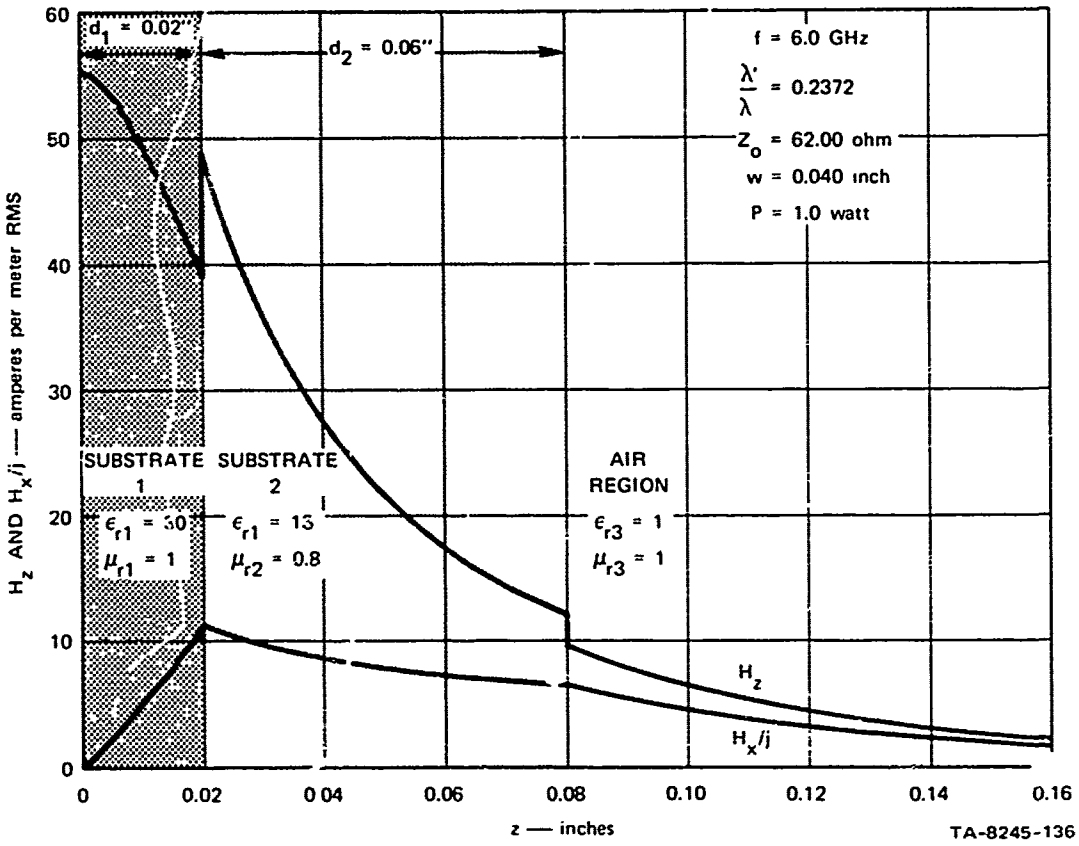

FIGURE IV-5 FIELDS H_z AND H_x/j vs. z IN y = 0 PLANE, ϵ_{rl} = 30

about 1.5 λ', which is large enough so that the magnetic walls have negligible effect on the computed data. Values of λ'/λ and Z_0 obtained from Eqs. (IV-1) through (IV-8) are also given in the figures. The frequency is 6.0 GHz, and the field strengths are in amperes per meter rms for one watt of power flow. This power normalization was obtained by letting $V_0 = \sqrt{Z_0}$ volts rms across the slot.

Inspection of Figures IV-4 and IV-5 shows that ϵ_{rl} has a major effect on the magnitude of H_x/j in the substrates. A large value of ϵ_{rl} yields a relatively large H_x/j in Substrate 2, which is a favorable condition for ferrite reciprocal phase shifters. The case of ϵ_{rl} = 9.6

Equations (IV-22) and (IV-23) hold for $|z|$ out to about 0.75 w (unless d_1 is smaller), while for greater $|z|$ the mode-summation equations, Eqs. (IV-9) through (IV-19), are valid. In the vicinity of $|z| = 0.75$ w, accuracy may be improved by plotting the two solutions and judiciously blending the curves together.

Graphs of H_x/j and H_z versus z are shown in Figures IV-4 and IV-5. The quasi-static and mode-summation formulas were used in plotting the curves. The discontinuities in H_z are the result of μ_{r2} discontinuities at the interfaces. In both graphs, the second substrate is characterized by $\epsilon_{r2} = 13$ and $\mu_{r2} = 0.8$, which are typical values for ferrite phase shifters. Figure IV-4 has $\epsilon_{r1} = 9.6$ and $\mu_{r1} = 1$, while Figure IV-5 has $\epsilon_{r1} = 30$ and $\mu_{r1} = 1$. The dimensions w, d_1, and d_2 are the same in both cases, and their values are shown in the figures. In each case b was

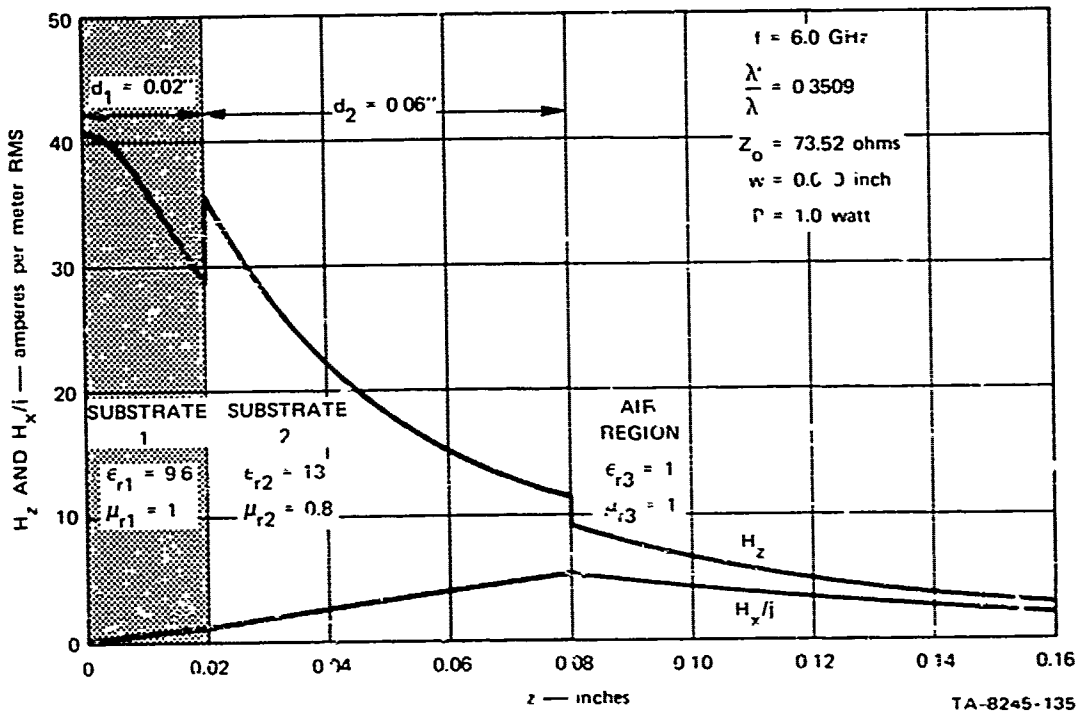

FIGURE IV-4 FIELDS H_z AND H_x/j vs. z IN y = 0 PLANE, $\epsilon_{r1} = 9.6$

yields almost zero H_x/j in Substrate 1. In fact, Eq. (IV-22) shows that H_x/j will be negative in Substrate 1 when $\epsilon_{r1}\mu_{r1} < (\lambda/\lambda')^2$. Examples in which this occurs were computed, showing that H_x/j versus z crosses zero at a point within Substrate 2 and is positive thereafter. Twenty-seven sets of H_z and H_x/j versus z were computed with $\mu_{r1} = \mu_{r2} = 1$, $\epsilon_{r2} = 13$, w = 0.040 inch, and f = 6.0 GHz, and with all combinations of $\epsilon_{r1} = 9.6$, 13, and 30; $d_1 = 0.02$, 0.03, and 0.04 inches; and $d_2 = 0.02$, 0.06, and 0.10 inches. The computer printouts were furnished to Sedco Systems, Inc. to aid their USAECOM-supported program on slot-line phase shifters. Plots of the 27 cases are included in their latest report.[33] These substantiate that a large value of ϵ_{r1} in the dielectric substrate 1 is needed to achieve high H_x/j in the ferrite substrate 2.

C. Coupling Between Slot Lines

Coupling between a pair of parallel slot lines on the same substrate will be treated in terms of even- and odd-mode characteristic impedances Z_{oe}, Z_{oo}, and wavelengths λ'_e, λ'_o. For weak to moderate coupling, these can be computed from solutions already available.

Figure IV-6(a) shows the single-substrate slot-line cross section previously analyzed.[19] The configuration is bounded by a pair of parallel electric or magnetic walls with spacing b. For b about 1.5 λ' or greater, these walls have negligible effect on slot line Z_0 and λ', while for smaller b these values are increasingly perturbed as b is decreased.

Images in a pair of electric walls yield the equivalent even-mode infinite array of Figure IV-6(b), while a pair of magnetic walls yields the odd-mode infinite array of Figure IV-6(c). Note that the slot voltages are codirected for the even mode and alternately directed for the odd mode. We will define Z_0 and λ' for the electric-wall, even-mode cases as Z_E

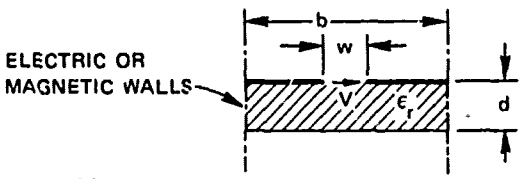

(a) SLOT-LINE CROSS SECTION SOLVED IN REF. 19

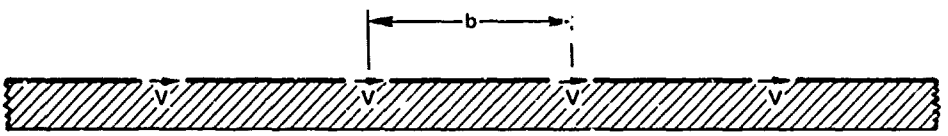

(b) INFINITE ARRAY OF SLOTS, EVEN-MODE CASE

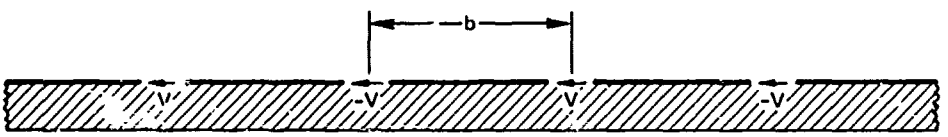

(c) INFINITE ARRAY OF SLOTS, ODD-MODE CASE

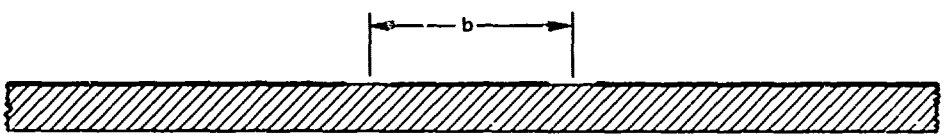

(d) PAIR OF COUPLED SLOTS

TA-8245-137

FIGURE IV-6 BASIC SLOT-LINE CROSS SECTION, EQUIVALENT INFINITE ARRAYS, AND COUPLED SLOT PAIR

and λ'_E, and for the magnetic-wall odd-mode case as Z_M and λ'_M. These may be computed by the formulas of Ref. 19. The symbols Z_0 and λ' will be applied to the limiting case $Z_E \to Z_M \to Z_0$ and $\lambda'_E \to \lambda'_M \to \lambda'$ as $b \to \infty$. When b is chosen such that Z_E, Z_M, and λ'_E, λ'_M are perturbed by relatively small amounts from Z_0 and λ', computation shows these perturbations to be opposite pairs:

$$Z_E \approx Z_0 + 2\Delta Z \quad , \quad Z_M \approx Z_0 - 2\Delta Z \tag{IV-24}$$

$$\lambda'_E \approx \lambda' + 2\Delta\lambda' \quad , \quad \lambda'_M \approx \lambda' - 2\Delta\lambda' \tag{IV-25}$$

where

$$\Delta Z = \frac{1}{4}(Z_E - Z_M) \tag{IV-26}$$

$$\Delta\lambda' = \frac{1}{4}(\lambda'_E - \lambda'_M) \quad . \tag{IV-27}$$

The case of a pair of coupled slots with center-to-center spacing b is shown in Figure IV-6(d). Each slot has close proximity to one adjacent slot, while in the infinite arrays each slot has close proximity to two adjacent slots. Therefore, when b is sufficiently large that the perturbations are small, the even and odd parameters of the pair of slots (Z_{oe}, Z_{oo}, λ'_e, λ'_o) are perturbed by half the amounts of the infinite array:

$$Z_{oe} \approx Z_0 + \Delta Z \quad , \quad Z_{oo} \approx Z_0 - \Delta Z \tag{IV-28}$$

$$\lambda'_e \approx \lambda' + \Delta\lambda' \quad , \quad \lambda'_o \approx \lambda' - \Delta\lambda' \tag{IV-29}$$

where ΔZ and $\Delta\lambda'$ are given by Eqs. (IV-26) and (IV-27).

For an input-wave amplitude of unity, the various output-wave amplitudes are as follows for Figure IV-7:

$$c = \frac{1}{2}(t_e - t_o) \qquad \text{(IV-30)}$$

$$t = \frac{1}{2}(t_e + t_o) \qquad \text{(IV-31)}$$

$$i = \frac{1}{2}(\rho_e - \rho_o) \qquad \text{(IV-32)}$$

$$\rho = \frac{1}{2}(\rho_e + \rho_o) \qquad \text{(IV-33)}$$

where ρ_e and t_e are the voltage reflection and transmission coefficients of a length of transmission line with parameters Z_{oe} and φ_e, while ρ_o and t_o are the same but with Z_{oo} and φ_o.

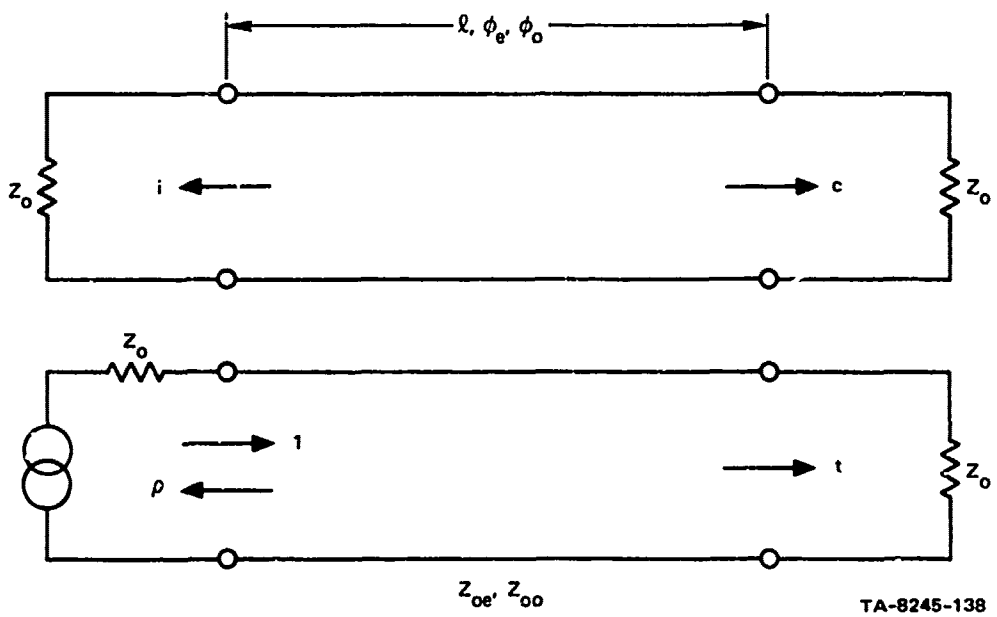

FIGURE IV-7 EQUIVALENT CIRCUIT OF COUPLED SLOT LINES

The inequality of φ_e and φ_o for a pair of coupled slots causes predominant forward coupling. Let coupling and directivity be defined as follows:

$$C = 20 \log_{10} |c| \text{ dB} \qquad \text{(IV-34)}$$

$$D = 20 \log_{10} \left|\frac{c}{i}\right| \text{ dB} \quad . \qquad \text{(IV-35)}$$

Curves of C and D versus f were computed and plotted in Figure IV-8 for $\varepsilon_r = 16$, d = 0.050 inch, w = 0.020 inch, ℓ = 1 inch, and b = 0.25, 0.35, and 0.5 inch. Junction effects are ignored, and will strongly affect the measured directivity of a practical coupler.

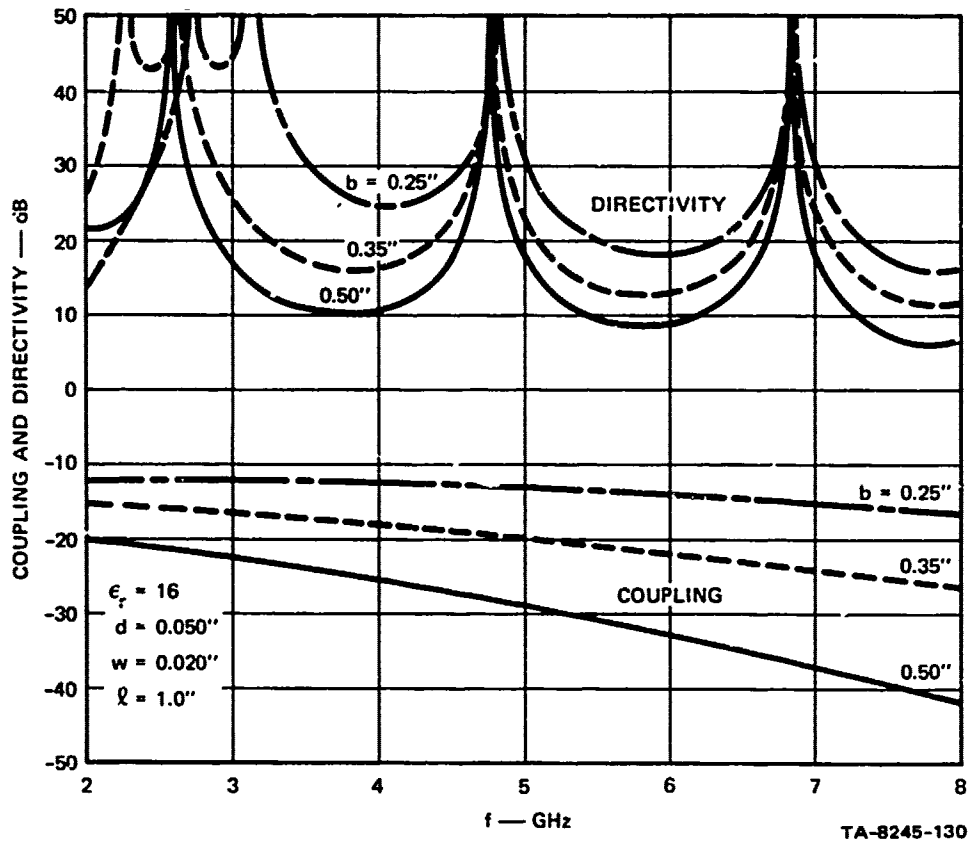

FIGURE IV-8 COUPLING AND DIRECTIVITY vs. FREQUENCY FOR A PAIR OF COUPLED SLOTS

V CONCLUSIONS

A. Meander-Line and Hybrid Meander-Line Transformers

A table of meander-line transformers having 2 to 6 turns, impedance transformation ratios of from 1.1 to 20, and bandwidth ratios of from 2.5:1 to 10:1 was presented. The transformer responses are, for all practical purposes, equal-ripple responses. For a given ripple, the bandwidth of meander-line transformers is less than what can be obtained with stepped-impedance transformers of the same degree of complexity. However, the principal advantage of meander-line transformers is their compactness.

The concept of hybrid meander-line transformers was introduced. Hybrid meander-line transformers permit circuit designers considerable flexibility in choosing the geometrical shape of the transformer design. The bandwidth of hybrid transformers lies between that of meander-line and stepped-impedance designs for the same passband VSWR. Several examples of hybrid transformers were illustrated in the text.

Experimental three-turn meander-line and N = 4 hybrid meander-line transformers were designed and constructed in stripline. The experimental data agreed extremely well with the theoretically computed responses.

B. Negative-Impedance Converters

It has been shown that active filters can be built to operate at power levels above 1 watt at UHF frequencies. In addition, negative feedback can be used to stabilize these filters so that changes in

operating conditions have little effect on the filter performance. Although care must be taken with large transistors to prevent spurious oscillations, one-watt active filters are now practical for operation up to 1 or 2 GHz.

The FET-NIC can be used to make filters that are stable, low-noise, and tiny (less than 0.2 cm^3). These filters can be made variable in both bandwidth and center frequency. A 1.2-percent-bandwidth, one-pole filter would have typically a 7- to 10-dB noise figure, +12 dBm power-handling capability, and a +23 dBm third-order intercept.

C. Slot Line

Symmetrical four-layer sandwich slot line appears better suited for ferrite-phase-shifter use than a two-layer all-ferrite configuration. The outer layers should be ferrite material, and the inner layers dielectric material. The use of high- rather than low-permittivity dielectric material results in far more favorable magnetic-field distributions in the ferrite layers.

Two parallel slots couple to each other predominantly in the forward direction. The formulas in this report are valid for moderate and weak couplings. The curves show that good directivity may be achieved in certain frequency bands.

REFERENCES

1. G.L. Matthaei, L. Young, and E.M.T. Jones, Design of Microwave Filters, Impedance-Matching Networks, and Coupling Structures (McGraw Hill Book Co., New York, N.Y., 1964).

2. R.E. Collin, "Theory and Design of Wide-Band Multisection Quarter-Wave Transformers," Proc. IRE, Vol. 43, pp. 179-185 (February 1955).

3. H.J. Riblet, "General Synthesis of Quarter-Wave Impedance Transformers," IRE Trans. on Microwave Theory and Techniques, Vol. MTT-5, pp. 36-43 (January 1957).

4. L. Young, "Tables for Cascaded Homogeneous Quarter-Wave Transformers," IRE Trans. on Microwave Theory and Techriques, Vol. MTT-7, pp. 233-237 (April 1959).

5. H. Ozaki and J. Ishii, "Synthesis of Transmission-Line Networks and the Design of UHF Filters," IEEE Trans. on Circuit Theory, Vol. CT-2, pp. 325-335 (December 1955).

6. G.L. Matthaei, "Short-Step Chebyshev Impedance Transformers," IEEE Trans. on Microwave Theory and Techniques, Vol. MTT-14, pp. 372-384 (August 1966).

7. P.N. Butcher, "The Coupling Impedance of Tape Structures," Proc. IEE, Vol. 104, Pt. 8, pp. 177-187 (March 1957).

8. J.T. Bolljahn and G.L. Matthaei, "A Study of the Phase and Filter Properties of Arrays of Parallel Conductors Between Ground Planes," Proc. IRE, Vol. 50, pp. 299-311 (March 1962).

9. H.S. Hewitt, "A Computer D igned 720 to 1 Microwave Compression Filter," IEEE Trans. on Microwave Theory and Techniques, Vol. MTT-15, pp. 687-694 (December 1967).

10. R. Sato, "A Design Method for Meander-Line Networks Using Equivalent Circuit Transformations," IEEE Trans. on Microwave Theory and Techniques, Vol. MTT-19, pp. 431-442 (May 1971).

11. P.I. Richards, "Resistor Transmission-Line Circuits," Proc. IRE, Vol. 36, pp. 217-220 (February 1948).

12. J.A. Bandler, "Optimization Methods for Computer-Aided Design," IEEE Trans. on Microwave Theory and Techniques, Vol. MTT-17, pp. 533-552 (August 1969).

13. W.J. Getsinger, "Coupled Rectangular Bars Between Parallel Plates," IRE Trans. on Microwave Theory and Techniques, Vol. MTT-10, pp. 65-73 (January 1962).

14. R. J. Wenzel, "Small Elliptic-Function Low-Pass Filters and Other Applications of Microwave C Sections," IEEE Trans. on Microwave Theory and Techniques, Vol. MTT-18, pp. 1150-1158 (December 1970).

15. G.I. Zysman and A. Matsumoto, "Properties of Microwave C-Sections," IEEE Trans. on Circuit Theory, Vol. CT-12, pp. 74-82 (March 1965).

16. E.G. Cristal, A. Podell, and S.B. Cohn, "Microwave Active Network Synthesis," Semiannual Report 1, SRI Project 8245, Contract DAAB07-70-C-0044, Stanford Research Institute, Menlo Park, California (October 1971).

17. E.G. Cristal, D. Chamber, S.B. Cohn, and A. Podell, "Microwave Active Network Synthesis," Interim Report, SRI Project 8245, Contract DAAB07-70-C-0044, Stanford Research Institute, Menlo Park, California (November 1970).

18. E.G. Cristal, D.K. Adams, R.Y.C. Ho, and S.B. Cohn, "Microwave Synthesis Techniques," Annual Report, Contract DAAB07-68-C-0088, SRI Project 6884, Stanford Research Institute, Menlo Park, California (September 1968).

19. R.Y.C. Ho, D.K. Adams, S.B. Cohn, and E.G. Cristal, "Microwave Synthesis Techniques," Semi-Annual Report 1, Contract DAAB07-68-C-0088, SRI Project 6884, Stanford Research Institute, Menlo Park, California (May 1969).

20. E.G. Cristal, R.Y.C. Ho, D.K. Adams, S.B. Cohn, L.A. Robinson, and L. Young, "Microwave Synthesis Techniques," Final Report, Contract DAAB07-68-C-0088, SRI Project 6884, Stanford Research Institute, Menlo Park, California (November 1969).

21. D. Chambers, S.B. Cohn, E.G. Cristal, and L. Young, "Microwave Active Network Synthesis, "Semi-Annual Report, Contract DAAB07-70-C-0044, SRI Project 8245, Stanford Research Institute, Menlo Park, California (June 1970).

22. S.B. Cohn, "Slot Line on a Dielectric Substrate," IEEE Trans. on Microwave Theory and Techniques, Vol. MTT-17, pp. 768-778 (October 1969).

23. E.A. Mariani, C.P. Heinzman, J.P. Agrios, and S.B. Cohn, "Slot Line Characteristics," IEEE Trans. on Microwave Theory and Techniques, Vol. MTT-17, pp. 1091-1096 (December 1969).

24. E.A. Mariani and J.P. Agrios, "Slot Line Filters and Couplers," IEEE Trans. on Microwave Theory and Techniques, Vol. MTT-18, pp. 1089-1095 (December 1970).

25. S.B. Cohn, "Sandwich Slot Line," IEEE Trans. on Microwave Theory and Techniques, Vol. MTT-19, pp. 773-774 (September 1971).

26. S.B. Cohn, "Slot-Line Field Components," to be published in the IEEE Trans. on Microwave Theory and Techniques, February 1972.

27. E.A. Mariani, "Evaluation of Slot Line Bends at S-band Frequencies," R&D Technical Report ECOM-3491, USAECOM, Fort Monmouth, N. J. (October 1971).

28. G.H. Robinson and J.L. Allen, "Slot Line Applied to Miniature Ferrite Devices," IEEE Trans. on Microwave Theory and Techniques, Vol. MTT-17, pp. 1097-1101 (December 1969).

29. F.C. de Ronde, "A New Class of Microstrip Directional Couplers," 1970 G-MTT International Symposium Digest, pp. 184-189 (May 11-14, 1970).

30. J.K. Hunton and J.S. Takeuchi, "Recent Developments in Microwave Slot-Line Mixers and Frequency Multipliers," 1970 G-MTT International Symposium Digest, pp. 196-199 (May 11-14, 1970).

31. H.J. Schmitt, "Fundamentals of Microwave Integrated Circuits," Proc. of Swedish Seminar on New Microwave Components, Stockholm, September 14-16, 1970.

32. J.A. Garcia, "A Wide-Band Quadrature Hybrid Coupler," IEEE Trans. on Microwave Theory and Techniques, Vol. MTT-19, pp. 660-661 (July 1971).

33. I. Bardash, "Slot Line Digital Ferrite Phase Shifter," Semiannual Report, Contract DAAB07-71-C-0056, Sedco Systems Corp., Farmingdale, N.Y. (January 1972).

UNCLASSIFIED
Security Classification

DOCUMENT CONTROL DATA - R & D

Security classification of title, body of abstract and indexing annotation must be entered when the overall report is classified

1 ORIGINATING ACTIVITY (Corporate author) Stanford Research Institute Menlo Park, California 94025	2a. REPORT SECURITY CLASSIFICATION UNCLASSIFIED 2b. GROUP N/A

3 REPORT TITLE

MICROWAVE ACTIVE NETWORK SYNTHESIS

4. DESCRIPTIVE NOTES (Type of report and inclusive dates)

Final Report Covering the Period 13 October 1969 to 27 December 1971

5 AUTHOR(S) (First name, middle initial, last name)

Edward G. Cristal Allen F. Podell Seymour B. Cohn

6 REPORT DATE	7a. TOTAL NO OF PAGES	7b. NO OF REFS
February 1972	118	33

8a. CONTRACT OR GRANT NO	9a. ORIGINATOR'S REPORT NUMBER(S)
Contract DAAB07-70-C-0044 b. PROJECT NO	Final Report SRI Project 8245
c.	9b. OTHER REPORT NO(S) (Any other numbers that may be assigned this report)
d.	ECOM-0044-F

10 DISTRIBUTION STATEMENT

Approved for public release; distribution unlimited.

11. SUPPLEMENTARY NOTES	12 SPONSORING MILITARY ACTIVITY
	U.S. Army Electronics Command Fort Monmouth, N.J. 07703 Attn: AMSEL-TL-MM

13 ABSTRACT

This report describes the application of meander lines to impedance transformers, and discusses two types of negative-impedance circuits and two slot-line topics.

It is demonstrated that meander lines constitute a class of impedance transformers of which stepped-impedance transformers are a special case. A design table is presented for nearly-equal-ripple meander-line transformers of from 2 to 6 turns, incorporating a wide range of bandwidths and impedance transformations. Experimental confirmation of the design table is given.

Two types of negative-impedance-converter (NIC) circuits were designed and constructed: (1) a high-power NUNIC, and (2) a FET-NIC filter. A high-power NUNIC circuit intended for operation at 200 to 500 MHz was built and produced negative resistance from below 80 MHz to above 680 MHz. A lossless one-pole filter incorporating the NUNIC was built for operation at 230 MHz and exhibited a 3-dB filter bandwidth of 2.7 MHz. The 1-dB compression point occurred at 1 watt of input power (+30 dBm) and the third-order intermodulation intercept measured +34.5 dB. A FET-NIC filter has been constructed in microwave integrated circuit (MIC) form. It was possible to vary the bandwidth of this filter electrically over a 7:1 range. The size of the complete MIC FET-NIC filter is comparable with a small power-transistor package, approximately 1/2 inch square by 1/16 inch high. (continue)

DD FORM 1 NOV 68 1473 (PAGE 1)

S/N 0101-807-6801

UNCLASSIFIED
Security Classification

14 KEY WORDS	LINK A		LINK B		LINK C	
	ROLE	WT	ROLE	WT	ROLE	WT
Meander-line transformers						
Negative-impedance converters						
Slot line						

ABSTRACT - continued

The slot-line topics treated are, [illegible], symmetrical four-layer-sandwich slot line, which is discussed for ferrite-phase-shifter applications. Formulas are given for wavelength, characteristic impedance, and magnetic-field-strength distribution. Curves of the latter are helpful for phase-shifter optimization. Secondly, coupling between two parallel slot lines is analyzed, and a few typical curves of coupling and directivity versus frequency are shown.